

**Understanding Selectivity and Activity in Z-selective Metathesis
with Cyclometallated Ru-based Catalysts**

Brendan Liam Quigley

in partial fulfillment of the requirements for the degree of
Doctor of Philosophy

Division of Chemistry and Chemical Engineering
California Institute of Technology
Pasadena, CA

2016

(Defended 23 May 2016)

© 2016

All rights reserved except where otherwise noted.

Acknowledgments

I would like to begin by thanking my advisor, Prof. Robert Grubbs. I first joined the Grubbs group in 2009 as a SURF student and I like to joke that I came back for grad school because I forgot to return the key. It was really Bob's passion for science and the strong sense of teamwork he fosters in the group that brought me back and have kept me going for the last six years. Bob has been an amazing support over my time at Caltech. He gave me the freedom to pursue projects in many different areas of olefin metathesis, allowing me to develop the skills required as an independent scientist. Whenever I needed guidance, Bob was always available and was an invaluable source of advice and direction not only for chemistry but also for life. I would also like to thank my committee, Profs. Linda Hsieh-Wilson, Harry Gray and Dennis Dougherty. I very much enjoyed discussing my research and proposals with you over the years and have benefited greatly from the engaging discussions. Your insights and advice have shaped my research and future endeavors.

Very little of the work included in this thesis would be possible without the assistance of the CCE staff. I would particularly like to thank David VanderVelde for maintaining the NMR facility and for his assistance and advice with NMR over the years. I would also like to thank Mona Shahgholi and Naseem Torian in the Mass Spectrometry facility and Larry Henley and Mike Takase in the X-ray crystallography facility for their work with my compounds. Scott Virgil has been invaluable in maintaining our analytical equipment. Linda Syme and Agnes Tong have both been extremely helpful in dealing with the administrative side of grad school. Rick Gerhart, Jeff Groseth and Joe Drew have all been helpful when things get broken and have made things run more smoothly. I

would also like to acknowledge Steve Gould, Elisa Brink, Silva Virgil, Guillermo Correa and Arthur Larenas for their work.

I have overlapped with a lot of people during my time in the Grubbs group and feel that I have learned something from each person. People have always been willing to give advice and the wealth of knowledge from different backgrounds and perspectives has been extremely beneficial. There are, however, a number of people I'd like to specifically thank. AJ Boydston was my mentor as a SURF student in 2009. He introduced me to the world of metathesis and experimental organometallic chemistry, which gave me a strong foundation for grad school. Chris Daeffler helped me pick up the cyclic polymers project as a grad student and together with Matthew Van Wingerden, Keith Keitz and Jean Li were invaluable sources of advice during my first couple of years. More recently, Julian Edwards began working on cyclic polymers and his enthusiasm and dedication have been invaluable in pushing the project forward. Paresma (Pinky) Patel helped me get started on my first Z-selective project and was an excellent source of advice. Siihong (Will) Lau joined me as a SURF student in 2015. He was a pleasure to work with and brought enthusiasm, hard work and fresh ideas to a project that turned out to be more challenging than either of us expected! I was extremely lucky that Prof. Dan O' Leary joined our group for a sabbatical. He has been an ever-enthusiastic collaborator and has greatly enhanced my knowledge of NMR spectroscopy. The studies in Chapter 3 would not have been possible without his help and insights. In addition, to the people mentioned above, I would particularly like to thank Nicholas Swisher, Melanie Pribisko Yen, Myles Herbert, Tonia Ahmed, Pablo Guzman, Chris Bates, Sarah Bronner, Jeff Cannon, John Hartung, Choonwoo Lee, Vanessa Marx, Garret Miyake and Raymond

Weitekamp for valuable discussions over the years.

I would like to thank my friends at Caltech for their support and friendship, including Matthew Van Wingerden, Catrina Pheeney, Chris Daeffler, Kristina Daeffler, Myles Herbert, Ryan Henning, Jonathan Chapman, Samantha Myers, Guy Edouard, Khai Chiong, Allyson Pellissier and Brad Hulse. You've made the last six years enjoyable outside the lab! I would also like to thank my friends in Ireland, who always made an effort to see me on one side of the Atlantic or the other. Melanie Pribisko, Nicholas Swisher, Tonia Ahmed, Ben Sveinbjornsson and Pablo Guzman have been great friends over the years and have been invaluable in helping me through the final year of grad school. I am extremely grateful for their support in writing this thesis.

Finally, I would like to thank my family, Maggie, Richard, Niamh, Aidan and Ailbhe. Despite being over 5,000 miles away for most of my time at Caltech, they have always managed to support me. This thesis would not have been possible without their encouragement.

Abstract

With the advent of well-defined highly active catalysts, olefin metathesis has become a powerful tool for the formation of carbon–carbon double bonds in a variety of settings. However, these traditional catalysts preferentially form the E-alkene product. Recent efforts have yielded several families of Z-selective metathesis catalysts, including a family of Ru complexes with cyclometallated NHC ligands developed in our group. The work in this thesis describes efforts to develop an improved understanding of the catalyst features that govern activity and selectivity in the cyclometallated Ru-based catalysts, as well as to expand the scope of reactivity in these systems.

Chapter 1 provides an outline of the key features that govern selectivity in cross metathesis applications.

Chapter 2 describes the application of cyclometallated Ru-based catalysts in Z-selective CM of allylic-substituted olefins. Efficient CM is demonstrated in the case of acrolein acetals providing a new route to access Z- α,β -unsaturated acetals and aldehydes. For a variety of other allylic-substituted olefins, reactivity was lower but could be correlated with the structure of the catalyst and substrate. The implications of the observed reactivity are discussed and contextualized with regard to reactivity of previous metathesis catalysts.

Chapter 3 describes the development of a series of cyclometallated Z-selective metathesis with varying N-aryl groups that allow elucidation of the key catalyst features that govern activity and selectivity in these systems. The synthesis of the catalyst series is described, including several strategies employed to circumvent unexpected side-reactions. The second part of the chapter focuses on the dynamic behavior of the catalysts

in solution and studies of an unusual C–H⋯F–C intramolecular interaction observed in some of these catalysts. Finally, the reactivity of these catalysts in a variety of CM applications are discussed, which allows for development of a refined model of how the N-aryl group affects Z-selectivity and activity in these catalysts systems and how this varies across different classes of substrate.

Table of Contents

Acknowledgements	iii
Abstract	vi
Table of Contents	viii
List of Figures	x
List of Tables	xiii
List of Schemes	xv
List of Abbreviations	xvii
Chapter 1: Introduction	
Olefin Metathesis	2
Selectivity in Cross Metathesis	3
Cis–trans Selectivity in Ru-based Metathesis Catalysts	5
Z-selective Ru-based Metathesis Catalysts	7
References	9
Chapter 2: Z-selective Cross Metathesis of Allylic-Substituted Olefins	
Abstract	13
Introduction	14
Z-selective Cross Metathesis of Acrolein Acetals	18
Optimization of Reaction Conditions	20
Substrate Scope: Allylic-substituted Olefin	23
Substrate Scope: Cross Partner	27
Deprotection of Z- α,β -unsaturated Acetals	29
CM of Other Allylic-substituted Olefins	32
Differences in Reactivity and Selectivity between Catalysts	34
CM of Allylic-substituted Olefins with Catalyst 2.1	37
Experimental Section	43
References	60

Chapter 3: Synthesis, Characterization and Activity of a Series of Cyclometallated Catalysts with Varying N-aryl Group

Abstract	65
Introduction	66
Synthesis of the Catalyst Series	71
NMR Characterization	85
Dynamics	85
An Unusual C–H····F–C Interaction	89
Reactivity	96
Homodimerization of Allylbenzene	96
Homodimerizations of Methyl-10-undecenoate and 4-Penten-1-ol	102
T.O.N. Experiments	105
Cross Metathesis of Allylic-substituted Olefins	107
Conclusion	110
Experimental Section	113
References	148

List of Figures

Chapter 1

- Figure 1.1. Key ruthenium-based metathesis catalysts. 5
- Figure 1.2. Possible orientations for metallacyclobutanes. 6
- Figure 1.3. *Syn* and *anti* geometries of bottom-bound metallacycles. 7
- Figure 1.4. Cyclometallated Ru catalysts that are Z-selective in metathesis. 8
- Figure 1.5. Model for Z-selectivity in cyclometallated Ru-based catalysts. 8

Chapter 2

- Figure 2.1. Cyclometallated Ru complexes commonly employed for
Z-selective olefin metathesis. 14
- Figure 2.2. Commonly employed metathesis catalysts. 15
- Figure 2.3. Key steric interactions governing Z-selectivity in CM reactions
of allylic-substituted olefins. 16
- Figure 2.4. Key scenarios representing the expected spectrum of reactivity
for allylic-substituted olefins compared to unhindered olefins. 17
- Figure 2.5. Proposed chelated catalyst species responsible for low activity. 30
- Figure 2.6. Key scenarios representing reactivity for allylic-substituted
olefins with catalyst 2.2 compared to catalyst 2.1 36

Chapter 3

- Figure 3.1. Cyclometallated Ru complexes commonly employed for
Z-selective olefin metathesis. 66

Figure 3.2. Previously prepared cyclometallated Ru-based Z-selective catalysts with various N-aryl groups.	67
Figure 3.3. Targeted series of Z-selective catalysts with varying N-aryl groups.	70
Figure 3.4. Fluoro-aryl catalyst 3.67, which demonstrated the presence of a F–Ru interaction.	85
Figure 3.5. Benzylidene region of ¹ H-NMR spectra of catalysts 3.1 and 3.10–3.16 in C ₆ D ₆ .	86
Figure 3.6. Solid-state structure of 3.61, with thermal ellipsoids drawn at 50% probability.	87
Figure 3.7. Rotation about the N-C(aryl) bond of 3.11	88
Figure 3.8. Through-space ¹ H– ¹⁹ F coupling to benzylidene proton observed in Ru-based metathesis model complex.	89
Figure 3.9. ¹ H-NMR spectra of 3.10 illustrating spin–spin coupling of the benzylidene proton signal with one F signal.	90
Figure 3.10. ¹ H-NMR spectra of 3.11 illustrating spin–spin coupling of downfield benzylidene proton signal with one F signal	91
Figure 3.11. Plot of chemical shift of benzylidene peak coupled to ¹⁹ F for each of catalysts 3.10, 3.11 and 3.13 against the σ_{meta} value for the other N-aryl substituent.	92
Figure 3.12. ¹ H– ¹⁹ F HOESY spectra illustrating almost equal NOE to both aromatic protons ortho to F.	93
Figure 3.13. ¹⁹ F-presaturation experiments for catalyst 3.10, illustrating decrease in intensity of non-irradiated ¹⁹ F peak.	94

Figure 3.14. Partial ^1H -ROESY/EXSY spectrum of catalyst 3.10 indicating exchange of meta aromatic protons.	95
Figure 3.15. A) Plot of conversion vs. time and B) Z-selectivity vs. conversion in the homodimerization of allylbenzene.	98
Figure 3.16. Plot of conversion vs. time in the homodimerization of allylbenzene,	99
Figure 3.17. Plots of Z-selectivity vs. conversion for homodimerization of allylbenzene.	100
Figure 3.18. A) Plot of conversion vs. time and B) Z-selectivity vs. conversion in the homodimerization of methyl-10-undecenoate.	103
Figure 3.19. A) Plot of conversion vs. time and B) Z-selectivity vs. conversion in the homodimerization of 4-penten-1-ol.	104
Figure 3.20. Yield and Z-selectivity of homodimer 3.71 at 6 h. in the homodimerization of allylbenzene	106
Figure 3.21. Yield and Z-selectivity of cross product 3.79 at 6 h.	108
Figure 3.22. Yield and Z-selectivity of cross product 3.79 at 6 h.	109
Figure 3.23. Comparison of Z-selectivity observed in formation of 3.70 (Scheme 3.11) at 1h. compared to Z-selectivity observed in formation of 3.78 (Scheme 3.15) at 6 h.	110

List of Tables

Chapter 2

Table 2.1. Optimization of CM reaction between 2-vinyl-1,3-dioxolane and 1-dodecene	21
Table 2.2. Varying the olefin in excess in CM of 2-vinyl-1,3-dioxolane and 1-dodecene.	22
Table 2.3. CM of various acrolein acetals with 1-dodecene.	24
Table 2.4. CM of vinyl pinacol boronate and 2-vinyloxirane with 1-dodecene.	25
Table 2.5. Varying the cross partner in CM of 2-vinyl-1,3-dioxolane.	27
Table 2.6. CM of 2-vinyl-1,3-dioxolane and <i>N</i> -allylaniline derivatives.	29
Table 2.7. Stereoretentive deprotection of <i>Z</i> - α,β -unsaturated acetals	31
Table 2.8. CM of allylic-substituted hydrocarbons with methyl-10-undecenoate.	32
Table 2.9. CM of allylic-substituted secondary alcohols.	33
Table 2.10. Comparison of catalysts in CM of 3-vinyl-1,2-dioxolane and 1-dodecene.	34
Table 2.11. CM of allylic-substituted hydrocarbons with methyl-10-undecenoate using catalyst 2.1.	37
Table 2.12. Optimization of CM between vinyl cyclohexane and methyl-10 undecenoate.	39
Table 2.13. CM of allylic-substituted hydrocarbons with methyl-10-undecenoate using catalyst 2.1.	40
Table 2.14. CM of protected secondary allylic alcohols with 1-dodecene using catalyst 2.1.	41

Table 2.15. Model for selectivity in CM, expanded to include cyclometallated Z-selective metathesis catalysts.	43
Chapter 3	
Table 3.1. Condensation of 2,6-substituted anilines and bromoacetyl chloride.	74
Table 3.2. Substitution of alkyl bromide with 1-adamantylamine.	75
Table 3.3. Reduction of amides with LiAlH_4 .	76
Table 3.4. Reduction of amides with $\text{BH}_3\cdot\text{THF}$.	78
Table 3.5. Formation of imidazolium chlorides from corresponding diamines.	79
Table 3.6. Formation of imidazolium chlorides from corresponding diamine dihydrochlorides.	80
Table 3.7. Metallation of NHCs using KO^tAm .	81
Table 3.8. Metallation of NHCs using KHMDs .	82
Table 3.9. C–H activation and anion metathesis to form cyclometallated Z-selective catalysts.	84

List of Schemes

Chapter 1

- Scheme 1.1. General mechanism for olefin metathesis. 2
- Scheme 1.2. Types of olefin metathesis reactions. 3
- Scheme 1.3. Products formed in cross metathesis of two terminal olefins. 4
- Scheme 1.4. Formation of metallacyclobutanes from phosphonium
alkylidene catalyst 1.4 at low temperature. 7

Chapter 2

- Scheme 2.1. CM of 2-vinyl-1,3-dioxolane and 1-dodecene. 20
- Scheme 2.2. Unreactive CM substrates with tertiary allylic substitution. 26
- Scheme 2.3. CM of allyl pinacol boronate with 2-vinyl-1,3-dioxolane
and conversion to corresponding allylic alcohol. 28

Chapter 3

- Scheme 3.1. Decomposition pathway observed for Z-selective
catalysts bearing N-aryl groups with ortho hydrogens. 68
- Scheme 3.2. General synthetic scheme for accessing cyclometallated
Z-selective Ru catalysts. 71
- Scheme 3.3. Proposed synthetic scheme for N-aryl, N'-1-adamantyl
imidazolium salts. 72
- Scheme 3.4 Preparation of anilines from corresponding carboxylic acids
using DPPA. 73
- Scheme 3.5. Negishi cross-coupling reaction to prepare 2-fluoro-6-isopropylaniline.
73

Scheme 3.6. Attempted reduction of amide 3.31 with LiAlH ₄ .	76
Scheme 3.7. Reduction of amide 3.31 with BH ₃ .THF	77
Scheme 3.8. Attempted reduction of amide 3.34 with LiAlH ₄ .	78
Scheme 3.9. Cyclization of 3.44 to form imidazolium salt and conversion to tetrafluoroborate.	81
Scheme 3.10. Metallation of NHC salt 3.44 using LiHMDS.	83
Scheme 3.11. Homodimerization of allylbenzene at 0.1 mol% catalyst loading.	97
Scheme 3.12. Homodimerization of methyl-10-undecenoate at 0.1 mol% catalyst loading.	102
Scheme 3.14. Homodimerization of allylbenzene at 0.01 mol% catalyst loading.	105
Scheme 3.15. CM of vinyl cyclohexane and methyl-10-undecenoate.	107

List of Abbreviations

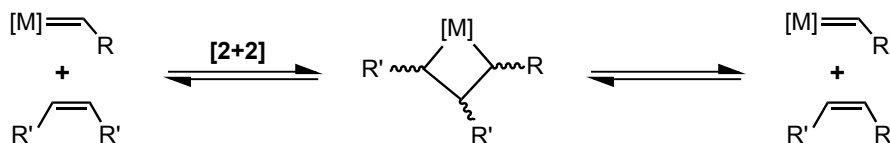
CM	Cross metathesis
Cy	Cyclohexyl
DCM	Dichloromethane
DFT	Density functional theory
DIPP	2,6-diisopropylphenyl
EXSY	Exchange spectroscopy
GC	Gas chromatography
h.	Hours
HMDS	Hexamethyldisilazane
HOESY	Heteronuclear Overhauser effect spectroscopy
Mes	2,4,6-trimethylphenyl
MIDA	<i>N</i> -methyliminodiacetic acid
min.	Minutes
NHC	N-heterocyclic carbene
NMR	Nuclear magnetic resonance
NOESY	Nuclear Overhauser effect spectroscopy
RCM	Ring-closing metathesis
ROCM	Ring-opening cross metathesis
ROESY	Rotating-frame Overhauser Spectroscopy
ROMP	Ring-opening metathesis polymerization
^t Am	Tert-amyl (2-methyl-2-butyl)
TEA	Triethylamine
THF	Tetrahydrofuran
TLC	Thin-layer chromatography

Chapter 1

Introduction to Selectivity in Olefin Metathesis

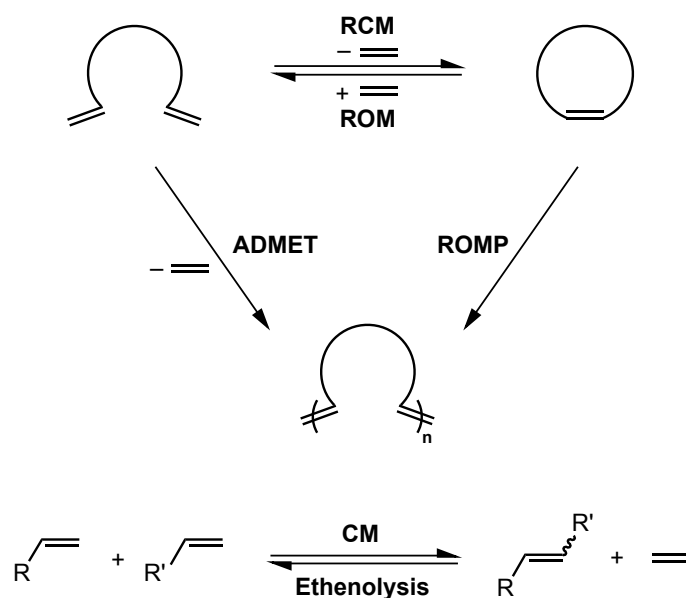
Olefin Metathesis

Over the past sixty years, olefin metathesis has transformed from an undesirable side reaction into a powerful and widely used method for the formation of carbon–carbon double bonds.^{1,2} While early catalysts were ill-defined heterogeneous mixtures, mechanistic experiments identified transition metal (TM) carbenes as the active catalysts in these systems³, which prompted the development of a wide variety of well-defined TM carbene complexes that were competent olefin metathesis catalysts.^{4,5} Olefin metathesis proceeds via a [2+2] cycloaddition between a TM carbene and an alkene to form a metallacyclobutane intermediate, which can then collapse to generate a new TM carbene and a new alkene product (**Scheme 1.1**).



Scheme 1.1. General mechanism for olefin metathesis.

By varying the type(s) of alkene starting materials employed in the reaction, a wide variety of alkene-containing products can be generated and this is used to define various classes of olefin metathesis reaction (**Scheme 1.2**).



Scheme 1.2. Types of olefin metathesis reactions.

Selectivity in Cross Metathesis

Of these reaction classes, initial attention was largely devoted to ring-opening metathesis polymerization (ROMP) and ring-closing metathesis (RCM), both of which have a strong driving force toward product formation. In ROMP reactions, release of ring strain from the cyclic starting material is the driving force for the reaction, whereas for RCM there is an entropic driving force due to the production of two molecules from one (the product and ethylene). Cross metathesis (CM) lacks either of these driving forces, making it a more challenging reaction that also presents several issues with regard to selectivity that are not present in other types of metathesis reactions. Typically, if two distinct terminal olefins (**A** + **B**, **Scheme 1.3**) undergo CM, multiple products result: the homodimers of **A** and **B** are formed (**A**₂ + **B**₂, respectively) in addition to the desired cross product (**AB**). Each of these products is also formed as a mixture of the cis and trans isomers, generating six different products.

The olefin classification type results from a combination of steric and electronic factors, with increased steric bulk proximal to the double bond and electron-withdrawing substituents generally leading to reduced reactivity. Notably, the “type” is specific to a given metathesis catalyst, which often allows for high selectivity to be achieved in the reaction of two given olefins, through careful choice of catalyst. The remaining major challenge in the field of CM was to achieve precise control over the olefin stereochemistry, allowing the generation of cis and trans olefins with high selectivity.

Cis–trans Selectivity in Ru-based Metathesis Catalysts

Two major families of well-defined TM complexes have enjoyed considerable success as olefin metathesis catalysts: those based on Mo and W complexes, pioneered by Schrock⁷⁻¹⁰, and those based on Ru, which have been a major focus of research in our group, as well as others^{11,12} (**Figure 1.1**). A focus on catalyst development in tandem with mechanistic studies has provided significant insight into the features that govern the stability and activity in Ru-based olefin metathesis catalysts.¹³⁻¹⁵ In contrast, the features that govern issues of selectivity, in particular cis–trans selectivity, have proved more challenging to elucidate. A key factor in understanding the cis–trans selectivity of typical

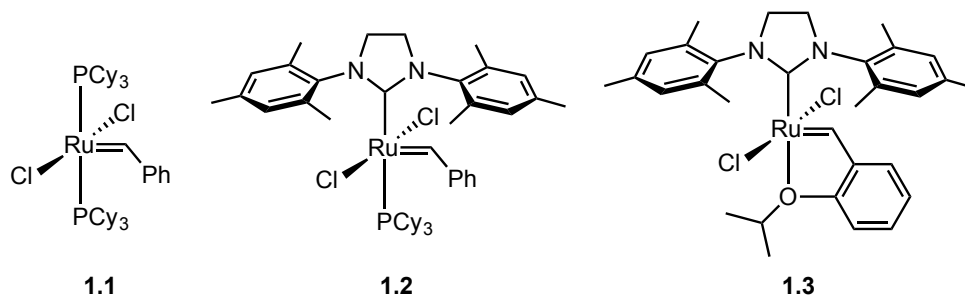


Figure 1.1. Key ruthenium-based metathesis catalysts.

Ru-based metathesis catalysts (such as **1.1-1.3**) is the orientation of the metallacyclobutane intermediate with respect to the other ligands on Ru, for which two distinct pathways have been proposed (**Figure 1.2**).

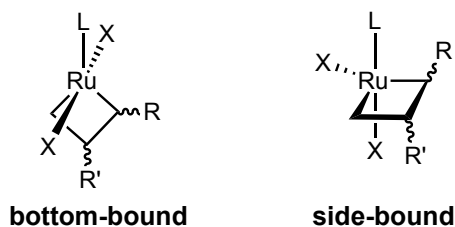
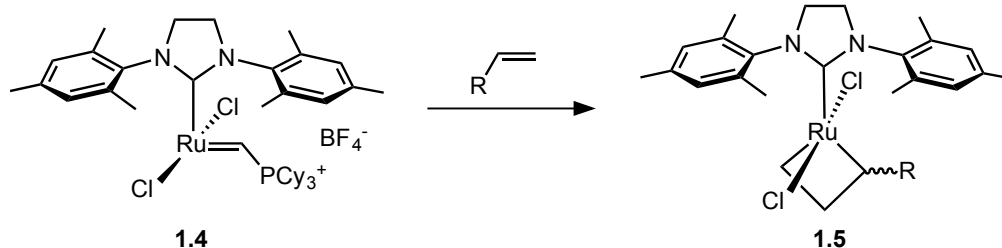


Figure 1.2. Possible orientations for metallacyclobutanes.

In the “bottom-bound” pathway, metallacycle formation takes place with an olefin bound trans to the L-type ligand (PCy_3 in **1.1**, NHC in **1.2** and **1.3**), leading to a metallacycle on the opposite face to the L-type ligand and the two X-type ligands trans to each other. In the alternative “side-bound” pathway, metallacycle formation takes place with an olefin bound cis to the L-type ligand and the resulting metallacycle is oriented in a perpendicular plane to the L-type ligand with the result that the two X-type ligands are cis to each other. Indirect experimental¹⁶⁻²⁰ and computational²¹⁻²³ investigations have provided evidence for both side-bound and bottom-bound pathways in the case of conventional metathesis catalysts such as **1.1-1.3**. The first direct evidence arose when 14-electron metathesis catalyst **1.4** was demonstrated to react with terminal olefins at low temperatures forming metallacycles, which could be studied using low-temperature NMR spectroscopy.²⁴⁻²⁸ These studies have supported the formation of bottom-bound metallacycles, in which the metallacycle lies coincident with the span of the NHC ligand (**1.5**), for NHC–Ru complexes, such as **1.2** and **1.3**, (**Scheme 1.4**).



Scheme 1.4. Formation of metallacyclobutanes from phosphonium alkylidene catalyst **1.4** at low temperature.

The substituents of the bottom-bound metallacycle can be in either a *syn* orientation, which leads to formation of the *Z*-olefin product, or in an *anti* orientation, which leads to formation of the *E*-olefin product (**Figure 1.3**). Steric repulsion between substituents in the *syn* metallacycle is believed to be responsible for the kinetic preference for formation of the *E*-olefin by catalysts such as **1.4** and **1.5**.¹³

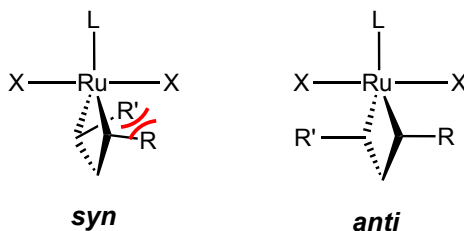


Figure 1.3. *Syn* and *anti* geometries of bottom-bound metallacycles.

Z-selective Ru-based Metathesis Catalysts

Our group has recently developed a series of cyclometallated Ru-based metathesis catalysts that show a kinetic preference for formation of *Z*-olefin products (**Figure 1.4**). **1.6** was the first Ru-based catalyst that demonstrated catalyst-driven *Z*-selectivity, which was discovered after a serendipitous C–H activation in the reaction of **1.3** with silver pivalate.²⁹ Replacement of the cyclometallated substituent by an *N*-adamantyl group resulted in catalyst **1.7**, which displayed both improved activity and *Z*-

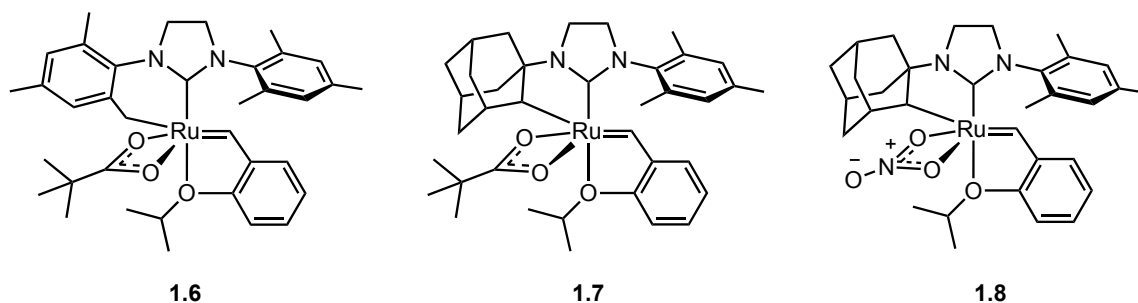


Figure 1.4. Cyclometallated Ru catalysts that are Z-selective in metathesis reactions.

selectivity.²⁹ Replacement of the remaining pivalate ligand by nitrate resulted in catalyst **1.8**, which demonstrated significant improvements in stability.³⁰ In contrast to previous Ru-based metathesis catalysts, catalysts **1.6–1.8** are believed to proceed via a side-bound pathway, in which the metallacycle lies under the N-aryl group of the catalyst (**Figure 1.5**).²⁹⁻³⁴ Steric repulsion between the metallacyclobutane substituent and the N-aryl group destabilizes the anti metallacycle geometry, with the result that the syn metallacycle geometry is preferred.

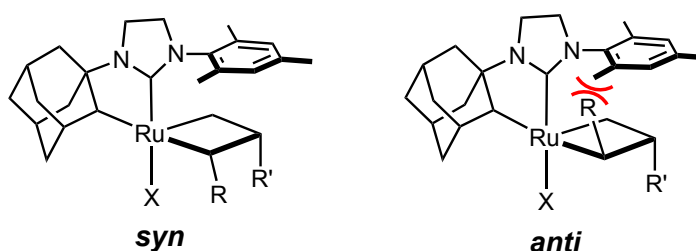


Figure 1.5. Model for Z-selectivity in cyclometallated Ru-based catalysts.

Thesis Research

While cyclometallated Ru-based complexes have demonstrated promising results in a number of metathesis reactions, their known scope of reactivity is rather limited in

comparison to more established catalysts, such as **1.1–1.3**. The primary focus of this thesis is to develop an improved understanding of the factors that govern reactivity and selectivity in the cyclometallated Z-selective catalysts. Chapter 2 focuses on the application of the cyclometallated catalysts in the Z-selective CM of allylic-substituted olefins. These more challenging substrates allow us to probe the boundaries of reactivity with the cyclometallated catalysts, providing insights into how the reactivity and Z-selectivity are influenced by the structure of both the catalyst and the substrate. Chapter 3 reports the development of a series of cyclometallated catalysts that systematically vary the steric and electronic nature of the N-aryl group. Studies of the reactivity of this catalyst series in a variety of CM applications have allowed further refinement of our understanding of the interplay between catalyst structure, activity and Z-selectivity. In addition, studies of an unusual C–H···F–C interaction observed in a number of these catalysts are described.

References

- (1) *Handbook of Metathesis*; Grubbs, R. H., Ed.; Wiley-VCH Verlag GmbH: Weinheim, Germany, 2003.
- (2) *Handbook of Metathesis*, 2nd ed.; Grubbs, R. H., Wenzel, A. G., O'Leary, D. J., Khosravi, E., Eds.; Wiley-VCH Verlag GmbH & Co. KGaA: Weinheim, Germany, 2015.
- (3) Hérisson, J.-L. P.; Chauvin, Y. *Makromol. Chem.* **1971**, *141* (1), 161.
- (4) Murdzek, J. S.; Schrock, R. R. *Organometallics* **1987**, *6* (6), 1373.
- (5) Schrock, R.; Rocklage, S.; Wengrovius, J.; Rupprecht, G.; Fellmann, J. *J. Mol. Catal.* **1980**, *8* (1-3), 73.
- (6) Chatterjee, A.; Choi, T.-L.; Sanders, D. P.; Grubbs, R. H. *J. Am. Chem. Soc.* **2003**, *125* (37), 11360.
- (7) Schrock, R. R. *Acc. Chem. Res.* **1990**, *23* (5), 158.

- (8) Schrock, R. R.; Murdzek, J. S.; Bazan, G. C.; Robbins, J.; Dimare, M.; O'Regan, M. *J. Am. Chem. Soc.* **1990**, *112* (10), 3875.
- (9) Schrock, R. R. *Tetrahedron* **1999**, *55* (27), 8141.
- (10) Schrock, R. R. *Chem. Rev.* **2009**, *109* (8), 3211.
- (11) Trnka, T. M.; Grubbs, R. H. *Acc. Chem. Res.* **2001**, *34* (1), 18.
- (12) Vougioukalakis, G. C.; Grubbs, R. H. *Chem. Rev.* **2010**, *110* (3), 1746.
- (13) Ritter, T.; Hejl, A.; Wenzel, A. G.; Funk, T. W.; Grubbs, R. H. *Organometallics* **2006**, *25* (24), 5740.
- (14) Dias, E. L.; Nguyen, S. T.; Grubbs, R. H. *J. Am. Chem. Soc.* **1997**, *119* (17), 3887.
- (15) Sanford, M. S.; Ulman, M.; Grubbs, R. H. *J. Am. Chem. Soc.* **2001**, *123* (4), 749.
- (16) Tallarico, J. A.; Bonitatebus, P. J.; Snapper, M. L. *J. Am. Chem. Soc.* **1997**, *119* (30), 7157.
- (17) Trnka, T. M.; Day, M. W.; Grubbs, R. H. *Organometallics* **2001**, *20* (18), 3845.
- (18) Anderson, D. R.; Hickstein, D. D.; O'Leary, D. J.; Grubbs, R. H. *J. Am. Chem. Soc.* **2006**, *128* (26), 8386.
- (19) Anderson, D. R.; O'Leary, D. J.; Grubbs, R. H. *Chem. Eur. J.* **2008**, *14* (25), 7536.
- (20) Stewart, I. C.; Benitez, D.; O'Leary, D. J.; Tkatchouk, E.; Day, M. W.; Goddard, W. A., III; Grubbs, R. H. *J. Am. Chem. Soc.* **2009**, *131* (5), 1931.
- (21) Cavallo, L. *J. Am. Chem. Soc.* **2002**, *124* (30), 8965.
- (22) Straub, B. F. *Angew. Chem. Int. Ed.* **2005**, *44* (37), 5974.
- (23) Adlhart, C.; Chen, P. *J. Am. Chem. Soc.* **2004**, *126* (11), 3496.
- (24) Romero, P. E.; Piers, W. E. *J. Am. Chem. Soc.* **2005**, *127* (14), 5032.
- (25) Romero, P. E.; Piers, W. E. *J. Am. Chem. Soc.* **2007**, *129* (6), 1698.
- (26) van der Eide, E. F.; Romero, P. E.; Piers, W. E. *J. Am. Chem. Soc.* **2008**, *130* (13), 4485.
- (27) Wenzel, A. G.; Blake, G.; VanderVelde, D. G.; Grubbs, R. H. *J. Am. Chem. Soc.* **2011**, *133* (16), 6429.
- (28) Wenzel, A. G.; Grubbs, R. H. *J. Am. Chem. Soc.* **2006**, *128* (50), 16048.
- (29) Endo, K.; Grubbs, R. H. *J. Am. Chem. Soc.* **2011**, *133* (22), 8525.
- (30) Keitz, B. K.; Endo, K.; Patel, P. R.; Herbert, M. B.; Grubbs, R. H. *J. Am. Chem. Soc.* **2012**, *134* (1), 693.
- (31) Liu, P.; Xu, X.; Dong, X.; Keitz, B. K.; Herbert, M. B.; Grubbs, R. H.; Houk, K. N. *J. Am. Chem. Soc.* **2012**, *134* (3), 1464.

- (32) Dang, Y.; Wang, Z.-X.; Wang, X. *Organometallics* **2012**, *31* (20), 7222.
- (33) Dang, Y.; Wang, Z.-X.; Wang, X. *Organometallics* **2012**, *31* (24), 8654.
- (34) Miyazaki, H.; Herbert, M. B.; Liu, P.; Dong, X.; Xu, X.; Keitz, B. K.; Ung, T.; Mkrtumyan, G.; Houk, K. N.; Grubbs, R. H. *J. Am. Chem. Soc.* **2013**, *135* (15), 5848.

Chapter 2

Z-selective Cross Metathesis of Allylic-substituted Olefins

Portions of this chapter are adapted/reproduced from:

Quigley, B. L.; Grubbs, R. H. *Chem. Sci.* **2014**, 5 (2), 501.

licensed under a

Creative Commons Attribution-Non-Commercial 3.0 Unported Licence.

Abstract

This chapter describes the application of cyclometallated Ru-based catalysts **2.1** and **2.2** in *Z*-selective cross metathesis of allylic-substituted olefins. The observed activity and selectivity of the catalysts are correlated with the catalyst structure by developing models for catalyst behavior. **2.2** was demonstrated to be an efficient catalyst for CM of acrolein acetals, providing a new synthetic route to *Z*- α,β -unsaturated acetals with excellent stereoselectivity (typically, >95% *Z*). The reaction conditions were compatible with a variety of acrolein acetals and terminal olefin cross partners, varying in functionality and steric profile. In addition, methods for the stereoretentive conversion of *Z*- α,β -unsaturated acetals to the corresponding aldehydes are also disclosed. The ability of catalyst **2.2** to carry out *Z*-selective CM of a wide variety of other allylic-substituted olefins was also explored. For a number of olefins that displayed poor reactivity with catalyst **2.2**, significantly improved reactivity was observed with more sterically accessible catalyst **2.1** under re-optimized conditions. Finally, the implications of the observed reactivity are discussed, allowing for extension of the “model for selectivity in CM” to the cyclometallated *Z*-selective catalysts.

Introduction

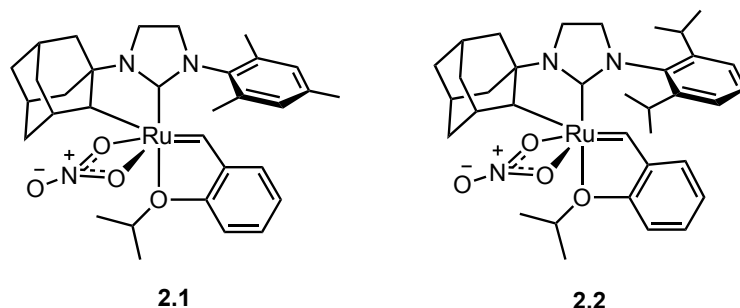


Figure 2.1. Cyclometallated Ru complexes commonly employed for Z-selective olefin metathesis.

Previous work in our group demonstrates the utility of the cyclometallated Ru-based metathesis catalysts, such as **2.1** and **2.2** (**Figure 2.1**), in a variety of Z-selective metathesis reactions, including CM¹⁻⁷, ethenolysis⁸ and macrocyclic RCM^{5,9,10}. These classes of reaction differ from ROMP^{11,12} and ROCM¹³⁻¹⁵ in that they lack the additional driving force from release of ring strain. Without the “spring-loaded” cyclic starting material, the other classes of reaction display a higher sensitivity to the steric environment of the starting olefin. In the case of CM reactions, the reactivity demonstrated to-date had been limited to relatively unhindered terminal and internal Z-olefins.¹⁻⁷ Allylic-substituted olefins were identified as an important substrate class to explore with the goal of augmenting the scope of reactivity of our Z-selective catalysts.

Olefins with allylic substitution have been explored as CM substrates with previous generations of Ru-based metathesis catalysts, including catalysts **2.3–2.5** (**Figure 2.2**).¹⁶⁻¹⁸ In these studies, two general trends were noted: allylic-substituted olefins are less reactive than unhindered olefins in CM applications and they tend to form cross products with improved selectivity for the E-olefin. This enhanced selectivity for

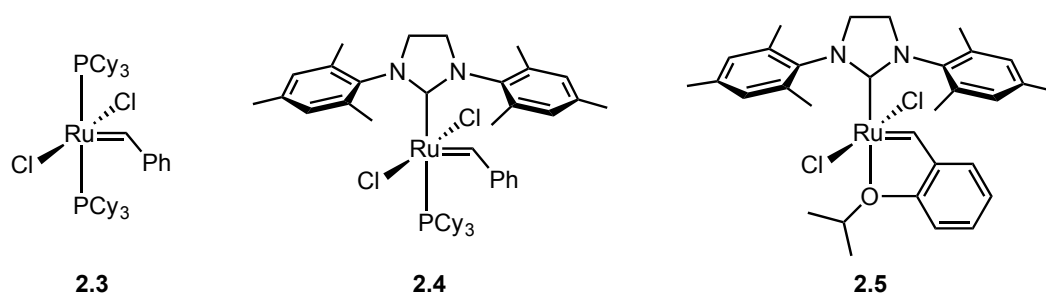


Figure 2.2. Commonly employed metathesis catalysts.

the E-olefin is attributed to increased steric repulsion between substituents in the syn metallacyclobutane, further disfavoring formation of the Z-olefin. In many cases, this allows the E-olefin to be generated with high stereoselectivity, lending the products to further synthetic applications where the olefin stereochemistry can be exploited. Access to the complementary Z-olefins *via* metathesis would provide a useful synthetic tool, extending the utility of these methods.

In the cyclometallated Z-selective catalysts, **2.1** and **2.2**, this increased steric clash between substituents in the syn metallacycle is expected to play a similar role. DFT calculations suggest that the rate-limiting step for product formation is either formation or collapse of the 1,2-disubstituted metallacyclobutane.¹⁹⁻²¹ The increased steric bulk of the alkene substituent is expected to result in a larger steric clash in the syn metallacyclobutane, and hence in the rate-limiting step, increasing the energy required to form the Z-olefin product (**Figure 2.3**).

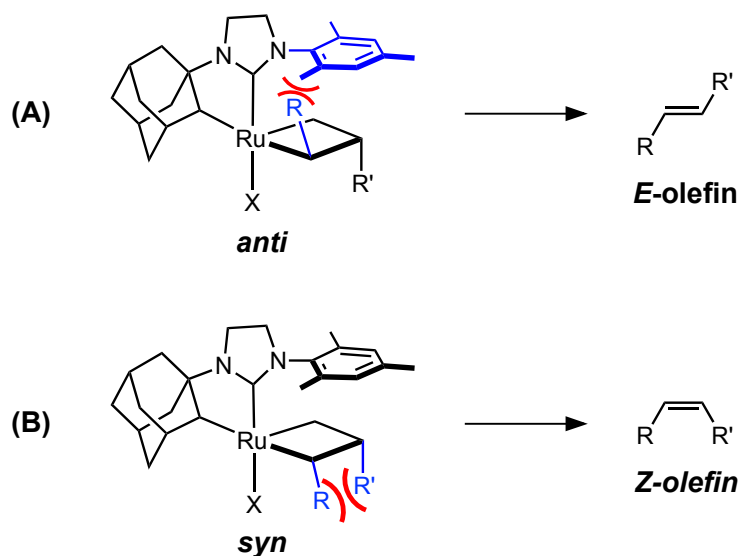
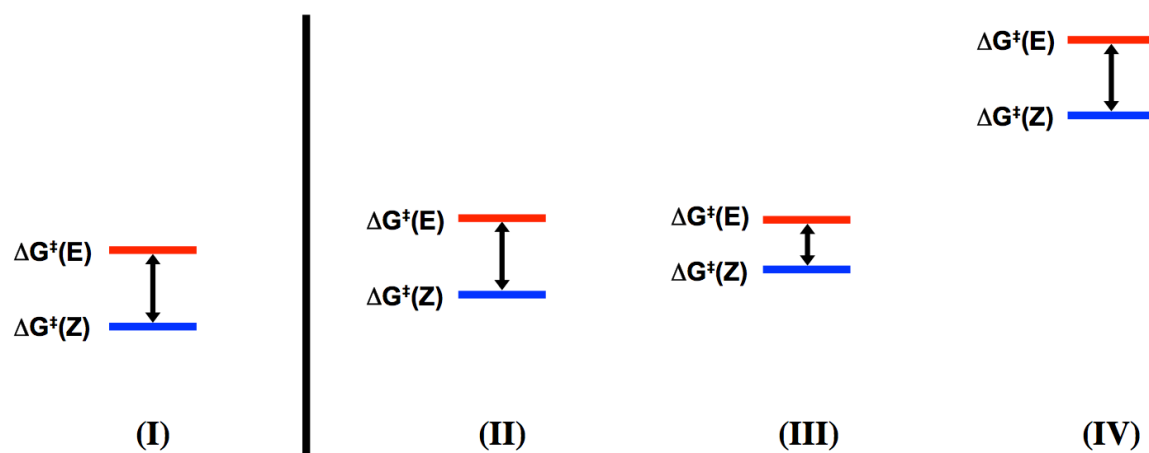


Figure 2.3. Key steric interactions governing *Z*-selectivity in CM reactions of allylic-substituted olefins. **A)** Negative steric interaction between metallacycle substituent and *N*-aryl group in *anti* metallacycle. **B)** Negative steric interaction between the two metallacycle substituents in the *syn* metallacycle. As *R'* increases in size, the steric clash in the *syn* metallacycle will become more significant, raising the energy of the pathway to form the *Z*-olefin.

Increased steric bulk of the metallacycle substituent(s) may also affect reactivity due to their interactions with other ligands on the catalyst. In the case of the *anti* metallacycle, this may result in a larger steric clash between the substituent and the *N*-aryl group. Additionally, there is the possibility for increased steric clashing with either the adamantyl group or the *X*-type ligand, which may play a role in destabilizing either or both of these competing pathways. **Figure 2.4** presents three possible scenarios for the expected reactivity of allylic-substituted olefins compared to non-allylic-substituted olefins, which arise from differences in how the increased steric bulk affects the energy of the pathways leading to the *E*-olefin and the *Z*-olefin.

Scenario (I) represents the case of CM of unhindered terminal olefins and Scenarios (II-IV) represent different possibilities for the reactivity of allylic-substituted olefins relative to Scenario (I). In Scenario (II), both pathways increase in energy by a similar but small amount, resulting in lowered reactivity but maintaining high Z-selectivity. In Scenario (III), the pathway leading to the Z-olefin increases in energy more than that of the E-olefin, with the result that the product will still be formed but with diminished Z-selectivity compared to the case of unhindered olefins. Scenario (IV) represents a third case where the increased steric clash is large, rendering both pathways leading to the Z-olefin and the E-olefin high in energy and largely inaccessible, leading to



	(II) vs. (I)	(III) vs. (I)	(IV) vs. (I)
$\Delta G^\ddagger(\text{Z})$	small increase	moderate increase	large increase
$\Delta G^\ddagger(\text{E}) - \Delta G^\ddagger(\text{Z})$	similar	reduced	similar
reactivity	good	good	poor
Z-selectivity	good	reduced	good

Figure 2.4. Key scenarios representing the expected spectrum of reactivity for allylic-substituted olefins compared to unhindered olefins, based on the differences in energy between the pathways for forming the E- and Z-olefin products.

minimal product formation.

A second consideration that may erode the initial Z-selectivity in allylic-substituted olefins is a difference in the propensity for the E- and Z-olefin products to undergo secondary metathesis. In the cyclometallated catalysts, secondary metathesis is believed to occur primarily *via* the “ethenolysis” pathway^{4,8}, which, being the reverse of the Z-selective forward CM reaction, will have a lower transition state for secondary metathesis of the Z-olefin product compared to the E-olefin product. In addition, increased steric bulk of alkene substituents is correlated with a larger energy difference in the stability of the E- and Z-olefin products.²² This typically results in the Z-olefin being higher in energy than the E-olefin and therefore more likely to undergo side-reactions, including secondary metathesis processes. As such, the Z-olefin product is both thermodynamically and kinetically more susceptible to secondary metathesis and, therefore, will be selectively consumed, leading to erosion of the Z-content of the product mixture if significant secondary metathesis occurs.

Z-selective Cross Metathesis of Acrolein Acetals

We selected acrolein acetals as the initial substrate class with which to begin cross metathesis studies of allylic-substituted olefins. Previous studies had demonstrated the viability of acrolein acetals as cross metathesis substrates with earlier generations of Ru metathesis catalysts, in particular, with catalyst **2.3**, which allowed the synthesis of cross products with high selectivity for the trans olefin product.^{17,23} However, Z-selective metathesis of acrolein acetals had yet to be demonstrated with either Ru-based catalysts or Mo/W-based catalysts prior to these studies.

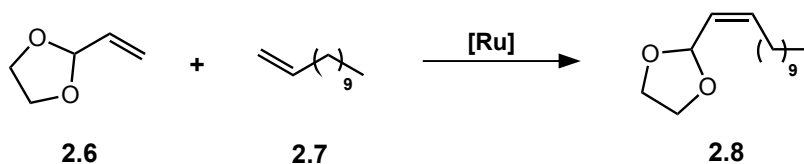
It was envisioned that the *Z*- α,β -unsaturated acetals formed from *Z*-selective CM of acrolein acetals would serve as useful precursors for the corresponding *Z*- α,β -unsaturated aldehydes, which are challenging to access via other methods. This would complement the *E*- α,β -unsaturated aldehydes that can be accessed either directly from CM of acrolein or from the corresponding acetals using catalysts **3.2–3.5**.^{17,18,23} *Z*- α,β -unsaturated aldehydes have significant interest for industry, due to their uses in fragrances^{24,25} and as semiochemicals for pest control applications.^{26,27} They are also formed as metabolites in various plants and animals and their detection has been used as a diagnostic for cancer and in food quality assays.²⁸⁻³¹ *Z*- α,β -unsaturated acetals and aldehydes also serve as useful synthetic intermediates, which have been exploited in the synthesis of a number of natural products.³²⁻³⁶ In addition, α,β -unsaturated acetals have been extensively explored as substrates for a number of base- and metal-promoted rearrangements.³⁷

Despite the significant interest in *Z*- α,β -unsaturated acetals and aldehydes, general, broad methods for their synthesis are rare. Reagents have been developed for the two-carbon homologation of aldehydes to the corresponding α,β -unsaturated compounds; however, achieving high *Z*-stereoselectivity is often challenging and unpredictable.³⁸⁻⁴³ This results in the employment of less efficient, multi-step methods. For example, the Still–Gennari modification of the Horner–Wadsworth–Emmons reaction affords the *Z*- α,β -unsaturated ester, which can then be reduced to the allylic alcohol and oxidized to afford the aldehyde.^{44,45} In an alternative strategy, α,β -alkynyl acetals can be accessed either by cross-coupling or alkylation and the desired product is then afforded after

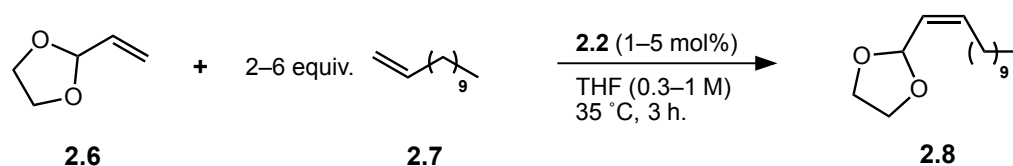
subsequent semi-hydrogenation (typically with Lindlar's catalyst) and deprotection.³⁷ Z-selective metathesis offers an attractive route to α,β -unsaturated acetals and aldehydes that avoids several shortcomings associated with the abovementioned strategies. Alternative methods require the use of strong bases, sensitive organometallic complexes or redox reagents, necessitating the use of protective groups in complex molecules. In contrast, Z-selective metathesis is a more direct method with generally good functional group tolerance, reducing the need for protecting groups. In addition, both starting materials are readily available/accessible: vinyl acetals can be efficiently prepared from acrolein⁴⁶ and cross partners can be sourced from the vast olefin chemical feedstock.

Optimization of Reaction Conditions

Initial studies began with 2-vinyl-1,3-dioxolane (**2.6**), which has been explored in CM applications with previous generations of Ru metathesis catalyst, allowing the generation of cross products with enhanced selectivity for the E-olefin (**Scheme 2.1**).²³ 1-Dodecene (**2.7**) was selected as a cross partner due to its low volatility and in order to avoid any possible effects due to the presence of other functional groups. Catalyst **2.2** was used, since it had demonstrated improved Z-selectivity over **2.1** in previous CM applications.^{5,6} Initial conditions, which employed 5 mol% **2.2** and 6 equivalents of 1-



Scheme 2.1. CM of 2-vinyl-1,3-dioxolane and 1-dodecene.

Table 2.1. Optimization of CM reaction between 2-vinyl-1,3-dioxolane and 1-dodecene.

Entry	2.2 (mol%)	Equiv. of 2.7	Conc. (M)	Yield (%) ^a	Z-selectivity (%) ^a
1	5	6	0.5	84	93
2	5	4	0.5	87	94
3	5	2	0.5	80	95
4	2	2	0.5	80	95
5	2	2	1.0	66	95
6	2	2	0.3	82	95
7	2	4	0.5	83	95
8	2	4	0.3	92	94
9	1	2	0.5	74	95

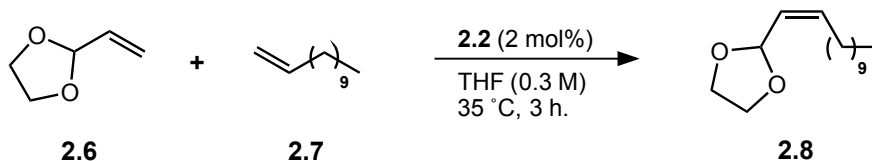
^a Yield and Z-selectivity determined by GC using tridecane as an internal standard; average of two experiments.

dodecene, were highly promising, yielding the desired cross product (**2.8**) in 84% yield and with 93% Z-selectivity at 3 h. (**Table 2.1, Entry 1**).

A number of reaction conditions were investigated in order to determine if reduced catalyst loading and/or reduced equivalents of 1-dodecene would be tolerated. The Z-selectivity was found to be largely independent of catalyst loading, excess of 1-dodecene or reaction concentration, giving a consistent value of 93–95% Z-selectivity across the various conditions investigated. This is suggestive that secondary metathesis of **2.8** is not occurring to a significant extent under these reactions conditions, the implications of which will be discussed further (*vide infra*). A similar yield was obtained

using a lower catalyst loading of 2 mol% **2.2** and 4 equivalents of 1-dodecene. Reducing the concentration of the reaction to 0.3 M in **2.6** led to an increase in yield, allowing the product to be generated in 92% yield and 94% Z-selectivity (**Entry 8**). We then employed these optimal conditions to investigate whether the reaction could also be carried out efficiently using the allylic-substituted olefin as the reagent in excess (**Table 2.2**). A comparable yield of the cross product (**2.8**) could be achieved using 4 equivalents of **2.6** and 1 equivalent of **2.7** and only a small reduction in Z-selectivity was noted (91% vs. 94%), although a longer reaction time of 7 h. was required. If only 2 equivalents of the olefin in excess were used, regardless of which olefin was used in excess, similar Z-selectivity was observed but with a reduction in yield of ~10%.

Table 2.2. Varying the olefin in excess in CM of 2-vinyl-1,3-dioxolane and 1-dodecene.



Entry	Equiv. of 2.6	Equiv. of 2.7	Yield ^a (%)	Z-selectivity ^a (%)
1	2	1	63 [84] ^b	93 [92] ^b
2	4	1	65 [94] ^b	91 [91] ^b
3	1	2	82	95
4	1	4	92	94

^a Yield and Z-selectivity determined by GC using tridecane as an internal standard; average of two experiments. ^b Value at 7 h. in square brackets.

Substrate Scope: Allylic-substituted Olefin

The substrate scope was then investigated on a preparative scale (~0.8–1.0 mmol), where it was found that increasing the reaction concentration to 0.5 M in the allylic-substituted olefin and extending reaction time to 5 h. led to conditions that were optimal for the range of substrates explored (**Table 2.3**). Under these conditions, cross product **2.8** was isolated in 82% yield and 96% Z-selectivity. The corresponding vinyl-1,3-dioxane (**2.9**) performed similarly, yielding cross product **2.14** in 79% yield and 96% Z-selectivity. Potentially bulkier vinyl acetals derived from hexylene glycol and pinacol (**2.10** and **2.11**, respectively) yielded products with marginally higher yield and Z-selectivity. In the case of a di(acrolein acetal) derived from pentaerythritol, **2.12**, the difunctionalized cross product **2.17** was obtained as a mixture of the Z,Z and E,Z diastereomers in an 89:11 ratio and 77% combined yield. This is consistent with the statistical outcome of two independent metathesis events occurring with ~94% Z-selectivity, as would be expected for the two distal alkenes. The two isomers of **2.17** could be separated by column chromatography on silica gel, allowing the Z,Z isomer to be isolated in 69% yield and >98% stereoselectivity. The reaction conditions were also found to be tolerant of acrolein diethyl acetal (**2.13**), which is known to be less stable than cyclic acetals.⁴⁷ The corresponding cross product, **2.18**, was obtained with high Z-selectivity (>98%) but a lower yield (70%) than that observed with the cyclic acetals. Overall, CM with 1-dodecene could be achieved for a wide variety of acrolein acetals, allowing the desired products to be isolated in 69–85% yield and with Z-selectivity of ≥96% in all cases.

Table 2.3. CM of various acrolein acetals with 1-dodecene.

Starting material	Product	Yield (%) ^a	Z-selectivity (%) ^b
		82	96
		79	96
		85	>98
		84	98
		77	89 (Z,Z)
		70	>98

^a Isolated yield. ^b Z-selectivity determined by ¹H-NMR spectroscopy.

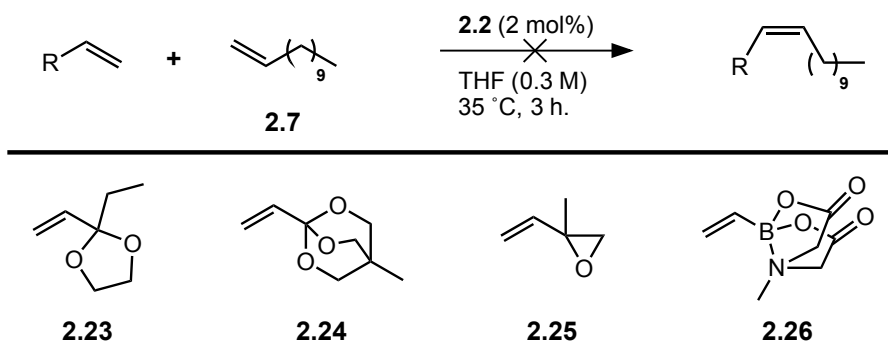
Having had promising results with vinyl acetals, our attention turned to related

Table 2.4. CM of vinyl pinacol boronate and 2-vinyloxirane with 1-dodecene.

Starting material	Product	Yield (%) ^a	Z-selectivity (%) ^b
 2.19	 2.21	81	92
 2.20	 2.22	40 ^c	>98

^a Isolated yield. ^b Z-selectivity determined by ¹H-NMR spectroscopy. ^c Z-selectivity determined by ¹H-NMR spectroscopy.

types of olefins with tertiary allylic carbons that are also of interest for their synthetic utility (**Table 2.4**). α,β -Unsaturated pinacol boronates are useful substrates in Suzuki cross-coupling reactions, where olefin geometry can be efficiently transferred to the cross-coupled products.⁴⁸⁻⁵⁰ Previous work has demonstrated that vinyl pinacol boronate (**2.19**) is a useful substrate for accessing E- α,β -unsaturated pinacol boronates using catalysts **3.3–3.5**.^{17,18,51} **2.19** was found to undergo CM efficiently with catalyst **2.2**, generating alkenyl boronate **2.21** in comparable yield (81%) to **2.8** and slightly reduced Z-selectivity (92%). This is complementary to a recent report by Schrock, Hoveyda and co-workers, where they used vinyl pinacol boronate as the reagent in excess.⁵² In addition, 2-vinyl oxirane was investigated as a substrate for Z-selective CM. While catalyst **2.3** failed yield the desired cross product for 2-vinyl oxirane (**2.20**), Z-selective



Scheme 2.2. Unreactive CM substrates with tertiary allylic substitution.

catalyst **2.2** was able to form the desired cross product, **2.22**, with excellent *Z*-selectivity but, though metathesis was carried out at room temperature in order to minimize loss of the volatile substrate, only a modest yield of **2.22** was obtained (40%).

Given the high yields observed in the case of acrolein acetals, we decided to investigate related substrates bearing quaternary allylic carbons, including ketal **2.23** and orthoester **2.24** (Scheme 2.2). In both cases, negligible formation of the desired cross product was observed. Similarly, 2-methyl-2-vinylloxirane **2.25** and vinyl MIDA boronate **2.26** led to only minimal conversion. For these reactions, lack of formation of homodimer from **2.7** (11-docosene) under the reaction conditions can be used as an indicator of catalyst sequestration or decomposition. If the hindered olefin is causing either of these effects, this is expected to impact formation of 11-docosene under the reaction conditions. Indeed, low conversion of 1-dodecene was noted with substrates **2.24** and **2.25**, which is suggestive of either catalyst sequestration or decomposition. In contrast, appreciable formation of 11-docosene occurred in CM reactions with **2.23** and **2.26**. This is consistent with an inherent low reactivity of the starting material limiting product formation (*cf.* Scenario (IV), Figure 2.4) and not catalyst decomposition or sequestration.

Substrate Scope: Cross Partner

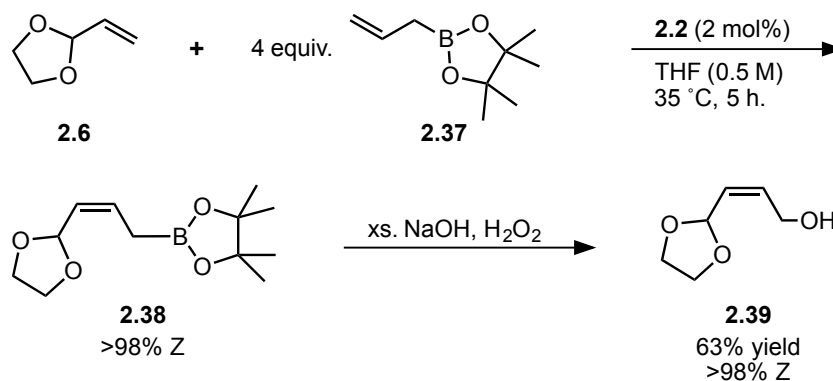
In order to investigate the compatibility of the reaction with various functional groups, a number of cross partners other than 1-dodecene were screened (**Table 2.5**).

Table 2.5. Varying the cross partner in CM of 2-vinyl-1,3-dioxolane.

Starting Material	Product	Yield (%) ^a	Z-selectivity (%) ^b
 2.7	 2.8	82	96
 2.28	 2.32	84	97
 2.29	 2.33	88	97
 2.30	 2.34	74 ^c	97
 2.31	 2.35	83	95

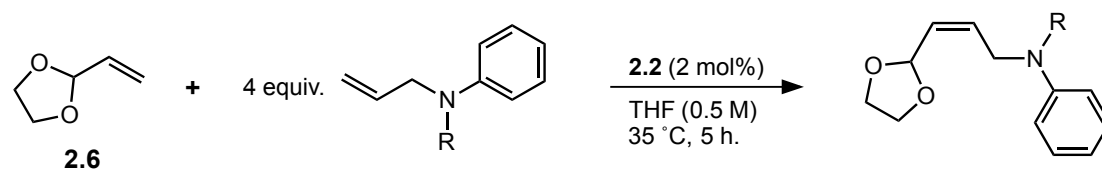
^a Isolated yield. ^b Z-selectivity determined by ¹H-NMR spectroscopy. ^c Reaction stopped at 3h.

Cross products were generated with similar yield and high Z-selectivity for methyl-10-undecenoate (**2.28**) and allylbenzene (**2.29**). In addition, a primary alcohol (**2.30**) and primary alkyl bromide (**2.31**) were both tolerated under the reaction conditions. Since a reaction time of 5 h. was found to result in a lower Z-selectivity of product **2.34**, reducing the reaction time to 3 h. allowed the product to be isolated in good yield and with excellent Z-selectivity. The anomalous degradation of Z-content has been observed in previous CM reactions with **2.30** and will be discussed further in **Chapter 3**. In addition, allyl pinacol boronate (**2.37**) was also tolerated as a cross partner, demonstrating excellent Z-selectivity (**Scheme 2.3**). Due to the instability of cross product **2.38** to purification, it was converted *in situ* to the corresponding Z-allylic alcohol (**2.39**) with excellent retention of stereochemistry and in good yield over the two steps.



Scheme 2.3. CM of allyl pinacol boronate with 2-vinyl-1,3-dioxolane and conversion to corresponding allylic alcohol.

N-allylaniline (**2.40**) was also investigated as a cross partner and, while cross product **2.43** was formed with high Z-selectivity, the yield was low (18%) (**Table 2.6**). Previously, *N*-allylaniline has been employed successfully as the limiting reagent in CM of unhindered olefins with catalyst **2.2**.⁶ Here, when **2.40** is used in excess in combination

Table 2.6. CM of 2-vinyl-1,3-dioxolane and *N*-allylaniline derivatives.

Starting material	Product	Yield (%) ^a	Z-selectivity (%) ^b
 2.40	 2.43	18	94
 2.41	 2.44	<5 ^c	–
 2.42	 2.45	72	89

^a Isolated yield. ^b Z-selectivity determined by ¹H-NMR spectroscopy. ^c Conversion, not yield, determined by ¹H-NMR spectroscopy.

with a less reactive olefin partner, coordination of the free amine to Ru may become a significant factor limiting reactivity. Protection of substrate **2.40** as the acetamide derivative resulted in an even less reactive substrate, **2.41**, with minimal conversion to cross product **2.44** noted. In this case, metathesis of the *N*-allyl acetamide onto Ru would produce a species that could form a potentially stable six-membered chelate by coordination of the O atom to Ru, thereby sequestering the catalyst (**Figure 2.5**). Consistent with this theory, low formation of 11-docosene (1-dodecene homodimer) was

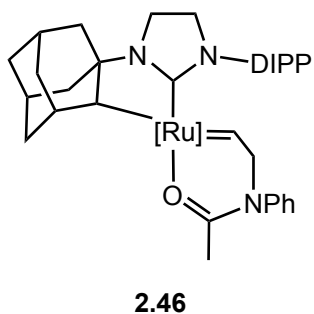
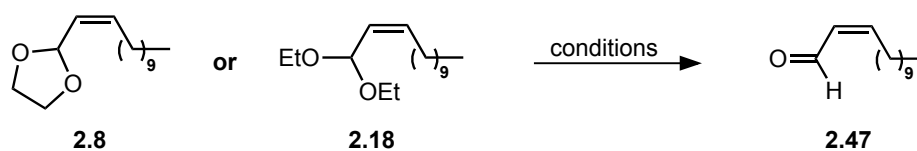


Figure 2.5. Proposed chelated catalyst species responsible for low activity.

noted under the reaction conditions. Reactivity was restored with the installation of an N-benzyl protecting group (**2.42**), allowing isolation of the cross product (**2.45**) in 72% yield. The *Z*-selectivity of the cross product was lower compared to the unprotected compound, **2.43**, (89% vs. 94%), presumably due to the increased steric bulk of **2.42** causing increased repulsion in the syn metallacycle.

Deprotection of *Z*- α,β -unsaturated Acetals

Much of the interest in formation of *Z*- α,β -unsaturated acetals is to use them as precursors to the corresponding *Z*- α,β -unsaturated aldehydes, which are useful substrates for a variety of further organic transformations. Methods for the clean deprotection of *Z*- α,β -unsaturated acetals without erosion of the olefin stereopurity, however, have been limited, due to the ease of isomerization from the *Z*-enal to *E*-enal.⁵³⁻⁵⁵ The use of oxalic acid adsorbed onto silica had previously been demonstrated for successful deprotection of *Z*-vinyl acetals and was found to offer a convenient method for deprotection of products **2.8** and **2.18** with retention of stereochemistry (**Table 2.7**).⁵⁶ The corresponding aldehyde, **2.47**, could be simply obtained in quantitative yield by filtration and

Table 2.7. Stereoretentive deprotection of Z- α,β -unsaturated acetals

Entry	Substrate	Reagent(s)	Yield (%) ^a	Z-selectivity (%) ^b	
				Initial	Final
1	2.8	SiO ₂ , oxalic acid ^c	quant.	>95	>95
2	2.8	LiBF ₄ ^d	95	>95	>95
3	2.18	SiO ₂ , oxalic acid ^c	quant.	>95	>95
4	2.18	LiBF ₄ ^d	92	>95	>95

^a Isolated yield. ^b Z-selectivity determined by ¹H-NMR spectroscopy. ^c SiO₂ 2.5 g/mmol with **2.8/2.18**; 5% aq. oxalic acid 10% w/w with SiO₂; DCM (0.05 M); r.t., 10 mins. ^d 1.3 eq. LiBF₄; 97:3 MeCN:H₂O (0.1 M); r.t. 10 mins.

concentration of the reaction mixture with complete stereoretention. LiBF₄ also could effect deprotection of the acetal in a 97:3 mixture of MeCN:H₂O with excellent stereoretention and afforded the desired aldehyde in high yield after work-up.⁵⁷ This offers a mild method for deprotection, which demonstrates good compatibility with functional groups that may be sensitive to Brønsted acid.^{57,58}

Cross Metathesis of Other Allylic-substituted Olefins

Our attention then turned to allylic-substituted hydrocarbon substrates. Here, we employed methyl-10-undecenoate (**2.28**) as the cross partner in order to facilitate separation of the product from the other olefins in the reaction mixture by column chromatography (**Table 2.8**). Vinyl cyclopentane (**2.48**) was found to undergo CM with good Z-selectivity (94%) but a significantly lower yield of the desired cross product, **2.17**, was obtained than in the case of the corresponding 5-membered cyclic acetal (44% vs. 82%). Vinyl cyclohexane (**2.49**) was also investigated as a CM substrate under identical conditions and only minimal cross product formation was noted (<5% conv.). This was unexpected given the relatively small variation in cross product yield between

Table 2.8. CM of allylic-substituted hydrocarbons with methyl-10-undecenoate.

Starting material	Product	Yield (%) ^a	Z-selectivity (%) ^b
 2.48	 2.51	44 ^a	94
 2.49	 2.52	<5 ^c	–
 2.50	 2.53	<5 ^c	–

^a Isolated yield. ^b Z-selectivity determined by ¹H-NMR spectroscopy. ^c Conversion (not yield) determined by ¹H-NMR spectroscopy

5- and 6-membered acrolein acetals (**2.8** and **2.14**). Low reactivity was also observed for the acyclic olefin, 3-methyl-1-hexene (**2.50**). This is suggestive that acrolein acetals may be privileged substrates for CM due an electronic factor, a difference in conformational preferences compared to the analogous hydrocarbons or both.

In addition, secondary allylic alcohol **2.54** was investigated as a substrate for *Z*-selective CM with catalyst **2.2** (Table 2.9). Under the standard conditions, minimal formation of cross product **2.58** was observed (<5%). Introduction of either a methyl- or

Table 2.9. CM of allylic-substituted secondary alcohols.

Starting Material	Product	Conversion (%) ^a
 2.54	 2.58	<5
 2.55	 2.59	<5
 2.56	 2.60	<5
 2.57	 2.61	<5

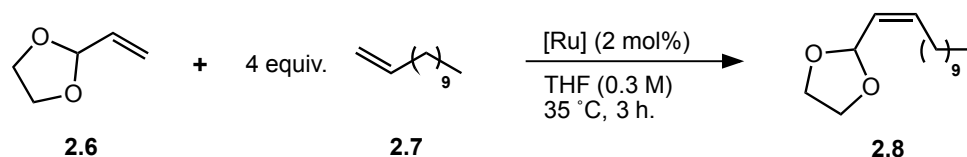
^a Conversion determined by GC and/or ¹H-NMR spectroscopy.

acetyl-protecting group (**2.55** and **2.56**) led to little improvement in CM under the same conditions. In the case of the acetyl-protected alcohol, which could potentially form a stable six-membered chelate similar to **2.46**, low formation of 1-dodecene homodimer was again noted. Poor reactivity was also observed in the case of the corresponding secondary allylic chloride (**2.57**).

Differences in Reactivity and Selectivity between Catalysts

In all of the Z-selective CM reactions discussed thus far, catalyst **2.2** has been used due to its higher Z-selectivity compared to **2.1** in CM of unhindered terminal olefins.^{5,6,59} According to our working model, the improved selectivity results from increased steric repulsion between the bulkier N-aryl group of **2.2** and the metallacycle substituents, which increases the energy of the anti metallacycle. In the case of CM of

Table 2.10. Comparison of catalysts in CM of 3-vinyl-1,2-dioxolane and 1-dodecene.



Entry	Catalyst	Yield (%) ^a	Z-selectivity (%) ^a
1	2.1	87	76
2	2.2	92	94
3	2.3	96	10
4	2.5	92	5

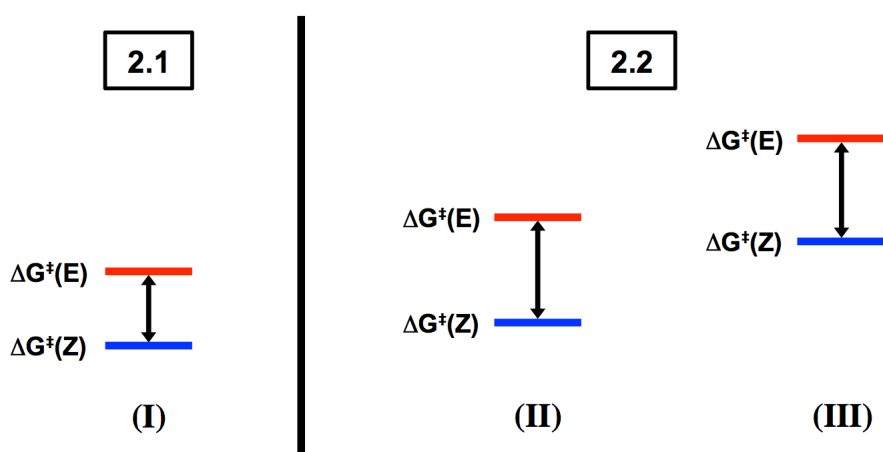
^a Yield and Z-selectivity determined by GC using tridecane as an internal standard; average of two experiments.

unhindered terminal olefins, both **2.1** and **2.2** display relatively high Z-selectivity at low conversion, with the difference typically being on the order of a few percent.

Z-selective catalyst **2.1** and catalysts **2.3** and **2.5** were compared to catalyst **2.2** in CM of **2.6** and **2.7** under identical conditions in order to examine how allylic substitution affects the Z-selectivity of the catalysts (**Table 2.10**). Here, the difference in Z-selectivity between **2.1** and **2.2** is considerably more pronounced than in previous examples with catalyst **2.1** forming cross product **2.8** with 76% Z-selectivity compared to the 94% achieved by **2.2**. Both Z-selective catalysts demonstrate high yields of cross product **2.8**, with **2.2** giving a marginally higher yield. Catalysts **2.3** and **2.5** complement the Z-selective catalysts, yielding **2.8** with 90% and 95% selectivity for the E-isomer. This allows both E- and Z-acrolein acetals to be accessed with excellent stereoselectivity and in high yield using Ru metathesis catalysts.

While both catalysts **2.1** and **2.2** were found to be efficient for CM of **2.6**, there were several examples of substrates for which **2.2** demonstrated extremely low activity. The difference in Z-selectivity between catalyst **2.1** and **2.2** is consistent with a more significant energy difference between the rate-limiting steps for formation of Z- and E-olefin products in **2.2** (larger $\Delta G^\ddagger(\text{E}) - \Delta G^\ddagger(\text{Z})$ in the case of **2.2**). This follows directly from the larger steric profile of the N-aryl group increasing $\Delta G^\ddagger(\text{E})$ due to increased steric clash in the anti metallacyclobutane. It is less obvious, however, how the N-aryl group significantly influences the energy required for formation of the Z-olefin, $\Delta G^\ddagger(\text{Z})$, since the substituents of the syn metallacyclobutane are pointed away from the N-aryl group. Two scenarios can be envisaged, which represent two extremes of reactivity

(Figure 2.6). If the N-aryl group has little effect on the Z-olefin pathway ($\Delta G^\ddagger(\text{Z})$ is similar for **2.1** and **2.2**), then there may be little chance of improved reactivity by employing catalyst **2.1** in place of **2.2** (Scenario (II)). If, however, $\Delta G^\ddagger(\text{Z})$ is significantly higher in energy for **2.2** than for the less bulky catalyst, **2.1** (Scenario (III)), then improved reactivity may be obtained by employing **2.1**. The exact energy differences between the two catalysts are expected to vary from substrate to substrate with differences in the bulk of the allylic substituent, which suggests that any improvements in reactivity may be specific to a given substrate class.



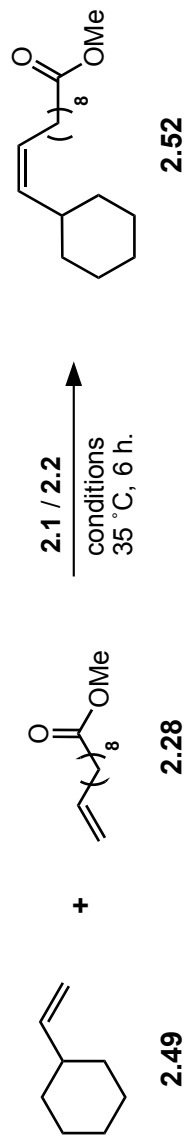
	(I) vs. (II)	(I) vs. (III)
$\Delta G^\ddagger(\text{E}) - \Delta G^\ddagger(\text{Z})$	larger	larger
$\Delta G^\ddagger(\text{Z})$	similar / small increase	significant increase
reactivity	slightly lower	significantly lower
Z-selectivity	good	good

Figure 2.6. Key scenarios representing reactivity for allylic-substituted olefins with catalyst **2.2** compared to catalyst **2.1**, based on the differences in energy between the pathways for forming the E- and Z-olefin products.

cross products were also noted for protected secondary allylic alcohols (**2.59** and **2.60**).

We then attempted to re-optimize conditions for the CM reaction using catalyst **2.1** in order to improve the yield for these more challenging substrates that performed poorly under the previous conditions. CM of vinyl cyclohexane (**2.49**) and methyl-10-undecenoate (**2.28**) was selected as the model reaction for optimization, using the previous best conditions in CM of acrolein acetals as the starting point (**Table 2.12**, Entry 1). Increasing the excess of methyl-10-undecenoate to 6 equivalents or the catalyst loading from 2 mol% to 5 mol% did not result in a significant improvement in the yield for catalyst **2.2** (Entries 2–3). Unlike in the previous optimization, employing an excess of the allylic-substituted olefin (**2.49**) led to significantly improved yields of **2.52**. A substantial increase in yield was obtained when doubling the equivalents of **2.49** from 2 to 4, with a smaller increase on further increasing the equivalents to 6 (Entries 5–7). Decreasing the overall concentration of the reaction led to a further increase in yield, reaching 40% (Entry 9). Subsequently, replacing THF with diglyme, an ethereal solvent with a higher boiling point, further improved the yield of the desired cross product to 50% (Entry 11). Under identical conditions, **2.2** generated only 16% yield of **2.52** but with 93% Z-selectivity, which supports the proposed difference in energy for the Z-olefin pathway in the two catalysts (**Figure 2.6**). The new conditions represent a *ca.* five-fold increase in yield when compared to the former conditions. Similar to the previously optimized reaction, the Z-selectivity observed for the cross product was largely unchanged across the various reaction conditions screened, giving a relatively consistent value of 73–75%. This is consistent with low levels of secondary metathesis occurring across these reaction conditions.

Table 2.12. Optimization of CM between vinyl cyclohexane and methyl-10-undecenoate.



Entry	Equiv. of 2.49	Equiv. of 2.28	Cat., (mol%)	Solvent	Conc. (M)	Yield (%) ^a	Z-sel. (%) ^a
1	1	4	2.2 (2)	THF	0.5	3	94
2	1	6	2.2 (5)	THF	0.5	4	90
3	1	6	2.1 (5)	THF	0.4	13	73
4	1	4	2.1 (5)	THF	0.45	12	73
5	2	1	2.1 (5)	THF	0.5	19	75
6	4	1	2.1 (5)	THF	0.5	26	75
7	6	1	2.1 (5)	THF	0.45	28	75
8	1	4	2.1 (5)	THF	0.22	18	73
9	6	1	2.1 (5)	THF	0.22	40	74
10	6	1	2.1 (2)	THF	0.22	30	75
11	6	1	2.1 (5)	diglyme	0.22	50	74
12	6	1	2.2 (5)	diglyme	0.22	16	93

^a Yield and Z-selectivity determined by GC using tridecane as an internal standard.

We then wanted to determine if these new conditions would lead to a similar increase in yield for other substrates that demonstrated low reactivity under previous conditions (**Table 2.13**). 4-vinyl-cyclohex-1-ene was also found to be a viable substrate, with 38% conversion and 78% Z-selectivity to cross product **2.64** achieved at 6 h. Under these reaction conditions, dihydromyrcenol (**2.63**) was found to undergo CM with 44% conversion and 82% Z-selectivity.

Table 2.13. CM of allylic-substituted hydrocarbons with methyl-10-undecenoate using catalyst **2.1**.

Starting Material	Product	Conversion (%) ^a	Z-selectivity (%) ^b
 2.49	 2.52	50 ^c	74
 2.62	 2.64	38	78
 2.63	 2.65	44	80

^a Conversion determined by GC using tridecane as an internal standard using $[\text{Cross product}] = [2.28]_{\text{initial}} - [2.28]_t - [2.28 \text{ homodimer}]_t$; ^b Z-selectivity determined by GC; ^c Yield of product determined by GC using tridecane as an internal standard.

In addition, several protected secondary allylic alcohols were examined under the new conditions (**Table 2.14**). For CM of 3-methoxy-1-octene (**2.55**), an improved conversion of 33% and 86% Z-selectivity was observed. However, in the case of the corresponding acetoxy-protected alcohol (**2.56**), no significant improvement was observed, with only 11% conversion to the desired cross product noted at 6 h. **2.56** can potentially form a stable 6-membered chelating alkylidene similar to that proposed for *N*-acetyl-*N*-allylaniline **2.41**. The corresponding benzyl-protected compound (**2.67**) performed similarly to the methyl-protected compounds under the new reaction conditions with marginally higher yield and slightly lower Z-selectivity.

Table 2.14. CM of protected secondary allylic alcohols with 1-dodecene using catalyst **2.1**.

Starting Material	Product	Conversion (%) ^a	Z-selectivity (%) ^b
 2.55	 2.59	33	86
 2.56	 2.60	11	84
 2.67	 2.68	36	84

^a Conversion determined by GC using tridecane as an internal standard using $[\text{Cross product}] = \frac{[\mathbf{2.7}]_{\text{initial}} - [\mathbf{2.7}]_t - [\mathbf{2.7} \text{ homodimer}]_t}{[\mathbf{2.7}]_{\text{initial}}}$ ^b Z-selectivity determined by GC ^c

Conclusions

The application of cyclometallated Ru-based catalysts in the Z-selective CM of allylic-substituted olefins was explored. CM of acrolein acetals by catalyst **2.2** provided a new synthetic method to access Z- α,β -unsaturated acetals and aldehydes with high stereoselectivity. While catalyst **2.2** demonstrated efficient CM for a wide variety of acrolein acetals, in addition to a number of other substrates, it demonstrated low reactivity for CM of other types of allylic-substituted olefins. Notably, **2.2** either catalyzed formation of the cross product with high Z-selectivity or it demonstrated low reactivity. This is consistent with the pathway for formation of the E-olefin not being low enough in energy to be accessible, even in the case of bulky allylic-substituted olefins. The reduced steric bulk of the N-aryl group in catalyst **2.1** allowed for improved CM reactivity in a number of cases where catalyst **2.2** performed poorly. Here, a lower difference in energy between the pathways for formation of the Z-olefin and the E-olefin allows formation of the E-olefin to become competitive, resulting in reduced Z-selectivity compared to that observed in CM of unhindered olefins. The relationship between the steric bulk of the N-aryl group and selectivity and activity in CM of allylic-substituted olefins is probed more extensively in **Chapter 3**, using seven additional catalysts that vary in the N-aryl group

The trends in the reactivity of allylic-substituted olefins allow us to extend the previous model for selectivity in CM to include the cyclometallated Z-selective catalysts (**Table 2.15**). This model provides a framework for determining whether CM can be rendered selective for formation of the desired cross product over the homodimers of the two starting materials. By choosing olefins of different “Type”, selectivity beyond that

Table 2.15 Model for selectivity in CM, expanded to include cyclometallated Z-selective metathesis catalysts. Adapted with permission from Chatterjee, A. K.; Choi, T.-L.; Sanders, D. P.; Grubbs, R. H. *J. Am. Chem. Soc.* **2003**, *125*, 11360. © 2003 American Chemical Society.

Catalyst	2.3	2.4	2.2
Type I (fast homodimerization)	<ul style="list-style-type: none"> terminal olefins allyl silanes 1° allylic alcohols 1° allylic ethers 1° allylic esters allyl boronates allyl halides 	<ul style="list-style-type: none"> terminal olefins 1° allylic alcohols 1° allylic esters allyl boronates allyl halides styrenes (no large ortho sub.) 	<ul style="list-style-type: none"> allyl phosphonates allyl silanes allyl phosphine oxides allyl sulfides protected allyl amines
Type II (slow homodimerization)	<ul style="list-style-type: none"> styrene 2° allylic alcohols vinyl dioxolanes vinyl boronates vinyl cyclopentane 	<ul style="list-style-type: none"> styrenes (large ortho sub.) acrylates / acrylic acid acrylamides acrolein vinyl ketones 	<ul style="list-style-type: none"> unprotected 3° allylic alcohols 2° allylic alcohols vinyl epoxides perfluoro-alkane olefins
Type III (no homodimerization)	<ul style="list-style-type: none"> vinyl siloxanes 	<ul style="list-style-type: none"> 1,1-disub. olefins non-bulky trisub. olefins vinyl phosphonates 	<ul style="list-style-type: none"> phenyl vinyl sulfone 4° allylic C olefins protected 3° allylic amines
Type IV (spectators to CM)	<ul style="list-style-type: none"> 1,1-disub. olefins disub. α,β-unsaturated carbonyls 4° allylic C olefins perfluoro-alkane olefins protected 3° allylic amines 	<ul style="list-style-type: none"> vinyl nitro olefins trisubstituted allyl alcohols, protected 	<ul style="list-style-type: none"> 1,1-disub. olefins 4° allylic C olefins

expected statistically can be achieved, which facilitates application of CM in synthetic applications. The model also allows us to directly compare the scope of reactivity of the Z-selective catalysts with conventional Ru-based metathesis catalysts. Interestingly, the reactivity of the Z-selective catalysts closely parallels that observed for catalyst **2.3** and is significantly lower than that of **2.4**.

Overall, the Z-selective CM of allylic-substituted olefins by catalysts **2.1** and **2.2** has allowed access to several classes of Z-olefins that are challenging to access *via* other methods. In addition, it has identified several areas where continued development of improved Z-selective catalysts would be beneficial.

Experimental Details

Materials and Methods

Unless otherwise stated, solvents and reagents were of reagent quality, obtained from commercial sources and used without further purification. Reactions involving catalysts **2.1–2.5** were carried out in a nitrogen-filled glovebox. Unless otherwise described, liquid substrates for cross metathesis were degassed by sparging with Ar and were filtered through a short plug of basic alumina prior to use. 2-vinyloxirane was degassed by sparging with Ar prior to use. Dihydromyrcenol and 8-octen-3-ol were distilled and degassed by sparging with Ar prior to use. THF was purified by passage through solvent purification columns and degassed prior to use.⁶⁰ Anhydrous diglyme was sparged with Ar, stored over 4 Å molecular sieves and filtered over basic alumina prior to use. DCM and CDCl₃ used for the analysis of CM reactions involving acetals were filtered through a plug of basic alumina prior to use. Flash chromatography was carried out with silica gel 60 (230-400 mesh). 2-vinyl-1,3-dioxane, 4,4,6-trimethyl-2-vinyl-1,3-dioxane, and 4,4,5,5-tetramethyl-2-vinyl-1,3-dioxolane⁶¹ were all prepared according to a previously reported procedure.⁶² *N*-allyl-*N*-benzylaniline was prepared as previously described.⁶³

Gas chromatography data was obtained using an Agilent 6850 FID gas chromatograph equipped with a HP-5 (5%-phenyl)-methylpolysiloxane capillary column (Agilent). High-resolution mass spectroscopy was completed at the California Institute of Technology Mass Spectrometry Facility. NMR spectra were recorded on a Varian Inova 400 (400 MHz for ¹H, 128 MHz for ¹¹B, 101 MHz for ¹³C), automated Varian Inova 500 (500 MHz for ¹H, 126 MHz for ¹³C), or Varian Inova 600 (500 MHz for ¹H, 151 MHz for

¹³C). ¹H and ¹³C chemical shifts are expressed in ppm downfield from tetramethylsilane using the residual protiated solvent as an internal standard (CDCl₃ ¹H: 7.26 ppm and ¹³C: 77.2 ppm; DMSO-*d*⁶ ¹H: 2.50 ppm and ¹³C: 39.5 ppm). ¹¹B chemical shifts are expressed in ppm downfield from BF₃·OEt₂ using the deuterium signal of the solvent as an internal standard.

Screening-scale Reactions

Typical procedure: CM of 2-vinyl-1,3-dioxolane and 1-dodecene

In a nitrogen-filled glovebox, 2-vinyl-1,3-dioxolane (16 μL, 0.016 mmol, 1 equiv.) and 1-dodecene (430 μL, 0.064 mmol, 4 equiv.) were combined in a 4 mL vial, to which tridecane (20 μL) was added as an internal standard. A solution of **2.2** (2.1 mg, 0.003 mmol, 2 mol%) in the required amount of THF was added. The reaction was stirred open to the atmosphere at 35 °C.

Samples for GC analysis were obtained by taking a 5 μL reaction aliquot and diluting to 1 mL with a 10% v/v solution of ethyl vinyl ether in DCM. Samples were shaken vigorously and allowed to stand for 10 minutes before GC analysis. All reactions were carried out in duplicate.

GC response factors were obtained for all starting materials and products using tridecane as an internal standard. Data was analyzed as previously described.⁶⁴

Instrument conditions: inlet temperature: 250 °C, detector temperature 300 °C, H₂ flow: 30 mL/min, air flow: 400 mL/min, makeup flow: 30 mL/min.

GC method: 80 °C for 1.5 minutes, followed by a temperature increase of 40 °C/min to 230 °C and held at that temperature for 2 minutes, then a temperature increase of 5 °C/min to 245 °C, and finally a temperature increase of 40 °C/min to 300 °C and held at that temperature for 2.5 minutes. Total run time: 14.1 minutes.

Compound	Response Factor	Retention Time (min)
tridecane	-	4.43
2-vinyl-1,3-dioxane	4.00	2.23
1-dodecene	1.10	4.88
(<i>Z</i>)-2-(dodec-1-en-1-yl)-1,3-dioxolane	1.07	6.74
(<i>E</i>)-2-(dodec-1-en-1-yl)-1,3-dioxolane	1.39	6.82
(<i>Z</i>)-11-docosene	0.56	9.34
(<i>E</i>)-11-docosene	0.56	9.38

Typical procedure: CM of vinylcyclohexane and methyl 10-undecenoate

In a nitrogen-filled glovebox, vinylcyclohexane (73 μ L, 0.53 mmol, 6 equiv.) and methyl 10-undecenoate (20 μ L, 0.09 mmol, 1 equiv.) were combined in a 4 mL vial, to which tridecane (10 μ L) was added as an internal standard. A solution of the appropriate catalyst (4.4 mmol, 5 mol%) in diglyme (300 μ L) was added and the reaction was stirred open to the atmosphere at 35 °C.

Samples for GC analysis were obtained by taking a 5 μ L reaction aliquot and diluting to 1 mL with a 10% v/v solution of ethyl vinyl ether in DCM. Samples were shaken vigorously and allowed to stand for 10 minutes before GC analysis.

GC response factors were obtained for all starting materials and products using tridecane as an internal standard. Data was analyzed as previously described.⁶⁴

Instrument conditions: inlet temperature: 250 °C, detector temperature 300 °C, H₂ flow: 30 mL/min, air flow: 400 mL/min, makeup flow: 30 mL/min.

GC method: 80 °C for 2 minutes, followed by a temperature increase of 30 °C/min to 250 °C and held at that temperature for 3 minutes, then a temperature increase of 5 °C/min to 270 °C, and finally a temperature increase of 30 °C/min to 300 °C and held at that temperature for 3 minutes. Total run time: 18.7 minutes.

Compound	Response Factor	Retention Time (min)
tridecane	-	5.86
vinylcyclohexane	1.71	2.27
methyl-10-undecenoate	1.24	6.44
Methyl (<i>Z</i>)-11-cyclohexylundec-10-enoate	0.79	9.21
methyl (<i>E</i>)-11-cyclohexylundec-10-enoate	0.79	9.36
dimethyl (<i>Z</i>)-icos-10-enedioate	0.71	13.90
dimethyl (<i>E</i>)-icos-10-enedioate	0.71	13.97

General Procedures

General Procedure 1: CM of allylic-substituted olefins and 1-dodecene

In a nitrogen-filled glovebox, the allyl-substituted olefin (0.8 mmol, 1 equiv.) and 1-dodecene (710 mL, 3.2 mmol, 4 equiv.) were combined in a 20 mL vial, to which tridecane (50 mL) was added as an internal standard. A solution of **2.2** (10.8 mg, 0.016 mmol, 2 mol%) in THF (700 mL) was added and the concentration of allyl-substituted

olefin adjusted to 0.5 M using THF. The reaction was stirred open to the atmosphere at 35 °C for 5 hours, at which time it was removed from the glovebox. The reaction mixture was quenched by addition of ethyl vinyl ether (200 mL) and subjected to silica gel chromatography.

General Procedure 2: CM of 2-vinyl-1,3-dioxolane with terminal olefins

In a nitrogen-filled glovebox, 2-vinyl-1,3-dioxolane (80 mL, 0.8 mmol, 1 equiv.) and terminal olefin (3.2 mmol, 4 equiv.) were combined in a 20 mL vial, to which tridecane (50 mL) was added as an internal standard. A solution of **2.2** (10.8 mg, 0.016 mmol, 2 mol%) in THF (700 mL) was added and the concentration of allyl-substituted olefin adjusted to 0.5 M using THF. The reaction was stirred open to the atmosphere at 35 °C for 5 hours, at which time it was removed from the glovebox. The reaction mixture was quenched by addition of ethyl vinyl ether (200 mL) and subjected to silica gel chromatography.

General Procedure 3: Deprotection of acetals with SiO₂/oxalic acid

SiO₂ (2.5 g/mmol with respect to acetal), 5% aq. oxalic acid (10% w/w with SiO₂) and DCM (1.1 mL) were stirred at 20 °C for 5 minutes. To this suspension, a solution of Z- α,β -unsaturated acetal (0.13 mmol) in DCM (1.1 mL) was added and the mixture was allowed to stir for a further 10 minutes. The suspension was then filtered through a SiO₂ plug and concentrated to yield the corresponding aldehyde.

General Procedure 4: Deprotection of acetals with LiBF₄

To *Z*- α,β -unsaturated acetal (0.13 mmol, 1 equiv.) in 97:3 MeCN:H₂O (1.25 mL), was added LiBF₄ (0.16 mmol, 1.3 equiv.) and the resultant solution was stirred at 20 °C for 10 minutes. Upon completion, Et₂O (8 mL), sat. aq. NaHCO₃ (6 mL) and H₂O (2 mL) were added to the reaction mixture. The organic layer was separated and the aqueous layer was back extracted with Et₂O (3 x 8 mL). The combined organic layers were washed with brine (5 mL, adjusted to pH 8 with NaHCO₃) and concentrated. The resultant residue was dissolved in DCM, dried over Na₂SO₄, and concentrated to yield the corresponding aldehyde.

Experimental Data**(*Z*)-2-(dodec-1-en-1-yl)-1,3-dioxolane (2.8)**

2-Vinyl-1,3-dioxolane (100 mg, 1.0 mmol) and 1-dodecene (670 mg, 4.0 mmol) were reacted according to general procedure 1. After purification by silica gel chromatography (pentane, then 92:8 pentane:Et₂O), product **2.8** was obtained as a clear, colorless oil (82% yield, 200 mg, 96% *Z*).

¹H NMR (400 MHz, CDCl₃) δ 5.77 (dt, *J* = 11.0, 7.7 Hz, 1H), 5.54 (d, *J* = 7.3 Hz, 1H), 5.42 (dd, *J* = 11.0, 7.3 Hz, 1H), 4.07 – 3.83 (m, 4H), 2.17 (q, *J* = 7.7 Hz, 2H), 1.47 – 1.15 (m, 16H), 0.88 (t, *J* = 6.8 Hz, 3H) ppm.

¹³C NMR (101 MHz, CDCl₃) δ 138.0, 125.8, 99.4, 65.1, 32.1, 29.9, 29.8, 29.7, 29.7, 29.6, 29.5, 29.3, 28.0, 22.8 ppm.

HRMS (FAB) calcd. for C₁₅H₂₉O₂ [M+H]⁺ 241.2168; found 241.2168.

(Z)-2-(dodec-1-en-1-yl)-1,3-dioxane (2.14)

2-Vinyl-1,3-dioxane (91 mg, 0.80 mmol) and 1-dodecene (540 mg, 3.2 mmol) were reacted according to general procedure 1. After purification by silica gel chromatography (pentane, then 90:10 pentane:Et₂O), product **2.14** was obtained as a pale yellow oil (79% yield, 160 mg, 96% Z).

¹H NMR (600 MHz, CDCl₃) δ 5.63 (dt, *J* = 11.1, 7.5 Hz, 1H), 5.43 (dd, *J* = 11.1, 6.4 Hz, 1H), 5.23 (d, *J* = 6.5 Hz, 1H), 4.13 (dd, *J* = 10.7, 5.0 Hz, 2H), 3.84 (td, *J* = 12.3, 2.5 Hz, 2H), 2.22 – 2.03 (m, 3H), 1.45 – 1.19 (m, 17H), 0.88 (t, *J* = 7.0 Hz, 3H) ppm.

¹³C NMR (101 MHz, CDCl₃) δ 135.9, 126.9, 98.1, 67.0, 32.0, 29.8, 29.7, 29.6, 29.5, 29.5, 29.3, 28.3, 25.8, 22.8, 14.2 ppm.

HRMS (FAB) calcd. for C₁₆H₃₁O₂ [M+H]⁺ 255.2324; found 255.2318.

(Z)-2-(dodec-1-en-1-yl)-4,4,6-trimethyl-1,3-dioxane (2.15)

4,4,6-Trimethyl-2-vinyl-1,3-dioxane (130 mg, 0.80 mmol) and 1-dodecene (540 mg, 3.2 mmol) were reacted according to general procedure 1. After purification by silica gel chromatography (pentane, then 92:8 pentane:Et₂O), product **2.15** was obtained as a clear, colorless oil (84% yield, 180 mg, >98% Z).

¹H NMR (600 MHz, CDCl₃) δ 5.62 (dt, *J* = 10.8, 7.5 Hz, 1H), 5.49 (d, *J* = 6.6 Hz, 1H), 5.45 (dd, *J* = 10.8, 6.6 Hz, 1H), 3.93 (ddh, *J* = 12.2, 6.1, 2.8 Hz, 1H), 2.11 (qd, *J* = 7.5, 1.3 Hz, 2H), 1.48 – 1.34 (m, 4H), 1.34 (s, 3H), 1.32 – 1.22 (m, 17H), 1.21 (d, *J* = 6.1 Hz, 3H), 0.87 (t, *J* = 7.0 Hz, 3H) ppm.

¹³C NMR (101 MHz, CDCl₃) δ 135.6, 127.5, 91.2, 72.1, 68.9, 43.5, 32.1, 31.9, 29.8, 29.7, 29.6, 29.5, 29.5, 29.4, 28.2, 22.8, 22.3, 22.0, 14.3 ppm.

HRMS (FAB) calcd. for $C_{19}H_{37}O_2$ $[M+H]^+$ 297.2794; found 297.2792.

(Z)-2-(dodec-1-en-1-yl)-4,4,5,5-tetramethyl-1,3-dioxolane (2.16)

4,4,5,5-Tetramethyl-2-vinyl-1,3-dioxolane (130 mg, 0.80 mmol) and 1-dodecene (540 mg, 3.2 mmol) were reacted according to general procedure 1. After purification by silica gel chromatography (pentane, then 96:4 pentane:Et₂O), product **2.16** was obtained as a clear, colorless oil (84% yield, 200 mg, 98% Z).

¹H NMR (600 MHz, CDCl₃) δ 5.73 (d, *J* = 8.0 Hz, 1H), 5.68 (dt, *J* = 11.0, 7.7 Hz, 1H), 5.38 (dd, *J* = 11.0, 8.0 Hz, 1H), 2.16 (q, *J* = 7.7 Hz, 2H), 1.40 – 1.23 (m, 16H), 1.22 (s, 12H), 0.87 (t, *J* = 7.0 Hz, 3H) ppm.

¹³C NMR (101 MHz, CDCl₃) δ 136.6, 128.4, 95.4, 82.2, 32.1, 29.8, 29.7, 29.6, 29.5, 29.3, 27.5, 24.2, 22.8, 22.2, 14.3 ppm.

HRMS (FAB) calcd. for $C_{19}H_{35}O_2$ $[(M+H)-H_2]^+$ 295.2637; found 295.2627.

3,9-di((Z)-dodec-1-en-1-yl)-2,4,8,10-tetraoxaspiro[5.5]undecane (2.17)

3,9-Divinyl-2,4,8,10-tetraoxaspiro[5.5]undecane (85 mg, 0.40 mmol) and 1-dodecene (540 mg, 3.2 mmol) were reacted according to general procedure 1. After purification by silica gel chromatography (pentane, then 92:8 pentane:Et₂O), product **2.17** was obtained as a white solid (77% yield, 150 mg, 89% Z,Z).

¹H NMR (600 MHz, CDCl₃) δ 5.66 (dt, *J* = 11.1, 7.6 Hz, 2H), 5.44 (dt, *J* = 11.1, 6.4 Hz, 2H), 5.14 (d, *J* = 6.4 Hz, 2H), 4.63 (dd, *J* = 11.5, 2.3 Hz, 2H), 3.66 – 3.58 (m, 4H), 3.43

(d, $J = 11.5$ Hz, 2H), 2.11 (q, $J = 7.6$ Hz, 4H), 1.40 – 1.19 (m, 32H), 0.87 (t, $J = 7.1$ Hz, 6H) ppm.

^{13}C NMR (151 MHz, CDCl_3) δ 136.5, 126.3, 98.7, 70.8, 70.3, 32.1, 32.1, 29.8, 29.7, 29.6, 29.5, 29.4, 29.3, 28.3, 22.8, 14.3 ppm.

HRMS (FAB) calcd. for $\text{C}_{31}\text{H}_{57}\text{O}_4$ $[\text{M}+\text{H}]^+$ 493.4257; found 493.4236.

(Z)-1,1-diethoxytridec-2-ene (2.18)

Acrolein diethyl acetal (130 mg, 1.0 mmol) and 1-dodecene (670 mg, 4.0 mmol) were reacted according to general procedure 1. After purification by silica gel chromatography (98.5:1.5 pentane: Et_3N , then 96.5:1.5:3 pentane: Et_3N : Et_2O), product **2.18** was obtained as a clear, colorless oil (70% yield, 190 mg, >98% *Z*).

^1H NMR (400 MHz, CDCl_3) δ 5.62 (dt, $J = 11.2, 7.5$ Hz, 1H), 5.46 (dd, $J = 11.2, 6.8$ Hz, 1H), 5.20 (d, $J = 6.8$ Hz, 1H), 3.64 (dq, $J = 9.4, 7.1$ Hz, 2H), 3.50 (dq, $J = 9.4, 7.1$ Hz, 2H), 2.13 (q, $J = 7.5$ Hz, 2H), 1.45 – 1.24 (m, 16H), 1.21 (t, $J = 7.1$ Hz, 6H), 0.88 (t, $J = 6.8$ Hz, 3H) ppm.

^{13}C NMR (101 MHz, CDCl_3) δ 135.1, 127.3, 97.8, 60.6, 32.1, 29.8, 29.8, 29.6, 29.6, 29.5, 29.4, 28.2, 22.8, 15.5, 14.3 ppm.

HRMS (FAB) calcd. for $\text{C}_{17}\text{H}_{33}\text{O}_2$ $[(\text{M}+\text{H})-\text{H}_2]^+$ 269.2481; found 269.2481.

(Z)-2-(dodec-1-en-1-yl)-4,4,5,5-tetramethyl-1,3,2-dioxaborolane (2.21)

Vinylboronic acid pinacol ester (120 mg, 0.80 mmol) and 1-dodecene (540 mg, 3.2 mmol) were reacted according to general procedure 1. After purification by silica gel

chromatography (pentane, then 92:8 pentane:Et₂O), product **2.21** was obtained as a clear, colorless oil (81% yield, 190 mg, 92% *Z*).

¹H NMR (400 MHz, CDCl₃) δ 6.43 (dt, *J* = 14.6, 7.5 Hz, 1H), 5.32 (d, *J* = 13.5 Hz, 1H), 2.38 (q, *J* = 7.5 Hz, 2H), 1.47 – 1.17 (m, 28H), 0.88 (t, *J* = 6.8 Hz, 3H) ppm.

¹³C NMR (101 MHz, CDCl₃) δ 155.45, 118.04, 82.91, 32.35, 32.08, 29.81, 29.78, 29.62, 29.60, 29.52, 29.22, 24.99, 22.85, 14.27 ppm.

¹¹B NMR (128 MHz, CDCl₃) δ 29.87 ppm.

HRMS (FAB) calcd. for C₁₈H₃₆BO₂ [M+H]⁺ 295.2808; found 295.2811.

(*Z*)-2-(dodec-1-en-1-yl)oxirane (2.22)

2-Vinyloxirane (70 mg, 1.0 mmol) and 1-dodecene (670 mg, 4.0 mmol) were reacted according to general procedure 1, except that the reaction was conducted at 20 °C. After purification by silica gel chromatography (98.5:1.5 pentane:Et₃N, then 96.5:1.5:2 pentane:Et₃N:Et₂O), product **2.22** was obtained as a clear, colorless oil (40% yield, 85 mg, >98% *Z*).

¹H NMR (600 MHz, CDCl₃) δ 5.74 (dtd, *J* = 10.9, 7.7, 0.9 Hz, 1H), 5.00 (ddt, *J* = 10.9, 9.0, 1.5 Hz, 1H), 3.61 (dddd, *J* = 9.0, 4.0, 2.7, 0.9 Hz, 1H), 2.98 (dd, *J* = 5.3, 4.0 Hz, 1H), 2.64 (dd, *J* = 5.3, 2.7 Hz, 1H), 2.38 – 2.10 (m, 2H), 1.48 – 1.20 (m, 16H), 0.88 (t, *J* = 7.1 Hz, 3H) ppm.

¹³C NMR (126 MHz, CDCl₃) δ 137.23, 126.94, 48.68, 48.08, 31.90, 29.61, 29.59, 29.58, 29.47, 29.33, 29.18, 27.74, 22.68, 14.12 ppm.

HRMS (FAB) calcd. for C₁₄H₂₇O [M+H]⁺ 211.2062; found 211.2027.

(Z)-methyl 11-(1,3-dioxolan-2-yl)undec-10-enoate (2.32)

2-Vinyl-1,3-dioxolane (80 mg, 0.80 mmol) and methyl-10-undecenoate (640 mg, 3.2 mmol) were reacted according to general procedure 2. After purification by silica gel chromatography (95:5 pentane:Et₂O, then 90:10 pentane:Et₂O), product **2.32** was obtained as a clear, colorless oil (84% yield, 180 mg, 97% Z).

¹H NMR (600 MHz, CDCl₃) δ 5.75 (dt, *J* = 11.1, 7.7 Hz, 1H), 5.53 (d, *J* = 7.3 Hz, 2H), 5.42 (dd, *J* = 11.1, 7.3 Hz, 1H), 4.07 – 3.81 (m, 4H), 3.66 (s, 3H), 2.29 (t, *J* = 7.5 Hz, 2H), 2.16 (q, *J* = 7.7 Hz, 2H), 1.61 (app. p, *J* = 7.5 Hz, 2H), 1.43 – 1.24 (m, 10H) ppm.

¹³C NMR (126 MHz, CDCl₃) δ 174.30, 137.71, 125.72, 99.18, 64.94, 51.43, 34.08, 29.43, 29.20, 29.13, 29.09, 29.06, 27.76, 24.91 ppm.

HRMS (FAB) calcd. for C₁₅H₂₇O₄ [M+H]⁺ 271.1909; found 271.1900.

(Z)-2-(3-phenylprop-1-en-1-yl)-1,3-dioxolane (2.33)

2-Vinyl-1,3-dioxolane (80 mg, 0.80 mmol) and allylbenzene (670 mg, 3.2 mmol) were reacted according to general procedure 2. After purification by silica gel chromatography (95:5 pentane:Et₂O, then 90:10 pentane:Et₂O), product **2.33** was obtained as a pale yellow oil (88% yield, 130 mg, 97% Z).

¹H NMR (600 MHz, DMSO-*d*⁶) δ 7.30 (t, *J* = 7.5 Hz, 2H), 7.25 – 7.16 (m, 3H), 5.83 (q, *J* = 8.7 Hz, 1H), 5.64 (d, *J* = 7.5 Hz, 1H), 5.53 – 5.43 (m, 1H), 4.02 – 3.79 (m, 4H), 3.49 (d, *J* = 7.9 Hz, 2H) ppm.

¹³C NMR (101 MHz, CDCl₃) δ 139.7, 135.5, 128.7, 128.6, 126.9, 126.4, 99.4, 65.2, 34.2 ppm.

HRMS (FAB) calcd. for $C_{12}H_{13}O_2$ [(M+H)-H₂]⁺ 189.0916; found 189.0886.

(Z)-5-(1,3-dioxolan-2-yl)pent-4-en-1-ol (2.34)

2-Vinyl-1,3-dioxolane (80 mg, 0.80 mmol) and 4-penten-1-ol (280 mg, 3.2 mmol) were reacted according to general procedure 2, except that the reaction was stopped at 3 h. After purification by silica gel chromatography (80:18:2 EtOAc:hexanes:Et₃N), product **2.34** was obtained as a clear colorless oil (74% yield, 94 mg, 97% Z).

¹H NMR (600 MHz, CDCl₃) δ 5.72 (dt, *J* = 10.8, 8.1 Hz, 1H), 5.56 (d, *J* = 6.6 Hz, 1H), 5.52 (dd, *J* = 10.8, 6.6 Hz, 1H), 4.05 – 3.85 (m, 4H), 3.62 (q, *J* = 5.7 Hz, 2H), 2.34-2.26 (m, 2H), 2.20 (s, 1H), 1.76-1.59 (m, 2H) ppm.

¹³C NMR (126 MHz, CDCl₃) δ 136.7, 127.0, 99.5, 65.1, 61.0, 31.6, 24.2 ppm.

HRMS (FAB) calcd. for $C_8H_{15}O_3$ [M+H]⁺ 159.1021; found 159.1017.

(Z)-2-(5-bromopent-1-en-1-yl)-1,3-dioxolane (2.35)

2-Vinyl-1,3-dioxolane (80 mg, 0.80 mmol) and 5-bromo-1-pentene (480 mg, 3.2 mmol) were reacted according to general procedure 2. After purification by silica gel chromatography (90:10 pentane:Et₂O, then 80:20 pentane:Et₂O), product **2.35** was obtained as a pale yellow oil (83% yield, 150 mg, 95% Z).

¹H NMR (600 MHz, CDCl₃) δ 5.72 (dt, *J* = 10.7, 7.8 Hz, 1H), 5.56 (d, *J* = 7.8 Hz, 1H), 5.52 (dd, *J* = 10.7, 7.1 Hz, 1H), 4.05 – 3.86 (m, 4H), 3.42 (t, *J* = 6.7 Hz, 2H), 2.40 – 2.32 (m, 2H), 1.96 (dt, *J* = 13.6, 6.7 Hz, 2H) ppm.

¹³C NMR (101 MHz, CDCl₃) δ 135.2, 127.8, 99.2, 65.1, 33.1, 32.4, 26.4 ppm.

HRMS (FAB) calcd. for $C_8H_{14}BrO_2$ $[M+H]^+$ 221.0177; found 221.0182.

(Z)-3-(1,3-dioxolan-2-yl)prop-2-en-1-ol (2.39)

2-Vinyl-1,3-dioxolane (80 mg, 0.80 mmol) and allylboronic acid pinacol ester (540 mg, 3.2 mmol) were reacted according to general procedure 2. The oxidation was carried out according to a modified literature procedure.⁶⁵ After removal from glovebox, the reaction mixture was diluted with additional THF (2 mL) and cooled to 0 °C. NaOH (15 w/w%, 2.6 mL, 9.6 mmol) and aqueous H_2O_2 (30 w/w%, 0.96 mL, 9.6 mmol) were added slowly and the reaction was allowed to gradually warm to room temperature over 2 h. The mixture was then diluted with sat. $NaHCO_3$ (4 mL) and the organic solvent removed under reduced pressure. The aqueous layer was extracted into EtOAc (3 x 10 mL), dried over Na_2SO_4 , filtered, and concentrated. After purification by silica gel chromatography (96.5:2:1.5 DCM:MeOH:Et₃N, then 94.5:4:1.5 DCM:MeOH:Et₃N), product **2.39** was obtained as a pale yellow oil (63% yield, 66 mg, >98% Z).

¹H NMR (400 MHz, $CDCl_3$) δ 5.95 (dt, $J = 10.8, 6.3$ Hz, 1H), 5.70 – 5.54 (m, 2H), 4.29 (app. t, $J = 6.2$ Hz, 2H), 4.12 – 3.85 (m, 4H), 1.84 (t, $J = 6.1$ Hz, 1H) ppm.

¹³C NMR (101 MHz, $CDCl_3$) δ 135.4, 128.2, 99.4, 65.1, 59.0 ppm.

HRMS (EI) calcd. for $C_6H_9O_3$ $[(M+H)-H_2]^+$ 129.0552; found 129.0540.

(Z)-N-(3-(1,3-dioxolan-2-yl)allyl)-N-benzylaniline (2.45)

2-Vinyl-1,3-dioxolane (80 mg, 0.80 mmol) and *N*-allyl-*N*-benzylaniline (720 mg, 3.2 mmol) were reacted according to general procedure 2. After purification by silica gel

chromatography (90:10 pentane:Et₂O, then 80:20 pentane:Et₂O), product **22** was obtained as an off-white solid (72% yield, 170 mg, 89% *Z*).

¹H NMR (400 MHz, CDCl₃) δ 7.36 – 7.16 (m, 7H), 6.78 – 6.68 (m, 3H), 5.87 (dt, *J* = 12.3, 6.3 Hz, 1H), 5.65 (dd, *J* = 11.2, 6.5 Hz, 1H), 5.49 (d, *J* = 6.5 Hz, 1H), 4.53 (s, 2H), 4.16 (d, *J* = 6.3 Hz, 2H), 4.07 – 3.82 (m, 4H) ppm.

¹³C NMR (101 MHz, CDCl₃) δ 148.9, 139.0, 134.0, 129.4, 128.7, 128.5, 127.0, 126.9, 117.1, 113.0, 99.2, 65.1, 54.4, 47.9 ppm.

HRMS (FAB) calcd. for C₁₉H₂₂NO₂ [M+H]⁺ 296.1650; found 296.1654.

(*Z*)-tridec-2-enal (2.47)

1. (Table 2.7, entry 1) SiO₂ (310 mg), 5% aq. oxalic acid (31 mg) and (*Z*)-2-(dodec-1-en-1-yl)-1,3-dioxolane (**2.8**) (30 mg, 0.13 mmol) were reacted according to general procedure 3. The product was obtained in quantitative yield (25 mg).

2. (Table 2.7, entry 2) (*Z*)-2-(Dodec-1-en-1-yl)-1,3-dioxolane (**2.8**) (30 mg, 0.13 mmol) and LiBF₄ (15 mg, 0.16 mmol) were reacted according to general procedure 4. The product was obtained in 95% yield (23 mg).

3. (Table 2.7, entry 3) SiO₂ (280 mg), 5% aq. oxalic acid (28 mg) and (*Z*)-1,1-diethoxytridec-2-ene (**2.18**) (30 mg, 0.11 mmol) were reacted according to general procedure 3. The product was obtained in quantitative yield (22 mg).

4. (Table 2.7, entry 4) (*Z*)-1,1-Diethoxytridec-2-ene (**2.18**) (30 mg, 0.11 mmol) and LiBF₄ (14 mg, 0.14 mmol) were reacted according to general procedure 4. The product was obtained in 92% yield (20 mg).

^1H NMR (400 MHz, CDCl_3) δ 10.08 (d, $J = 8.2$ Hz, 1H), 6.64 (dt, $J = 11.2, 8.2$ Hz, 1H), 5.95 (ddt, $J = 11.2, 8.2, 1.5$ Hz, 1H), 2.65 – 2.55 (m, 2H), 1.56 – 1.44 (m, 2H), 1.41 – 1.17 (m, 14H), 0.87 (t, $J = 7.0, 6.4$ Hz, 3H) ppm.

^{13}C NMR (101 MHz, CDCl_3) δ 191.1, 153.7, 130.3, 32.0, 29.7, 29.7, 29.5, 29.5, 29.3, 29.2, 28.2, 22.8, 14.3 ppm.

HRMS (FAB) calcd. for $\text{C}_{13}\text{H}_{25}\text{O}_2$ $[\text{M}+\text{H}]^+$ 197.1905; found 197.1888.

(Z)-methyl 11-cyclopentylundec-10-enoate (2.48)

Vinyl cyclopentane (96 mg, 1.0 mmol) and methyl-10-undecenoate (790 mg, 4.0 mmol) were reacted according to general procedure 1, with methyl-10-undecenoate used in place of 1-dodecene. After purification by silica gel chromatography (95:5 pentane: Et_2O), product **17** and unreacted methyl-10-undecenoate were isolated as a mixture. ^1H -NMR analysis showed the mixture (160 mg) contained 73 mol% of **2.48** (117 mg, 44% yield, 94% Z).

^1H NMR (600 MHz, CDCl_3) δ 5.35 – 5.25 (m, 2H), 3.68 (s, 3H), 2.78 – 2.62 (m, 1H), 2.32 (t, $J = 7.6$ Hz, 2H), 2.05 (q, $J = 6.8$ Hz, 2H), 1.84 – 1.73 (m, 1H), 1.73 – 1.49 (m, 6H), 1.44 – 1.12 (m, 12H) ppm.

^{13}C NMR (101 MHz, CDCl_3) δ 174.5, 135.5, 128.6, 51.6, 38.3, 34.3, 33.9, 30.1, 29.5, 29.4, 29.3, 29.3, 27.6, 25.5, 25.1 ppm.

HRMS (FAB) calcd. for $\text{C}_{17}\text{H}_{31}\text{O}_2$ $[\text{M}+\text{H}]^+$ 267.2324; found 267.2316.

2-vinyl-1,3-dioxane (2.14)

Prepared as previously described.⁶² ¹H NMR (500 MHz, CDCl₃) δ 5.85 (ddd, *J* = 17.4, 10.7, 4.5 Hz, 1H), 5.46 (dt, *J* = 17.4, 1.3 Hz, 1H), 5.29 (dt, *J* = 10.7, 1.3 Hz, 1H), 4.96 (d, *J* = 4.5 Hz, 1H), 4.16 (dd, *J* = 10.7, 5.0 Hz, 2H), 3.88 – 3.81 (m, 2H), 2.13 (dtt, *J* = 13.5, 12.4, 5.0 Hz, 1H), 1.37 (dtt, *J* = 13.5, 2.6, 1.4 Hz, 1H) ppm.

¹³C NMR (126 MHz, CDCl₃) δ 135.1, 118.6, 100.8, 67.1, 25.9 ppm.

4,4,6-trimethyl-2-vinyl-1,3-dioxane (2.10)

Prepared as previously described.⁶² ¹H NMR (400 MHz, CDCl₃) δ 5.86 (ddd, *J* = 17.4, 10.5, 5.0 Hz, 1H), 5.45 (d, *J* = 17.4 Hz, 1H), 5.28 (d, *J* = 10.5 Hz, 1H), 5.19 (d, *J* = 5.0 Hz, 1H), 3.99 – 3.89 (m, 1H), 1.51 – 1.37 (m, 2H), 1.33 (s, 3H), 1.27 (s, 3H), 1.23 (d, *J* = 6.2 Hz, 3H) ppm.

¹³C NMR (101 MHz, CDCl₃) δ 135.7, 118.6, 94.7, 72.2, 68.8, 43.5, 31.8, 22.4, 21.9 ppm.

References

- (1) Endo, K.; Grubbs, R. H. *J. Am. Chem. Soc.* **2011**, *133* (22), 8525–8527.
- (2) Keitz, B. K.; Endo, K.; Patel, P. R.; Herbert, M. B.; Grubbs, R. H. *J. Am. Chem. Soc.* **2012**, *134* (1), 693–699.
- (3) Keitz, B. K.; Endo, K.; Herbert, M. B.; Grubbs, R. H. *J. Am. Chem. Soc.* **2011**, *133* (25), 9686–9688.
- (4) Herbert, M. B.; Marx, V. M.; Pederson, R. L.; Grubbs, R. H. *Angew. Chem. Int. Ed.* **2013**, *52* (1), 310–314.
- (5) Rosebrugh, L. E.; Herbert, M. B.; Marx, V. M.; Keitz, B. K.; Grubbs, R. H. *J. Am. Chem. Soc.* **2013**, *135* (4), 1276–1279.
- (6) Cannon, J. S.; Grubbs, R. H. *Angew. Chem. Int. Ed.* **2013**, *52* (34), 9001–9004.
- (7) Mangold, S. L.; O’Leary, D. J.; Grubbs, R. H. *J. Am. Chem. Soc.* **2014**, *136* (35),

- 12469–12478.
- (8) Miyazaki, H.; Herbert, M. B.; Liu, P.; Dong, X.; Xu, X.; Keitz, B. K.; Ung, T.; Mkrtumyan, G.; Houk, K. N.; Grubbs, R. H. *J. Am. Chem. Soc.* **2013**, *135* (15), 5848–5858.
- (9) Mangold, S. L.; Grubbs, R. H. *Chem. Sci.* **2015**, *6* (8), 4561–4569.
- (10) Marx, V. M.; Herbert, M. B.; Keitz, B. K.; Grubbs, R. H. *J. Am. Chem. Soc.* **2013**, *135* (1), 94–97.
- (11) Rosebrugh, L. E.; Ahmed, T. S.; Marx, V. M.; Hartung, J.; Liu, P.; López, J. G.; Houk, K. N.; Grubbs, R. H. *J. Am. Chem. Soc.* **2016**, *138* (4), 1394–1405.
- (12) Keitz, B. K.; Fedorov, A.; Grubbs, R. H. *J. Am. Chem. Soc.* **2012**, *134* (4), 2040–2043.
- (13) Hartung, J.; Grubbs, R. H. *J. Am. Chem. Soc.* **2013**, *135* (28), 10183–10185.
- (14) Hartung, J.; Grubbs, R. H. *Angew. Chem. Int. Ed.* **2014**, *53* (15), 3885–3888.
- (15) Hartung, J.; Dornan, P. K.; Grubbs, R. H. *J. Am. Chem. Soc.* **2014**, *136* (37), 13029–13037.
- (16) O'Leary, D.; Blackwell, H.; Washenfelder, R.; Grubbs, R. H. *Tetrahedron Lett.* **1998**, *39* (41), 7427–7430.
- (17) Blackwell, H.; O'Leary, D.; Chatterjee, A.; Washenfelder, R.; Da Bussmann; Grubbs, R. H. *J. Am. Chem. Soc.* **2000**, *122* (1), 58–71.
- (18) Chatterjee, A.; Choi, T.-L.; Sanders, D. P.; Grubbs, R. H. *J. Am. Chem. Soc.* **2003**, *125* (37), 11360–11370.
- (19) Dang, Y.; Wang, Z.-X.; Wang, X. *Organometallics* **2012**, *31* (20), 7222–7234.
- (20) Dang, Y.; Wang, Z.-X.; Wang, X. *Organometallics* **2012**, *31* (24), 8654–8657.
- (21) Liu, P.; Xu, X.; Dong, X.; Keitz, B. K.; Herbert, M. B.; Grubbs, R. H.; Houk, K. N. *J. Am. Chem. Soc.* **2012**, *134* (3), 1464–1467.
- (22) Turner, R. B.; Jarrett, A. D.; Goebel, P. *J. Am. Chem. Soc.* **1973**, *95* (3), 790–792.
- (23) O'Leary, D.; Blackwell, H.; Washenfelder, R.; Miura, K.; Grubbs, R. H. *Tetrahedron Lett.* **1999**, *40* (6), 1091–1094.
- (24) Ohloff, G.; Pickenhagen, W.; Kraft, P. *Scent and Chemistry*; Verlag Helvetica Chimica Acta, Zürich, and Wiley-VCH, Weinheim, 2011.
- (25) Boelens, M. H.; van Gemert, L. J. *Perf. Flav.* **1987**, *12* (5), 31–43.
- (26) Howse, P. E.; Stevens, I. D. R.; Jones, O. T. *Insect Pheromones and their Use in Pest Management*; Springer Netherlands: Dordrecht, 1998.
- (27) Jang, E. B.; Siderhurst, M. S.; Hollingsworth, R. G.; Showalter, D. N.; Troyer, E. *J. Pest Manag. Sci.* **2010**, *66* (4), 454–460.

- (28) Balboa-Lagunero, T.; Arroyo, T.; Cabellos, J. M.; Aznar, M. *Am. J. Enol. Vitic.* **2011**, *62* (4), 527–535.
- (29) Haddada, F. M.; Manai, H.; Daoud, D.; Fernandez, X.; Lizzani-Cuvelier, L.; Zarrouk, M. *Food Chem.* **2007**, *103* (2), 467–476.
- (30) Johanningsmeier, S. D.; McFeeters, R. F. *J. Food Sci.* **2011**, *76* (1), C168–C177.
- (31) Jobu, K.; Sun, C.; Yoshioka, S.; Yokota, J.; Onogawa, M.; Kawada, C.; Inoue, K.; Shuin, T.; Sendo, T.; Miyamura, M. *Biol. Pharm. Bull. Jpn.* **2012**, *35* (4), 639–642.
- (32) Brodmann, T.; Janssen, D.; Kalesse, M. *J. Am. Chem. Soc.* **2010**, *132* (39), 13610–13611.
- (33) Roush, W.; Sciotti, R. *J. Am. Chem. Soc.* **1994**, *116* (14), 6457–6458.
- (34) Paterson, I.; Florence, G.; Gerlach, K.; Scott, J. *Angew. Chem. Int. Ed.* **2000**, *39* (2), 377–380.
- (35) Vostrowsky, O.; Paulus, H.; Billmann, W.; Stransky, W. *Tetrahedron Lett.* **1977**, *18* (1), 121–124.
- (36) Gerasyuto, A. I.; Hsung, R. P. *J. Org. Chem.* **2007**, *72* (7), 2476–2484.
- (37) Deagostino, A.; Prandi, C. *Curr. Org. Chem.* **2003**, *7* (9), 821–830.
- (38) Cresp, T.; Sargent, M.; Vogel, P. *J. Chem. Soc., Perkin Tran. 1* **1974**, 37–41.
- (39) Daubresse, N.; Francesch, C.; Rolando, C. *Tetrahedron* **1998**, *54* (36), 10761–10770.
- (40) Nuzillard, J.; Boumendjel, A.; Massiot, G. *Tetrahedron Lett.* **1989**, *30* (29), 3779–3780.
- (41) Petroski, R. J.; Vermillion, K.; Cossé, A. A. *Molecules* **2011**, *16* (12), 5062–5078.
- (42) Wittig, G.; Reiff, H. *Angew. Chem. Int. Ed.* **1968**, *7* (1), 7–14.
- (43) Wollenberg, R. H.; Albizati, K. F.; Peries, R. *J. Am. Chem. Soc.* **1977**, *99* (22), 348–352.
- (44) Shaw, S. J.; Sundermann, K. F.; Burlingame, M. A.; Zhang, D.; Petryka, J.; Myles, D. C. *Bioorg. Med. Chem.* **2006**, *16* (7), 1961–1964.
- (45) Zhou, S.; Xiao, T.; Song, H.; Zhou, X. *Tetrahedron Lett.* **2012**, *53* (42), 5684–5687.
- (46) Ikeda, C.; Braun, R.; Sorenson, B. *J. Org. Chem.* **1964**, *29* (2), 286–290.
- (47) Wuts, P. G. M.; Greene, T. W. *Protective Groups in Organic Synthesis*; John Wiley & Sons, Inc., 2006; pp 431–532.
- (48) Miyaura, N.; Suzuki, A. *Chem. Rev.* **1995**, *95* (7), 2457–2483.
- (49) Molander, G. A.; Felix, L. A. *J. Org. Chem.* **2005**, *70* (10), 3950–3956.

- (50) Woerly, E. M.; Struble, J. R.; Palyam, N.; O'Hara, S. P.; Burke, M. D. *Tetrahedron* **2011**, *67* (24), 4333–4343.
- (51) Hemelaere, R.; Carreaux, F.; Carboni, B. *J. Org. Chem.* **2013**, *78* (13), 6786–6792.
- (52) Kiesewetter, E. T.; O'Brien, R. V.; Yu, E. C.; Meek, S. J.; Schrock, R. R.; Hoveyda, A. H. *J. Am. Chem. Soc.* **2013**, *135* (16), 6026–6029.
- (53) Kelly, T. R.; Lee, Y.-J.; Mears, R. J. *J. Org. Chem.* **1997**, *62* (9), 2774–2781.
- (54) Dias, D. A.; Kerr, M. A. *Org. Lett.* **2009**, *11* (16), 3694–3697.
- (55) Cacchi, S.; Fabrizi, G.; Moro, L.; Pace, P. *Synlett* **1997**, No. 12, 1367–1370.
- (56) Sakai, T.; Miyata, K.; Tsuboi, S.; Takeda, A. *Bull. Chem. Soc. Jpn.* **1989**.
- (57) Lipshutz, B. H. *Synth. Commun.* **1982**, *12* (4), 267–277.
- (58) Bonin, M.; Royer, J.; Grierson, D. S.; Husson, H. P. *Tetrahedron Lett.* **1986**, *27* (14), 1569–1572.
- (59) Herbert, M. B.; Grubbs, R. H. *Angew. Chem. Int. Ed.* **2015**, *54* (17), 5018–5024.
- (60) Pangborn, A. B.; Giardello, M. A.; Grubbs, R. H. *Organometallics* **1996**, *15* (5), 1518–1520.
- (61) Wiedemann, S. H.; Bergman, R. G.; Ellman, J. A. *Org. Lett.* **2004**, *6* (10), 1685–1687.
- (62) Ikeda, C. K.; Braun, R. A.; Sorenson, B. E. *J. Org. Chem.* **1964**, *29* (2), 286–290.
- (63) Gómez-Ayala, S.; Gómez-Ayala, R.; Castrillón, J. A.; Palma, A.; Leal, R. M.; Escobar, P.; Bahsas, A.; Leal, S. M. *Bioorg. Med. Chem.* **2010**, *18* (13), 4721–4739.
- (64) Ritter, T.; Hejl, A.; Wenzel, A. G.; Funk, T. W.; Grubbs, R. H. *Organometallics* **2006**, *25* (24), 5740–5745.
- (65) Ely, R. J.; Morken, J. P. *J. Am. Chem. Soc.* **2010**, *132* (8), 2534–2535.

Chapter 3

Synthesis, Characterization and Activity of a Series of Cyclometallated Catalysts with Varying N-aryl Group

Abstract

In the family of cyclometallated Z-selective metathesis catalysts recently developed in our group, steric repulsion between the N-aryl group and the metallacycle substituents is key to determining the Z-selectivity. This chapter outlines studies involving a novel series of seven cyclometallated catalysts that differ in the identity of the 2,6-substituted N-aryl group of the cyclometallated NHC ligand. Through systematic variation of the steric and electronic nature of the N-aryl group, the specific aspects of the N-aryl group that affect catalyst behavior are elucidated. The first part of the chapter discusses the synthesis of the series of metathesis catalysts from the corresponding anilines, including several unexpected synthetic challenges. The second part of the chapter focuses on the behavior of the catalyst in solution. The dynamic behavior of the catalysts with respect to rotation about the N–C(aryl) bond is studied by NMR spectroscopy, revealing the presence of conformational isomers in a number of the catalysts. In addition, an unusual C–H···F–C hydrogen-bonding type interaction present in several of the catalysts is studied. Finally, the reactivity of the series of catalysts, in parallel with previously published catalysts **3.1** and **3.2**, is explored in homodimerization reactions of unhindered terminal olefins, as well as in CM of allylic-substituted olefins. These studies allow development of a more refined model for the influence of the N-aryl group on selectivity and activity. Distinct reactivity and selectivity patterns are observed in reactions with unhindered terminal olefins and allylic-substituted olefins, supporting observations made in the studies detailed in Chapter 2. Finally, improved reactivity is observed in CM with an allylic-substituted olefin, surpassing previous catalysts.

Introduction

Catalyst **3.1** (**Figure 3.1**) emerged as the first Z-selective Ru-based metathesis catalyst that demonstrated a good balance of activity, stability, and Z-selectivity, allowing it to be applied in a wide variety of metathesis applications.¹⁻¹¹ Replacement of the N-Mes group with the more sterically demanding N-DIPP group yielded catalyst **3.2**, which demonstrated improved Z-selectivity in a number of reactions, including the CM of allylic-substituted olefins discussed in **Chapter 2**.^{5,8,12-14} In the search for catalysts with further improved activity, stability and Z-selectivity, considerable efforts have generated a family of catalysts that have variations in the anionic (X-type) ligand(s)^{19,15}, the nature of the cyclometallated group^{4,12,16-18}, and replacement of the dihydroimidazolylidene ligand by other types of carbenes.¹⁹ From these studies, no new catalyst emerged that demonstrated significant improvements across a wide scope of metathesis reactions. While catalyst **3.2** performed well in the CM of unhindered terminal olefins, results in **Chapter 2** demonstrated its much poorer activity in the case of allylic substituted olefins, where it was surpassed in activity by less sterically bulky catalyst **3.1**. In addition, the difference in Z-selectivity between **3.1** and **3.2** was much larger in CM of allylic-

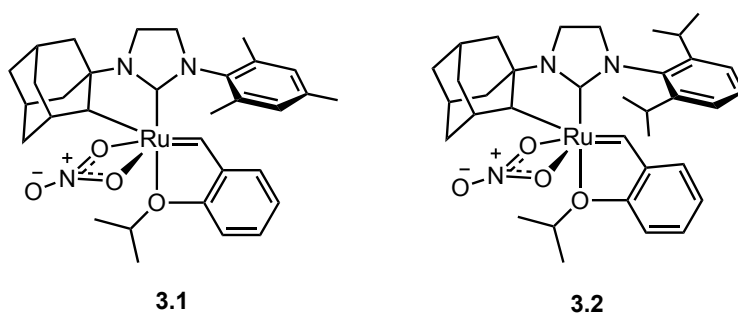


Figure 3.1. Cyclometallated Ru complexes commonly employed for Z-selective olefin metathesis.

substituted olefins. This suggests that alterations in the N-aryl group might have a much more significant impact in metathesis reactions involving allylic-substituted olefins and may provide an avenue for development of catalysts with an improved balance of activity and Z-selectivity. Previously, a limited number of analogues of **3.1** bearing alternative N-aryl groups have been prepared (**3.3–3.6**).^{1,12}

Catalysts **3.3** and **3.4** differ from catalyst **3.1** in the para substituent of the N-aryl group (**Figure 3.2**). As the para substituent of the N-aryl group is distal to the metallacycle, it was expected to have little steric influence on the metallacycle and, therefore, any changes would be a consequence of altering the electronics of the NHC ligand. Catalysts **3.3** and **3.4** were compared to **3.1** in a number of homodimerization reactions, where they demonstrated similar activity and Z-selectivity, with only relatively minor differences observed between the catalysts.¹ Similarly, replacement of the ortho-Me groups of catalyst **3.1** with ortho-Et groups, giving catalyst **3.5**, led to only marginal differences in either Z-selectivity or activity.¹ In this case, unhindered rotation about the methylene of the ethyl substituent likely renders the effective steric bulk of the two N-aryl groups similar. In addition, catalyst **3.6**, which bears an N-(2-isopropyl-6-

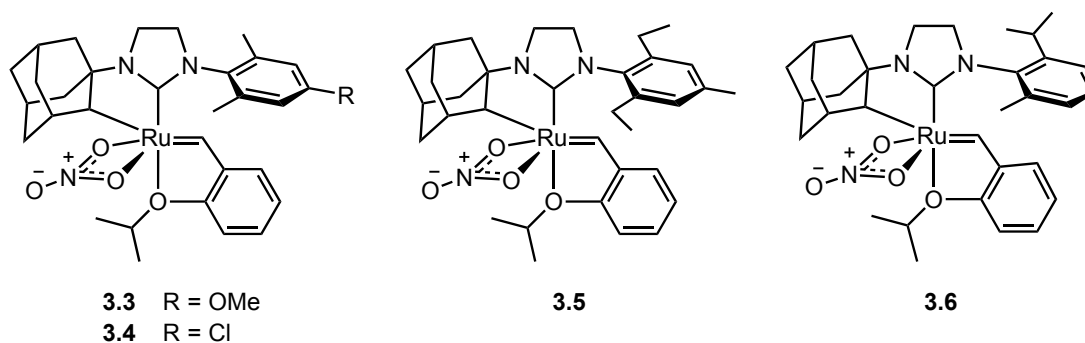
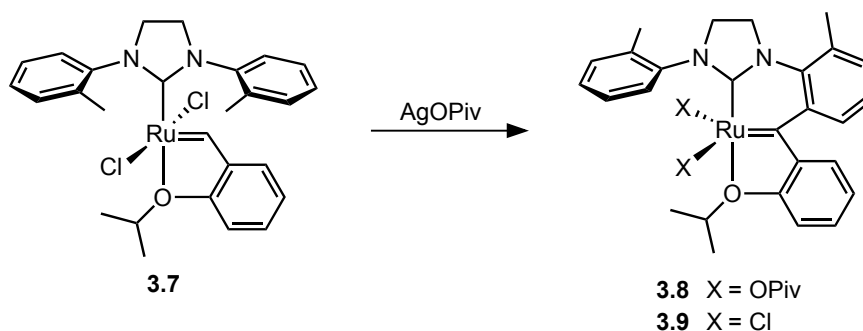


Figure 3.2. Previously prepared cyclometallated Ru-based Z-selective catalysts with various N-aryl groups.

methylphenyl) group, has been prepared previously.¹² However, **3.6** had poor solubility in THF, making direct comparison to previously reported reactivity of other catalysts challenging, and it displayed anomalously low reactivity in the homodimerization of one substrate.

More significant variation of the N-aryl group has proved challenging, with significant decomposition occurring under the C–H-activation conditions used to prepare the cyclometallated catalysts, making it difficult to isolate the desired catalysts.^{1,20} While catalysts bearing N-aryl groups with ortho hydrogens were of particular interest, the several catalysts targeted could not be isolated. These catalysts are believed to undergo C–H activation of the ortho H of the aryl group, followed by insertion of the resulting Ru–C bond into the carbene, forming a metathesis inactive species. A typical example of this decomposition route was observed for catalyst **3.7**, which upon exposure to AgOPiv and subsequent anion exchange was found to form species **3.9**, with **3.8** being the presumed initially formed species (**Scheme 3.1**).²⁰ DFT calculations supported the viability of the observed decomposition pathway for this catalyst and similar decomposition pathways have been observed previously in other Ru metathesis



Scheme 3.1. Decomposition pathway observed for Z-selective catalysts bearing N-aryl groups with ortho hydrogens.

catalysts.²⁰

While differences in the Z-selectivity associated with changes in the N-aryl group^{5,12-14} have been noted in a number of studies, the relationship with activity has generally been more tenuous to elucidate, as differences between **3.1** and **3.2** are often marginal in CM of unhindered olefins.^{5,12,14} In addition, given the limited number of catalysts available, it has been challenging to make specific correlations between the nature of the N-aryl group and the resultant behavior of the catalysts. We sought to develop an improved understanding of the relationship between catalyst structure and catalytic performance through examining a series of catalysts where the steric and electronic profile of N-aryl group was systematically varied.

Figure 3.3 depicts the series of catalysts targeted in this chapter, all of which have one or more fluorine (**3.10–3.14**) or methoxy substituents (**3.14–3.16**) in the ortho position of the N-aryl group. These catalysts were targeted to complement **3.1** and **3.2**, providing a range of catalysts that could be used to address which features of the N-aryl group play a role in these Z-selective metathesis catalysts. In particular, there were a number of specific questions that we hoped to address by employing a systematic series of catalysts to separate out steric and electronic influences. We wanted to explore if one or both of the ortho substituents play a significant role in governing the Z-selectivity of the reaction. In addition, we wanted to examine more extensively the effects of changing the electronic nature of the N-aryl group, by introducing more significant changes than in **3.3** and **3.4**. Previous results had demonstrated that substrates containing certain functional groups displayed activity and Z-selectivity distinct from other substrates.^{1,5,12,14,21} We wanted to establish if this was related purely to substrate-specific

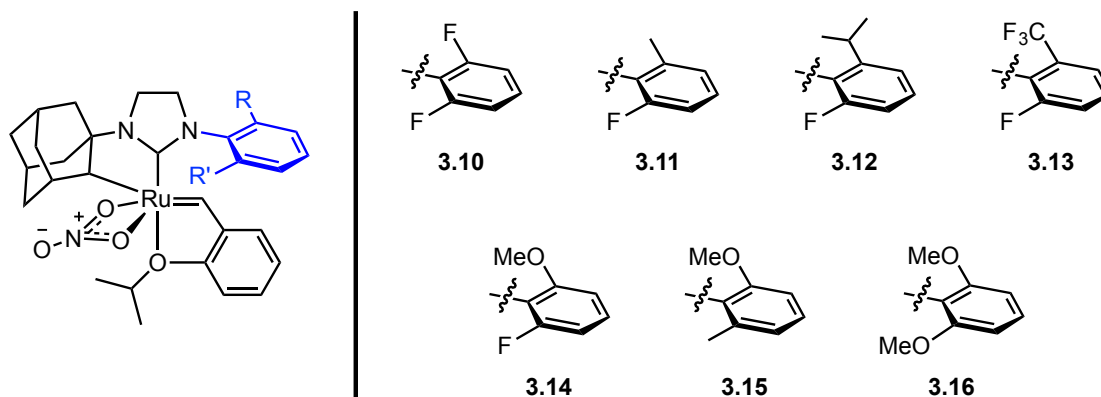


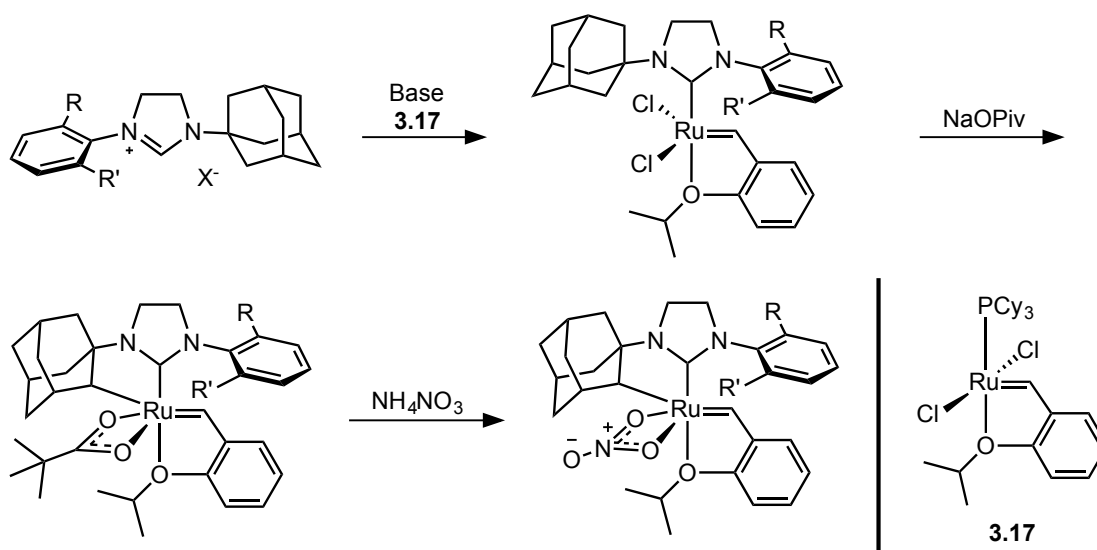
Figure 3.3. Targeted series of *Z*-selective catalysts with varying *N*-aryl groups.

parameters or if improved activity and/or *Z*-selectivity could be achieved by altering the *N*-aryl group of the catalyst. In addition, certain substrates exhibited enhanced degradation of *Z*-content at high conversions.¹ Whether this degradation is affected more strongly by the steric or electronic nature of the *N*-aryl group may indicate if factors other than the inherent activity of the catalysts (and, hence, secondary metathesis) are influencing reactivity.

Fluorine was selected as an ortho substituent as it is less sterically demanding than a Me group, allowing access to catalysts with a potentially less sterically demanding *N*-aryl group than **3.1**, but avoiding the decomposition pathway noted for the analogous catalysts that contain an ortho C–H bond (**Scheme 3.1**).²⁰ In comparison to a hydrogen substituent, however, fluorine is significantly more electron-withdrawing, changing the electronic nature of the *N*-aryl substituent. In order to complement the fluorinated *N*-aryl groups, a number of *N*-aryl groups bearing more electron-donating methoxy substituents were also targeted. The series of catalysts also allows for comparison of catalysts with an identical ortho substituent while varying the size of the other ortho substituent.

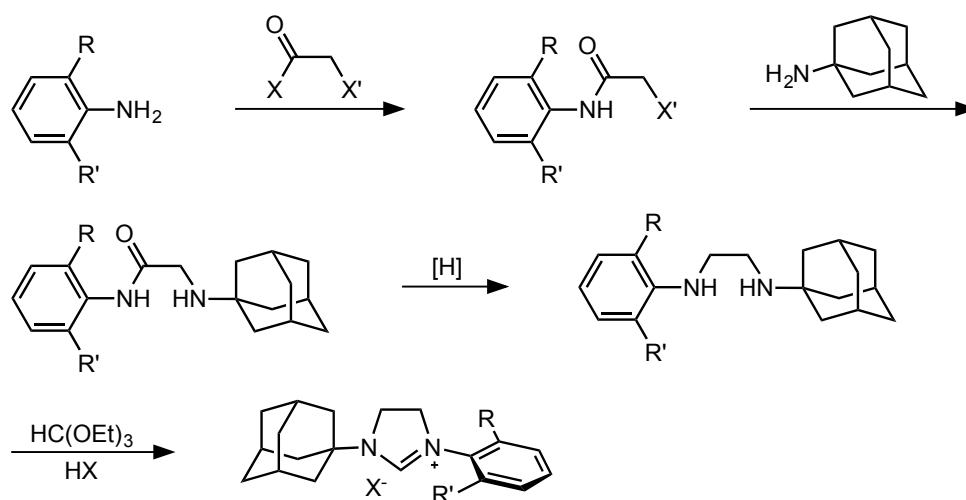
Synthesis of the Catalyst Series

Scheme 3.2 outlines the general synthetic route used to access the cyclometallated Z-selective metathesis catalysts, beginning from the corresponding imidazolium salt.^{1,12} The N-aryl N'-1-admantyl NHC is metallated onto **3.17** by displacement of the phosphine ligand. C–H activation is then achieved using NaOPiv¹², which allows for milder conditions than the initially disclosed method that employs AgOPiv.¹⁷ Anion metathesis using NH₄NO₃ then forms the corresponding nitrato complexes. In choosing a method for the synthesis of the NHC salts, the primary consideration was to employ a route that would be robust for a variety of aryl groups that vary in both their steric and electronic profile.

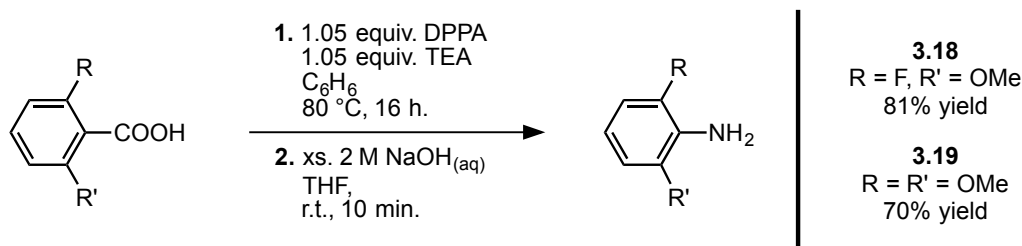


Scheme 3.2. General synthetic scheme for accessing cyclometallated Z-selective Ru catalysts.

The synthetic strategy chosen was developed by Paczal et al. and relies on an α -haloacetyl halide as the key building block (**Scheme 3.3**).²² This method has been widely employed by our group and others for the synthesis of N-aryl N'-alkyl NHC salts, as it allows installation of the two different amines with high chemoselectivity.^{1,23-25} The anilines necessary for synthesizing the catalyst series are either commercially available or readily accessible. Condensation of the aniline with the acyl halide is associated with a strong driving force, which should help minimize problems with sterically hindered or poorly nucleophilic anilines. Alternative synthetic approaches to NHC salts that rely on nucleophilic substitution or cross-coupling approaches may perform poorly for these substrates.²⁵ Installation of the N'-1-adamantyl group can then be achieved by nucleophilic substitution, which has previously been demonstrated to be efficient even for this relatively sterically hindered nucleophile.^{1,24} The amide can then be reduced to the corresponding diamine, which can then be cyclized using triethyl orthoformate to generate the desired imidazolium salt.

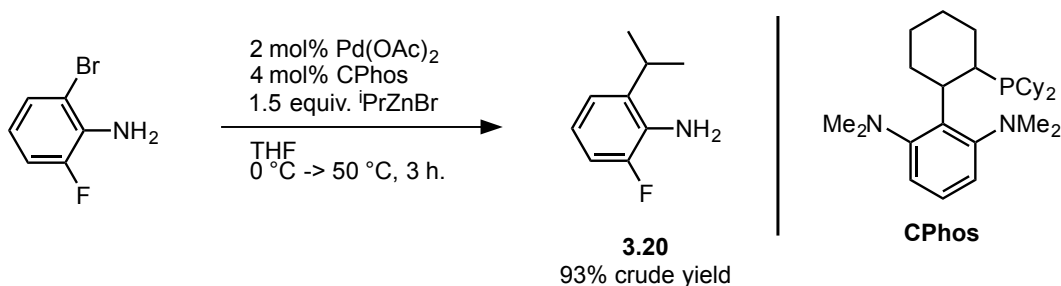


Scheme 3.3. Proposed synthetic scheme for N-aryl, N'-1-adamantyl imidazolium salts.



Scheme 3.4 Preparation of anilines from corresponding carboxylic acids using DPPA.

Seven anilines were employed to generate the targeted catalyst series, four of which were obtained from commercial sources. 2-fluoro-6-methoxyaniline (**3.18**) and 2,6-dimethoxyaniline (**3.19**) can be accessed in good yield from the corresponding carboxylic acids by employing diphenylphosphoryl azide (DPPA) to perform a modified Curtius-type rearrangement (**Scheme 3.4**).^{26,27} While the latter aniline was commercially available, freshly prepared starting material resulted in improved yield in the subsequent step. 2-Fluoro-6-isopropylaniline (**3.20**) was accessed from 2-bromo-6-fluoroaniline and isopropylzinc bromide by Pd-catalyzed Negishi coupling using conditions adapted from those developed by Han and Buchwald (**Scheme 3.5**).²⁸ The aniline was formed in high yield and with high selectivity for the branched product (>95:5) and could be used in the next step without further purification.

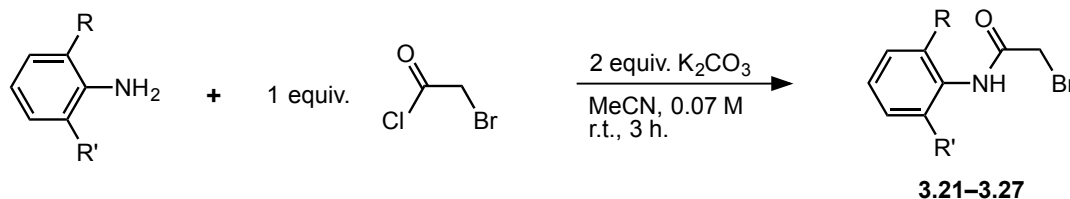


Scheme 3.5. Negishi cross-coupling to prepare 2-fluoro-6-isopropylaniline.

Bromoacetyl chloride was chosen over chloroacetyl chloride for the initial amide formation step, with the expectation of improved reactivity in the subsequent nucleophilic substitution reaction with 1-adamantylamine. The initial amide formation was carried out under more dilute conditions (~ 0.07 M in MeCN) and for shorter reaction time (~ 3 h.) than previously reported.^{1,24} These conditions were employed after initial experiments with 2-fluoro-6-trifluoromethylaniline demonstrated significant formation of the undesired 2,5-diketopiperazine under more forcing reaction conditions.

These milder conditions were found to work well for all seven anilines examined and the products could be obtained in good to excellent yields after purification (**Table 3.1**). Some substitution of the alkyl bromide by the displaced chloride was noted and the

Table 3.1. Condensation of 2,6-substituted anilines and bromoacetyl chloride.



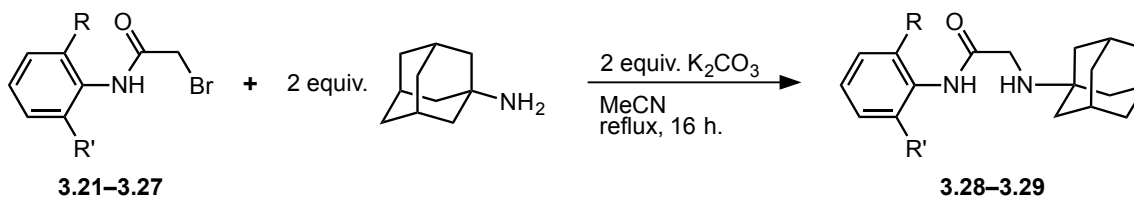
Entry	Product	R	R'	Yield (%) ^a
1	3.21	F	F	82
2	3.22	F	Me	92
3	3.23	F	ⁱ Pr	62
4	3.24	F	CF ₃	97
5	3.25	F	OMe	74
6	3.26	Me	OMe	80
7	3.27	OMe	OMe	85

^a Isolated yield. In all cases a small amount of the corresponding chloro product was present in **3.21–3.27**. The ratio of the two was determined by ¹H-NMR spectroscopy and the yield was adjusted accordingly.

products were isolated as a mixture of the two compounds, with the bromide being the major component. The mixture of compounds was used in the subsequent step and the reported yield and subsequent reaction stoichiometry were calculated accordingly.

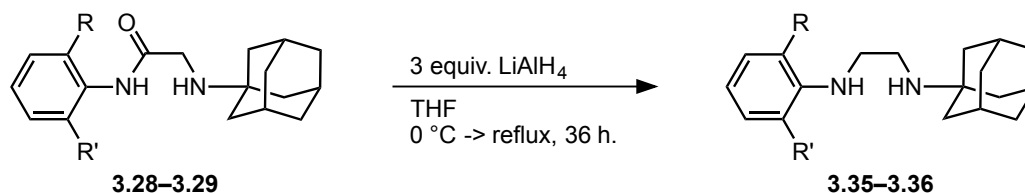
An excess of 1-adamantylamine was employed in the nucleophilic substitution step in order to promote efficient formation of the desired product and to minimize potential competitive formation of the 2,5-diketopiperazine or other byproducts. Under these conditions, the substitution proceeded with high efficiency across the series of compounds, allowing the desired α -aminoamides to be isolated in high yield after purification by column chromatography on silica gel (**Table 3.2**).

Table 3.2. Substitution of alkyl bromide with 1-adamantylamine.



Entry	Product	R	R'	Yield ^a (%)
1	3.28	F	F	95
2	3.29	F	Me	92
3	3.30	F	ⁱ Pr	94
4	3.31	F	CF ₃	96
5	3.32	F	OMe	91
6	3.33	Me	OMe	95
7	3.34	OMe	OMe	97

^a Isolated yield. In all cases a small amount of the corresponding chloro product was present in **3.21-3.37**. The ratio of the two was determined by ¹H-NMR spectroscopy and the reaction stoichiometry and yield were adjusted accordingly.

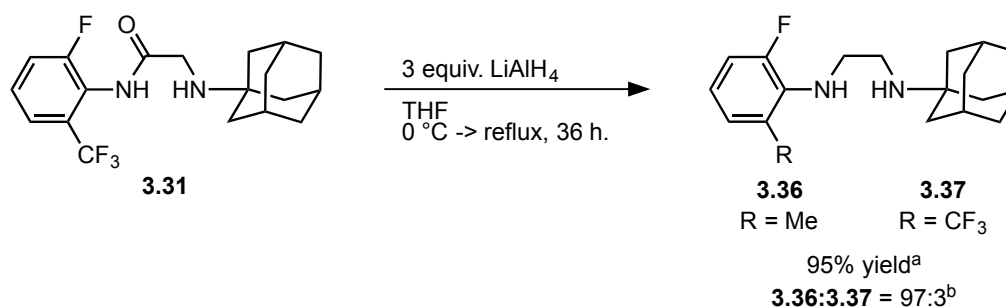
Table 3.3. Reduction of amides with LiAlH₄.

Entry	Product	R	R'	Yield (%) ^a
1	3.35	F	F	98
2	3.36	F	Me	93

^a Isolated yield.

In previous reports, reduction of the amide to form the corresponding diamine had typically been achieved using LiAlH₄.^{1,22-24} In the case of compounds **3.28** and **3.29**, the reaction proceeded efficiently using previously disclosed conditions to generate the desired diamines (**3.35** and **3.36**) in excellent yield (**Table 3.3**).

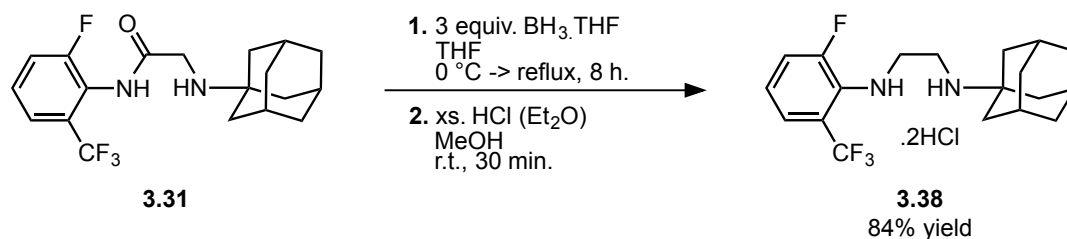
However, when compound **3.31** was subjected to the same reaction conditions, compound **3.36** was again found to be the major product with a small amount of the desired product (**3.37**) and trace amounts of other products present in the reaction mixture



^a Isolated yield. ^b Ratio determined using ¹H- and ¹⁹F-NMR spectroscopy.

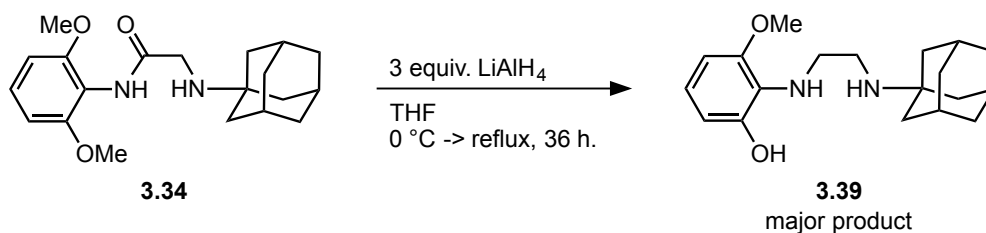
Scheme 3.6. Attempted reduction of amide **3.31** with LiAlH₄.

(**Scheme 3.6**). While trifluoromethyl groups are typically inert to LiAlH_4 , the reduction of aryl trifluoromethyl groups has been previously reported in the presence of activating ortho or para amino groups.²⁹ Borane-based reducing agents have previously been employed for reduction of oxalamide intermediates in an alternative synthetic procedure for the preparation of imidazolium salts.^{30,31} Employing $\text{BH}_3\cdot\text{THF}$ under similar conditions effected clean reduction of the amide with no reduction of the trifluoromethyl group observed under these reaction conditions (**Scheme 3.7**). The addition of HCl facilitated cleavage of the product–borane adducts in the work-up procedure and hence the diamine products were isolated as the dihydrochloride salts.



Scheme 3.7. Reduction of amide **3.31** with $\text{BH}_3\cdot\text{THF}$

In the reduction of amides bearing phenyl groups with ortho-methoxy substituents with LiAlH_4 , a second unexpected side reaction was noted where cleavage of the methyl group occurred. This was particularly evident in the reduction of **3.34** bearing the N-2,6-dimethoxyphenyl group, which, under similar reactions used for **3.28** and **3.29**, generated the corresponding diamine bearing a 2-hydroxy-6-methoxyphenyl group (**3.39**) as the major product (**Scheme 3.8**). This indicates that one methyl group had been selectively cleaved under the reaction conditions. To a lesser extent, cleavage of the methoxy group

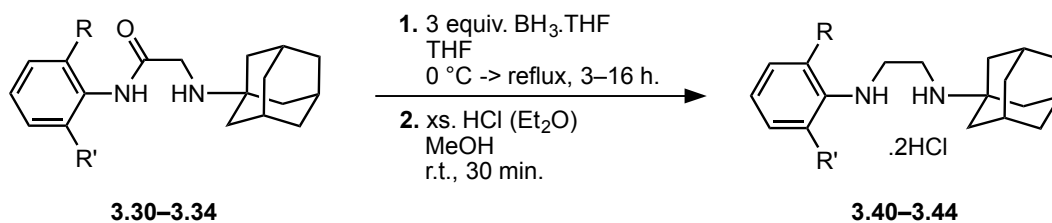


Scheme 3.8. Attempted reduction of amide **3.34** with LiAlH_4 .

was also observed when compound **3.33** bearing a 2-methyl-6-methoxyphenyl group was subjected to LiAlH_4 reduction.

Reducing the equivalents of LiAlH_4 and monitoring the reaction indicated that cleavage of the methyl group was competitive with amide reduction. When **3.34** was subjected to the conditions used for trifluoromethyl-containing compound **3.31**, some cleavage of the methoxy group was again noted. By limiting the reaction time to 3 h.

Table 3.4. Reduction of amides with $\text{BH}_3\cdot\text{THF}$.



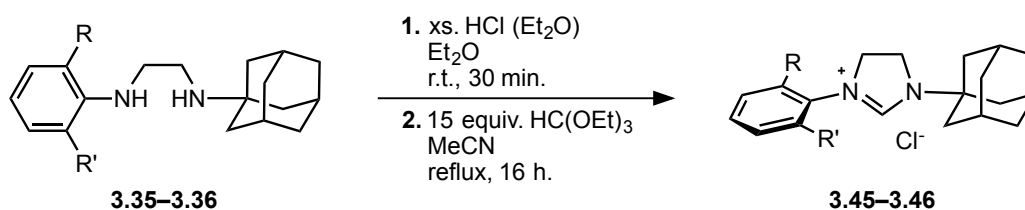
Entry	Product	R	R'	Yield (%) ^a
1	3.40	F	ⁱ Pr	91
2	3.41	F	CF_3	84
3	3.42	F	OMe	89
4	3.43	Me	OMe	85
5	3.44	OMe	OMe	60

^a Isolated yield.

appreciable conversion to the desired product could be achieved with minimal cleavage, allowing the desired diamine to be isolated in good yield (**Table 3.4**). In the work-up of the borane reduction, acid was added in order to promote complete cleavage of the product–borane adducts and the products were isolated as the dihydrochloride salts. This method was also efficient for the reduction of the remaining amides.

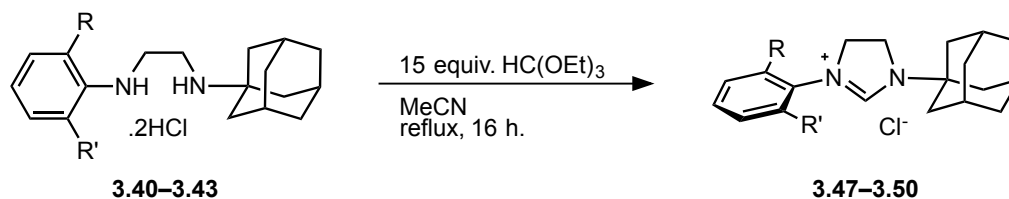
For compounds **3.35** and **3.36**, the diamines were converted to the dihydrochloride salts by addition of HCl in Et₂O before being subjected to cyclization conditions employing triethyl orthoformate as the carbon source (**Table 3.5**). The addition of one volume equivalent of MeCN (v/v with HC(OEt)₃) improved solubility during the cyclization step and resulted in higher yields of the desired product.

Table 3.5. Formation of imidazolium chlorides from corresponding diamines.



Entry	Product	R	R'	Yield (%) ^a
1	3.45	F	F	59
2	3.46	F	Me	63

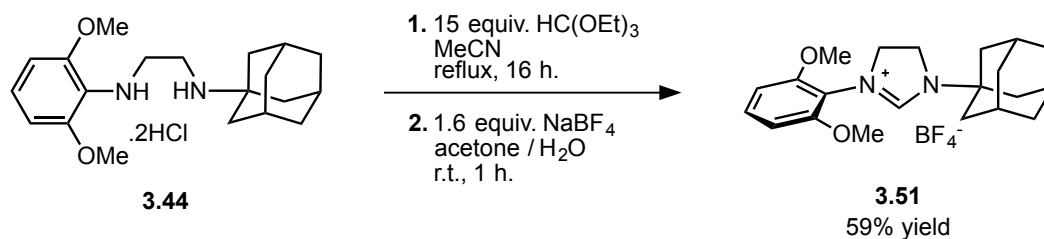
^a Isolated yield.

Table 3.6. Formation of imidazolinium chlorides from corresponding diamine dihydrochlorides.

Entry	Product	R	R'	Yield ^a (%)
1	3.47	F	ⁱ Pr	74
2	3.48	F	CF ₃	62
3	3.49	F	OMe	72
4	3.50	Me	OMe	76

^a Isolated yield.

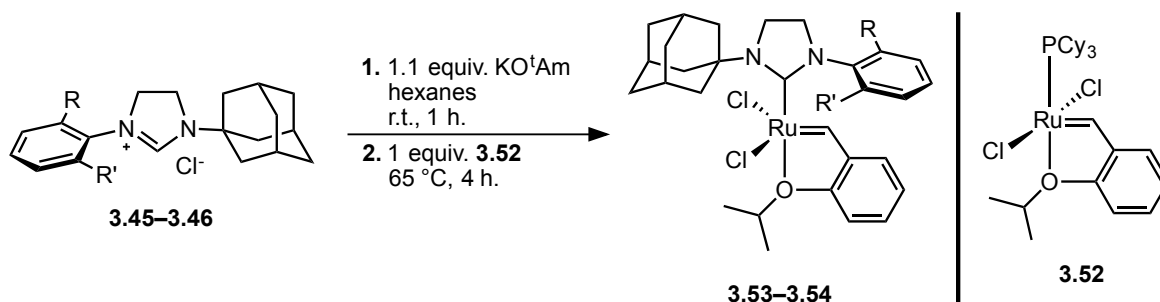
Identical cyclization conditions were applied to the diamine dihydrochloride salts prepared from the borane reduction, allowing isolation of the corresponding imidazolinium salts in good yield (**Table 3.6**). In the formation of **3.41** and **3.44**, cyclization was incomplete under these conditions with an intermediate crashing out under the reaction conditions, which upon aqueous hydrolysis was identified as the corresponding monoformate. Addition of two further equivalents of MeCN (v/v with HC(OEt)₃) was found to prevent this intermediate from crashing out, allowing cyclization to take place more efficiently. The imidazolinium chloride formed from **3.44** was found to be hygroscopic and so was converted to the less hygroscopic tetrafluoroborate salt before metallation was attempted (**Scheme 3.9**).



Scheme 3.9. Cyclization of **3.44** to form imidazolium salt and conversion to tetrafluoroborate.

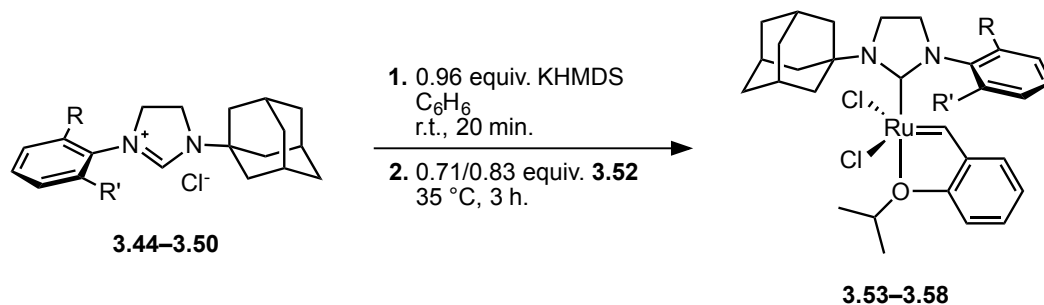
Previously, metallation of analogous NHCs, including in the preparation of **3.1** and **3.2**, had employed a method which utilized KO^tAm as the base and hexanes as the solvent. This method was found to generate **3.53** and **3.54** in moderate yields (**Table 3.7**). Improved yields were obtained using an alternative method, which employed KHMDS as the base and benzene as the solvent. **3.53–3.58** were found to be stable to purification on the benchtop and could be isolated in good yield using this procedure (**Table 3.8**).

Table 3.7. Metallation of NHCs using KO^tAm.



Entry	Product	R	R'	Yield (%) ^a
1	3.52	F	F	48
2	3.53	F	Me	67

^a Isolated yield.

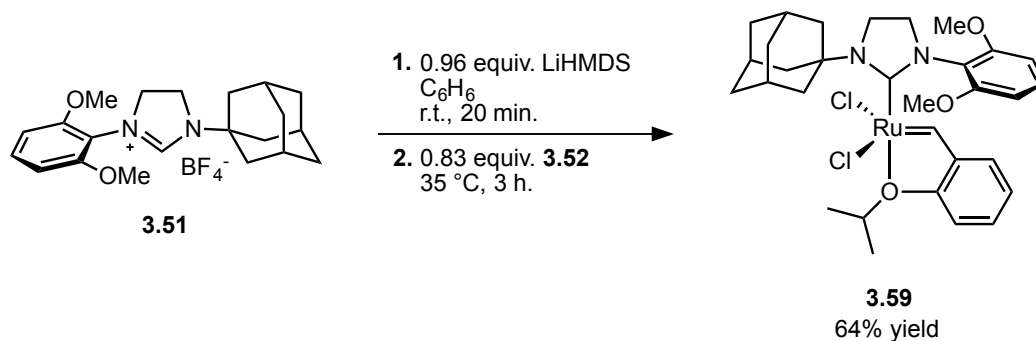
Table 3.8. Metallation of NHCs using KHMDS.

Entry	Product	R	R'	Yield (%) ^a
1	3.53	F	F	84
2	3.54	F	Me	80
3	3.55	F	ⁱ Pr	61
4	3.56	F	CF ₃	77
5	3.57	F	OMe	78
6	3.58	Me	OMe	69

^a Isolated yield.

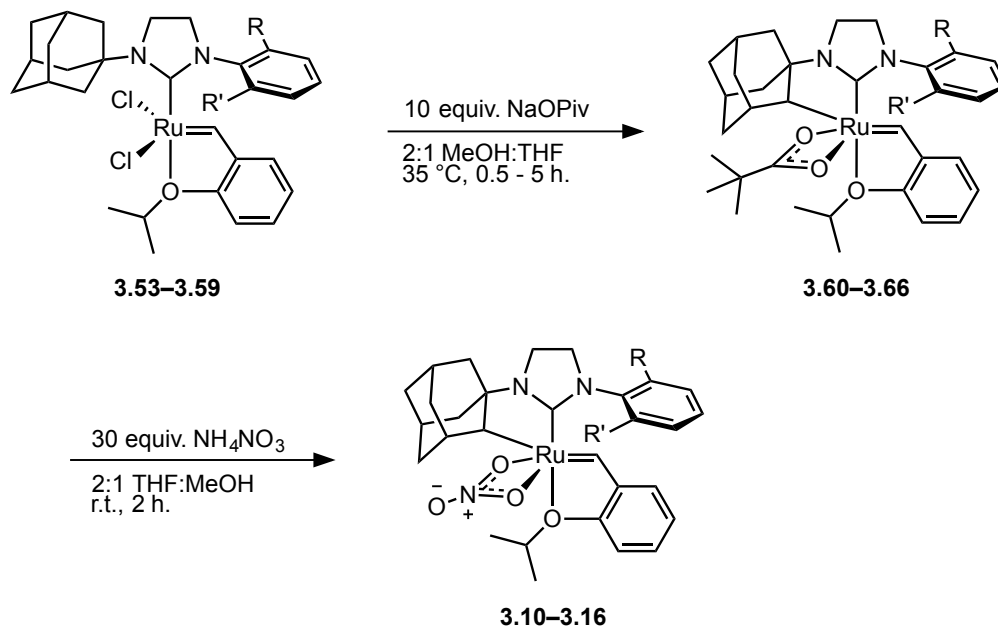
Attempts to metallate **3.51** using this method resulted in challenging purification and poor yield. In comparison to a number of known Ru metathesis catalysts that have NHCs bearing aryl groups with ortho-fluorine substituents, only a very limited number of catalysts have been reported with an ortho-ether substituent and attempts to metallate NHCs bearing ortho-phenols onto common Ru metathesis precursors have thus far been unsuccessful. The formation of stable potassium NHC complexes has been demonstrated in the case of NHCs bearing a hydroxyl-containing substituent. In order to investigate if the potassium counterion was negatively affecting reactivity, 18-crown-6 was added to the KHMDS to sequester the potassium before addition of the NHC salt. This resulted in improved conversion to the desired complex. Interestingly, a significant improvement

was also observed when LiHMDS was used in place of KHMDS, allowing isolation of the desired catalyst, **3.59**, in 64% yield (**Scheme 3.10**).



Scheme 3.10. Metallation of NHC salt **3.44** using LiHMDS.

The catalysts were then subjected to C–H activation conditions, using NaOPiv to effect the cyclometallation. Previous conditions employed a solvent mixture of 1:1 THF:MeOH for the anion exchange/cyclometallation step.¹² Here, it was found that employing a 2:1 mixture of MeOH:THF led to cleaner formation of the desired cyclometallated species (**Table 3.9**). Under these conditions, there was lower solubility of the starting catalyst, which may hinder bimolecular decomposition pathways involving the starting catalyst. In general, increased steric bulk of the N-aryl group was found to correlate with increased reaction time, as predicted based on previous studies. These reaction conditions allowed for generally good yields across the scope of the catalysts investigated. While the pivalate-containing cyclometallated catalysts could be isolated (**3.60–3.66**), they were found to demonstrate poor stability in solution and limited stability as solids at room temperature. Exchange of the pivalate to nitrate resulted in catalysts **3.10–3.16**, which were found to be significantly more stable and so these were employed in further studies. Previously, the anion metathesis was effected using NH₄NO₃ in THF, but improved yield was observed when the exchange was conducted in a 2:1

Table 3.9. C–H activation and anion metathesis to form cyclometallated Z-selective catalysts.

Entry	Product	R	R'	Yield (%) ^a
1	3.10	F	F	66
2	3.11	F	Me	63
3	3.12	F	ⁱ Pr	54
4	3.13	F	CF ₃	48
5	3.14	F	OMe	62
6	3.15	Me	OMe	53
7	3.16	OMe	OMe	54

^a Isolated yield over two steps.

mixture of THF:MeOH, which was associated with increased solubility of NH_4NO_3 under the reaction conditions.¹ In all cases, the desired catalysts (**3.10–3.16**) could be accessed in moderate to good yield over the two steps, representing a significant improvement over previously reported syntheses of related catalysts.^{1,12}

NMR Characterization

Dynamics

The $^1\text{H-NMR}$ spectra of Ru complexes **3.53–3.59** (pre-C–H activation) were relatively unremarkable with each catalyst demonstrating a single sharp benzyldiene peak and no indication of distinct conformational isomers at room temperature. Compared to the parent N-Mes catalyst ($\delta = 16.90$ p.p.m., CDCl_3), **3.53**, **3.57** and **3.59** showed significant downfield shifts (17.25–17.47 p.p.m), whereas the remaining catalysts showed a smaller change (16.87–17.01 p.p.m.). No evidence of F–Ru interactions, which had been observed previously in catalysts with fluorinated N-aryl groups, such as **3.67**, were observed in these catalysts (**Figure 3.4**).³² Previous studies on Ru metathesis catalysts bearing N-Ar, N'-Ak NHC have demonstrated that the NHC N-aryl group is typically located over the benzyldiene^{1,17,24,33,34}, whereas F–Ru interactions have been observed on the opposite face of the Ru from the benzyldiene.³⁵

In contrast, several interesting features were noted in the $^1\text{H-NMR}$ spectra of the C–H-activated catalysts, which are highlighted by examining the benzyldiene region of the $^1\text{H-NMR}$ spectra (**Figure 3.5**). Firstly, while catalysts **3.10**, **3.12**, and **3.16** were

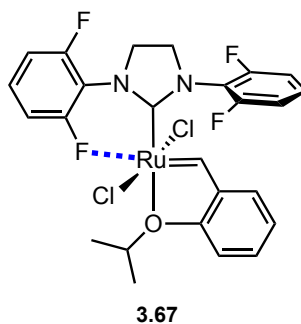


Figure 3.4. Fluoro-aryl catalyst **3.67**, which demonstrated the presence of a F–Ru interaction.

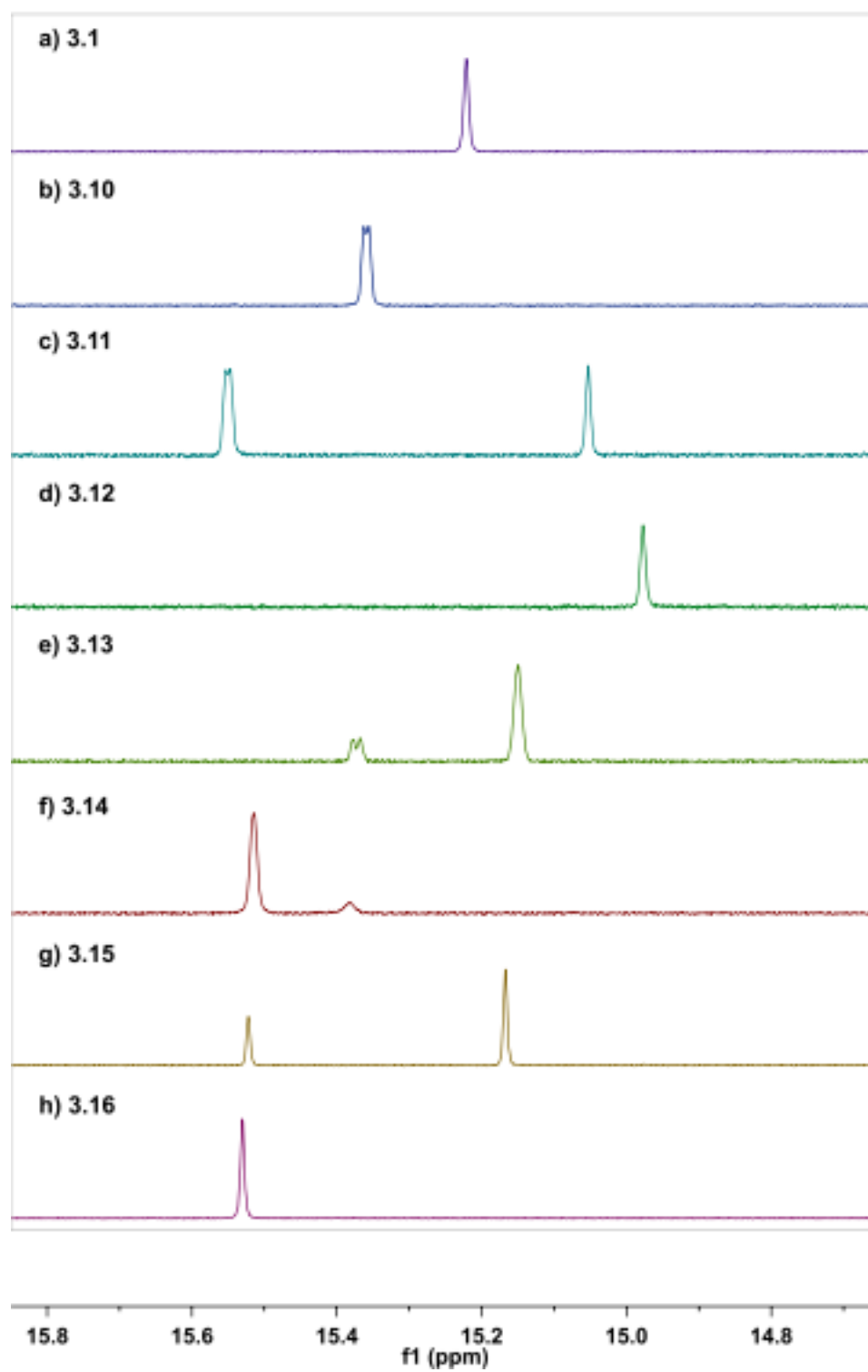


Figure 3.5. Benzylidene region of $^1\text{H-NMR}$ spectra of catalysts **3.1** and **3.10–3.16** in C_6D_6 .

present as a single species by $^1\text{H-NMR}$ spectroscopy, catalysts **3.11** and **3.13–3.15** all present as a mixture of two isomers at room temperature, as evidenced by two peaks in the benzylidene region of the spectrum. The catalysts that are present as a mixture of isomers all possess unsymmetrical N-aryl groups, in which the two ortho substituents are not identical.

In previous solid-state structures of cyclometallated Ru-based catalysts, the N-aryl group is oriented roughly perpendicular to the Ru=C(benzylidene) bond^{1,12,17}, with the result that one of the ortho substituents is pointed towards the benzylidene and the other ortho substituent is pointed away from it. A solid-state structure of **3.61** revealed a similar

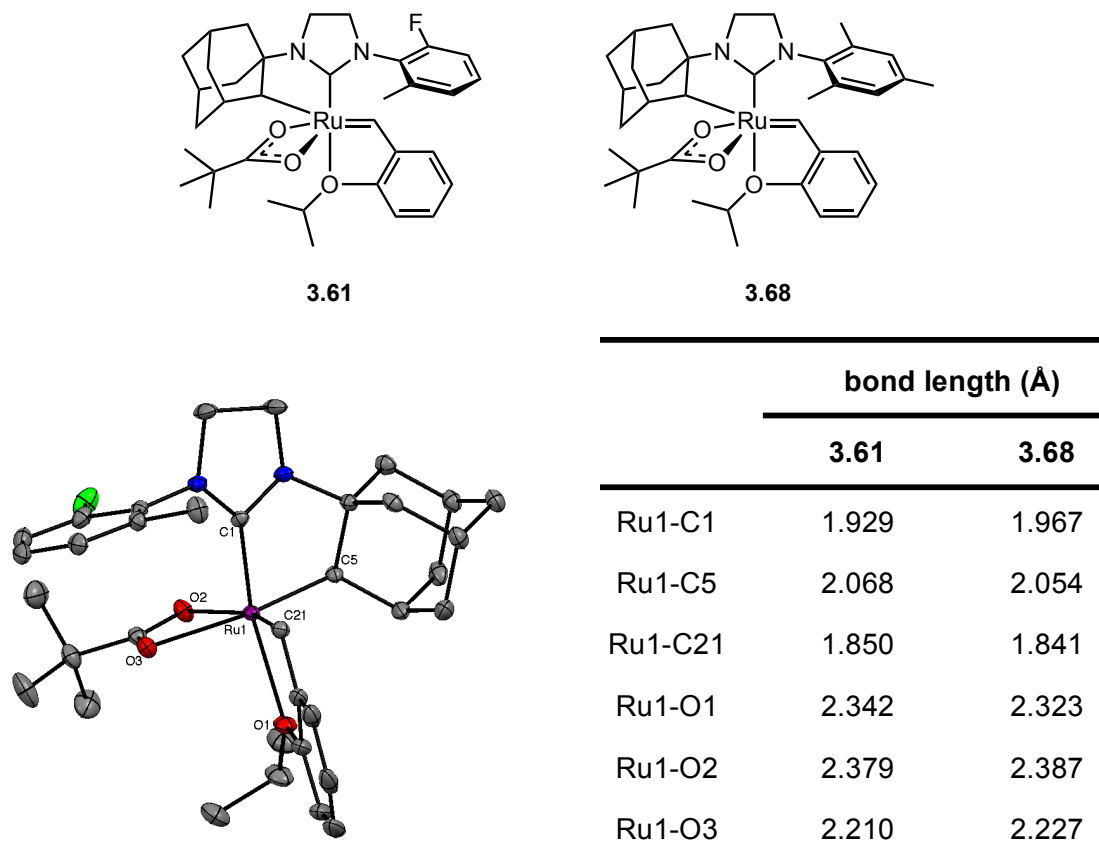


Figure 3.6. Solid-state structure of **3.61**, with thermal ellipsoids drawn at 50% probability. Selected bond lengths are compared to corresponding N-Mes species **3.68**.

overall geometry, in which the ortho methyl group was pointed toward the benzylidene (**Figure 3.6**). The bond lengths found in **3.61** were largely consistent with the corresponding N-Mes complex (**3.68**) apart from a slightly shorter Ru–C(NHC) bond, which is consistent with a more electron-deficient NHC ligand.

In the case of catalysts with unsymmetrical N-aryl groups, such as **3.61** or the corresponding nitrate analogue **3.11**, rotation about the N–C(aryl) bond results in two conformers that are chemically distinct and will hence have different properties (**Figure 3.7**). Two isomers were observed for all of the nitrate catalysts bearing unsymmetrical N-aryl groups (as well as the corresponding pivalate complexes) apart from **3.12**, which has the N-2-fluoro-6-isopropylphenyl group. Here, as in **3.2**, it is believed that rotation about the N–C(aryl) bond is restricted, due to the steric clash between the ⁱPr substituent and the backbone protons, which hence enforces a preferred orientation of the aryl group with respect to the benzylidene.

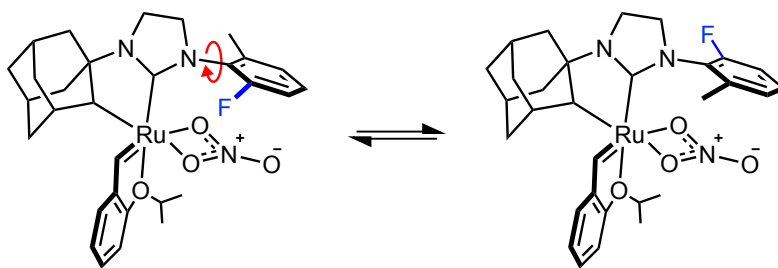


Figure 3.7. Rotation about the N–C(aryl) bond of **3.11** results in two different stereoisomers of the catalyst, which have distinct properties.

An Unusual C–H⋯F–C Interaction

In addition, a second interesting NMR feature is noted in all of the catalysts bearing an ortho F apart from **3.12**, where one of the benzyldiene signals displays evidence of splitting. ^1H – ^1H coupling of the benzyldiene proton is generally not observed in the case of NHC-containing Ru complexes with an o-isopropoxybenzyldiene, as the shortest possible coupling would be a $^4J_{\text{HH}}$ with the ortho proton of the benzyldiene. In previous studies of **3.69**, designed as a model complex for olefin binding, broadening of the benzyldiene was also observed and attributed to a through-space ^{19}F – ^1H coupling interaction (**Figure 3.8**).³⁶ In **3.69** and in the current catalysts (**3.10**–**3.14**), seven bonds separate the benzyldiene proton and the nearest fluorine atom and so a through-bond coupling mechanism was deemed unlikely.

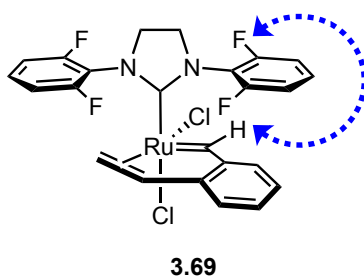


Figure 3.8. Previously observed through-space ^1H – ^{19}F coupling to benzyldiene proton observed in Ru-based metathesis model complex.

3.10 displays a single peak in the benzyldiene region of its ^1H -NMR spectrum. Selective $^1\text{H}\{^{19}\text{F}\}$ decoupling experiments of the two fluorine resonances illustrated that the coupling occurs specifically to the downfield fluorine resonance in the ^{19}F -NMR spectrum (**Figure 3.9**). Given that the two fluorine atoms are both seven bonds away from the benzyldiene, this also supports a through-space coupling mechanism. Catalyst

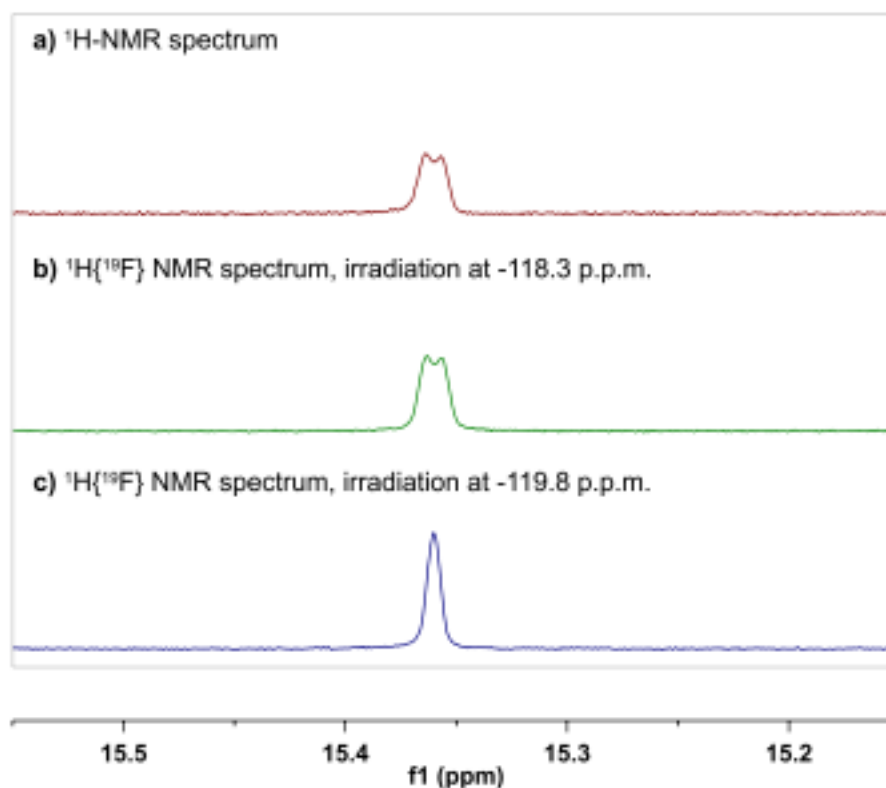


Figure 3.9. ^1H -NMR spectra of **3.10** illustrating spin–spin coupling of the benzylidene proton signal with one F signal. **a)** Benzylidene region of ^1H -NMR spectrum of catalyst **3.10**. Benzylidene region of $^1\text{H}\{^{19}\text{F}\}$ -NMR spectrum acquired with continuous-wave ^{19}F irradiation at **b)** -118.3 p.p.m. and **c)** -119.8 p.p.m.

3.11 displays two peaks in the benzylidene region of its ^1H -NMR spectrum: a singlet at 15.05 p.p.m. and a multiplet at 15.55 p.p.m. with two corresponding resonances in the ^{19}F -NMR spectrum (**Figure 3.10**). Selective $^1\text{H}\{^{19}\text{F}\}$ decoupling experiments demonstrated coupling between the benzylidene signal at 15.55 p.p.m. and the downfield ^{19}F resonance. Similar coupling was also observed in the case of the corresponding pivalate-containing precursors (**3.60–3.61**).

The existence of this fluorine–proton interaction was further supported by an interesting observation made with compounds **3.10**, **3.11**, and **3.13**. The chemical shift of the benzylidene proton resonance that is coupled to fluorine could be correlated with the

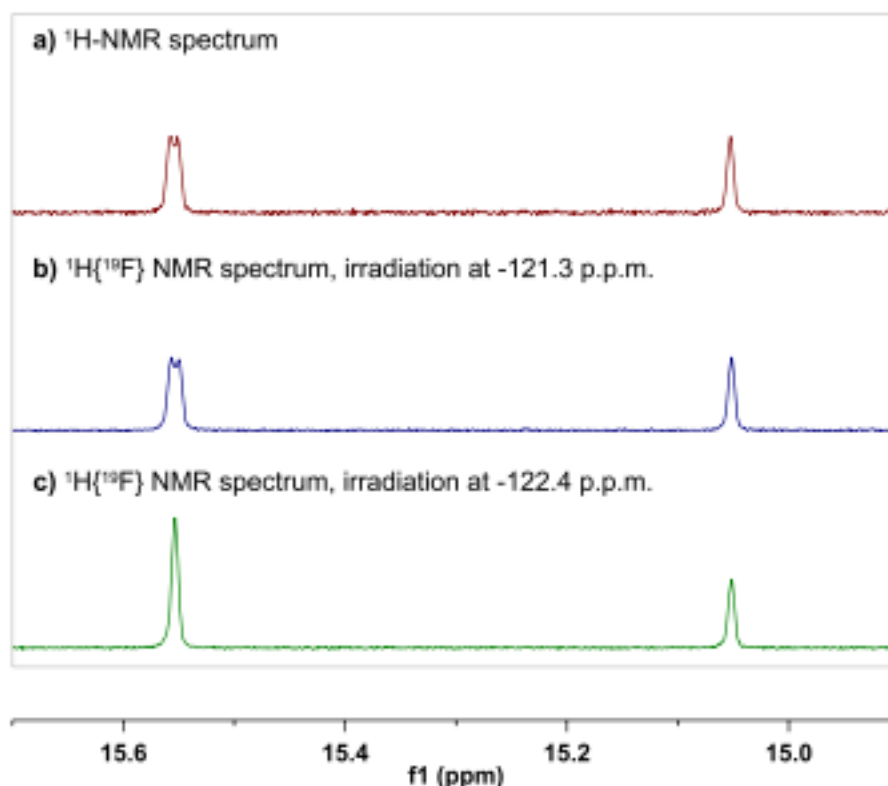


Figure 3.10. ^1H -NMR spectra of **3.11** illustrating spin–spin coupling of downfield benzyldene proton signal with one F signal. **a)** Benzyldene region of ^1H -NMR spectrum of catalyst **3.11**. Benzyldene region of $^1\text{H}\{^{19}\text{F}\}$ -NMR spectrum of **3.11** acquired with continuous-wave ^{19}F irradiation at **b)** -121.3 p.p.m. and **c)** -122.4 p.p.m.

identity of the other ortho substituent of the N-aryl group, which is located meta relative to the fluorine (**Figure 3.11**). A plot of the benzyldene chemical shift against the Hammett σ_{meta} parameter for the non-F ortho substituent of the N-aryl group revealed a good linear correlation ($R^2 = 0.97$) with a negative slope. Given the remote nature of the ortho-substituent (seven bonds away from the benzyldene), the correlation was unexpected. A linear correlation ($R^2 = 0.99$) was also observed in the chemical shifts of the corresponding pivalate-containing catalysts (**3.60**, **3.61**, and **3.63**). No such correlations were observed in the non-cyclometallated precursors (**3.53–3.59**) or the three cyclometallated catalysts bearing o-methoxy substituents (**3.14–3.16**).

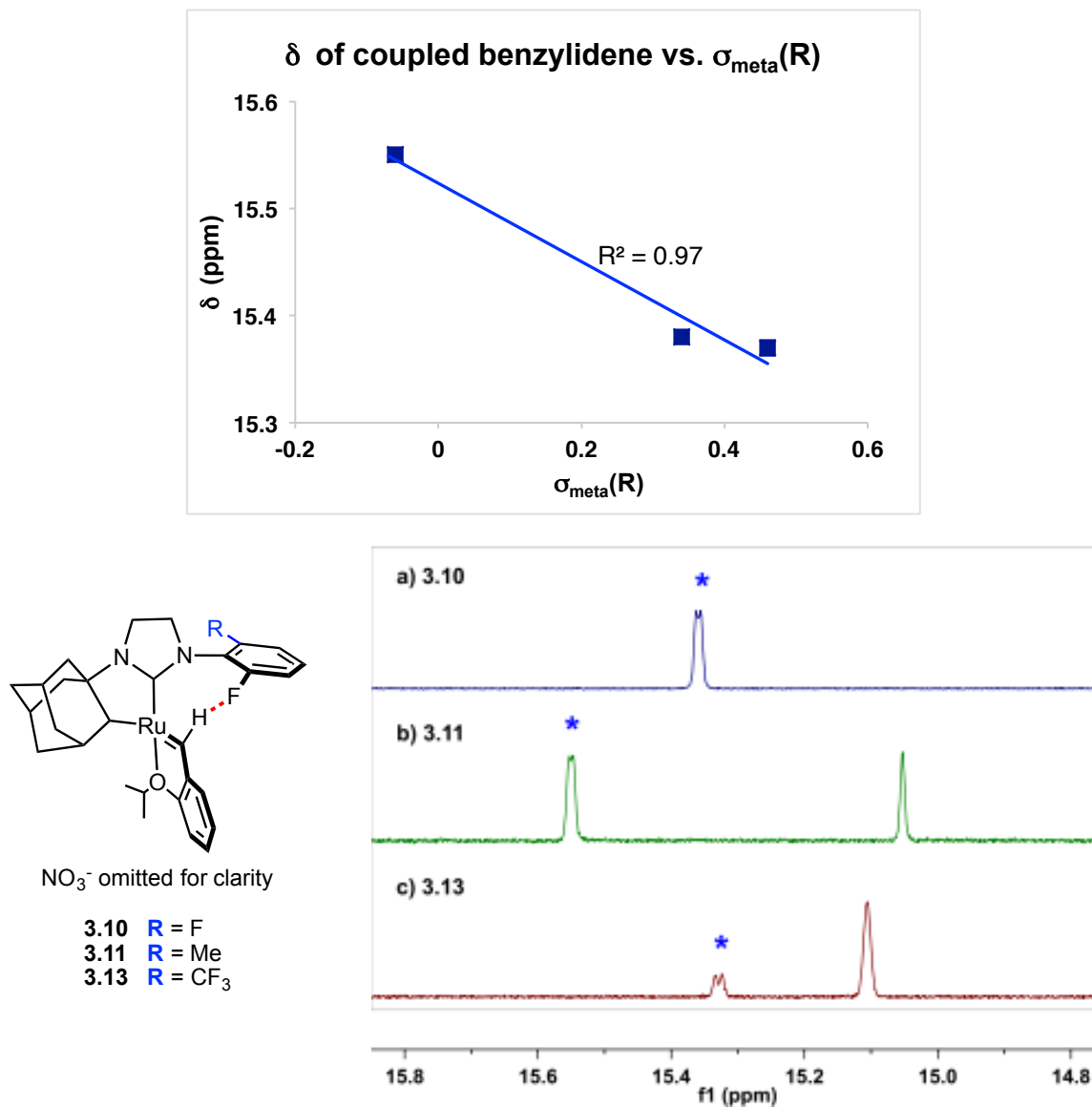


Figure 3.11. Plot of chemical shift of benzylidene peak coupled to ^{19}F for each of catalysts **3.10**, **3.11**, and **3.13** against the σ_{meta} value for the other N-aryl substituent. Benzylidene region of ^1H -NMR spectra of the catalysts, indicating the peaks used for the plot.

The negative slope of the plot in **Figure 3.11** is consistent with a weak

intramolecular hydrogen-bonding-type interaction.³⁷ A decreased σ_{meta} value correlates with increased electron density on the fluorine atom, which makes it a better hydrogen-bond acceptor. The improved acceptor ability of the F atom leads to a stronger hydrogen bond, which results in increased deshielding of the H-bond donor (the benzylidene hydrogen atom) and a downfield shift of the benzylidene proton signal in the ^1H -NMR spectrum. Evidence for $\text{C-H}\cdots\text{F-C}$ interactions has also been observed in a number of TM-based α -olefin polymerization catalysts, including group 4 complexes bearing fluorinated bis(phenoxyimine) or fluorinated pincer ligands, as well as in group 10 metal complexes bearing fluorinated phenoxyimine ligands.³⁸⁻⁴¹

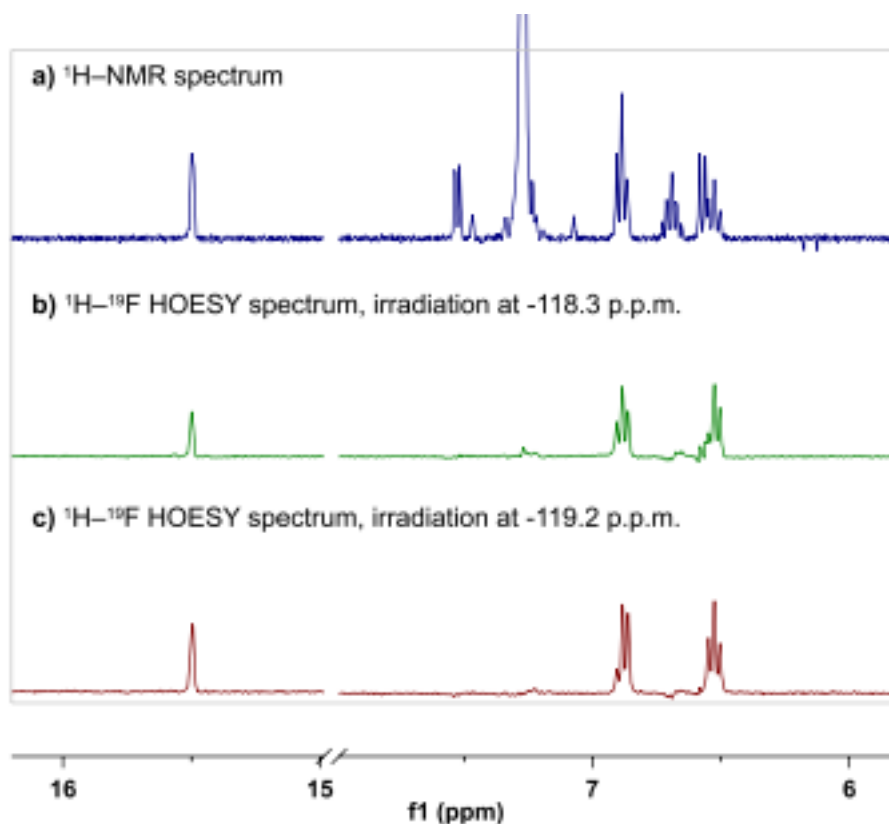


Figure 3.12. ^1H - ^{19}F HOESY spectra illustrating almost equal NOE to both aromatic protons ortho to F. **a)** Benzylidene and aromatic region of ^1H -NMR spectrum for catalyst **3.10**. **b)** and **c)** Benzylidene and aromatic region of ^1H - ^{19}F HOESY spectra with relaxation delay = 3.0 s and **b)** irradiation at -118.3 p.p.m. **c)** -119.2 p.p.m. (Gaussian resolution enhanced).

While the $^1\text{H}\{^{19}\text{F}\}$ selective decoupling experiments illustrated specific coupling between the benzylidene and one of the two fluorine atoms for catalyst **3.10**, ^1H - ^{19}F 1D-HOESY experiments with an irradiation time of 3.0 s demonstrated that excitation of either fluorine atom resulted in an almost equal NOE to both N-aryl meta protons (**Figure 3.12**).

In addition, ^{19}F -NMR experiments with continuous wave presaturation of the downfield ^{19}F resonance, the intensity of the upfield resonance was found to decrease with longer irradiation times (**Figure 3.13**). These observations are consistent with rotation about the N-C(aryl) bond occurring, which results in the two fluorine atoms undergoing exchange. A ^1H 2D-NOESY/EXSY experiment (mixing time = 400 ms)

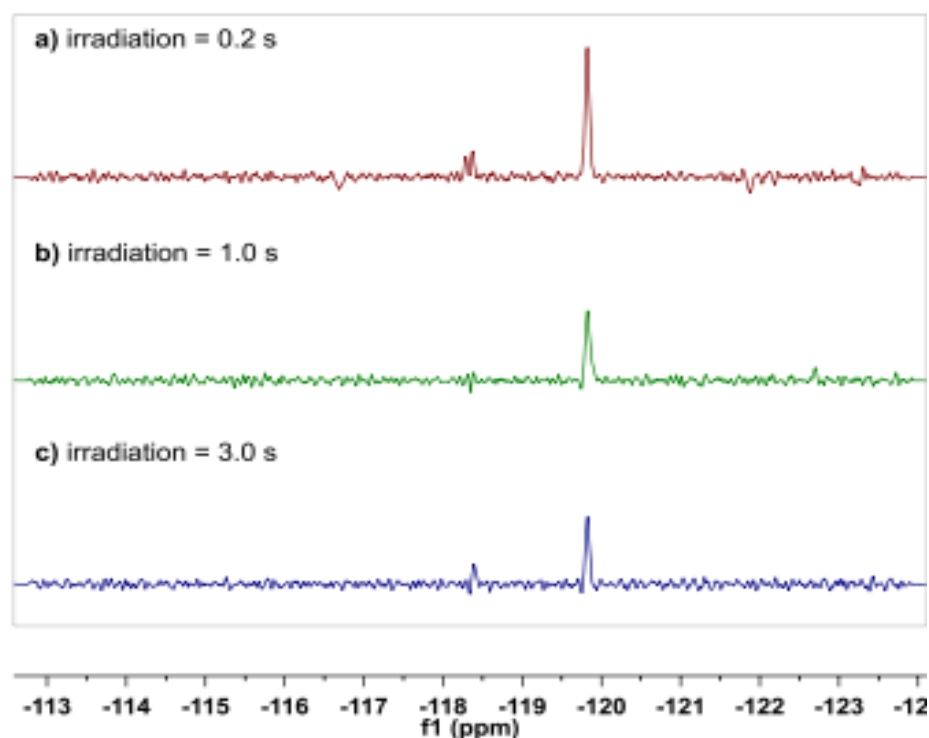


Figure 3.13. ^{19}F -presaturation experiments for catalyst **3.10**, illustrating decrease in intensity of non-irradiated ^{19}F peak. Presaturation carried out with continuous wave irradiation at -118.3 p.p.m. for **a)** 0.2 s. **b)** 1.0 s **c)** 3.0 s (Gaussian resolution enhanced).

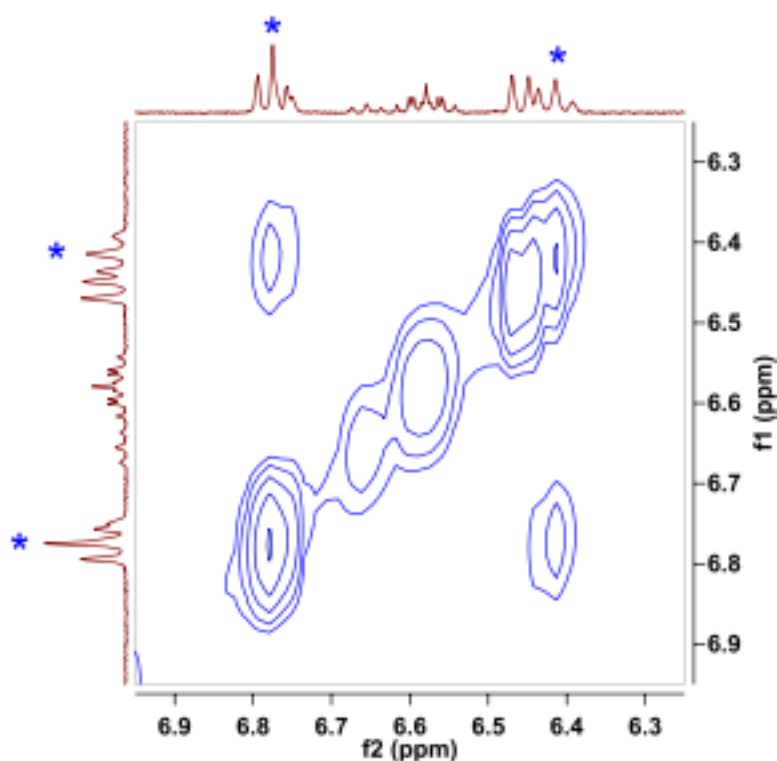


Figure 3.14. Partial ^1H -ROESY/EXSY spectrum of catalyst **3.10** indicating exchange of meta aromatic protons. Mixing time = 400 μs .

further supported rotation about the N–C(aryl) bond, as an exchange cross peak is observed for the meta protons of the N-aryl group (**Figure 3.14**). Rotation about the N–C(aryl) bond of the NHC is expected to be lower for **3.10** than for other catalysts, due to reduced steric clashing between the small ortho-F substituents and the NHC backbone which is consistent with the small fluorine substituent causing minimal steric clash with the NHC backbone.⁴²

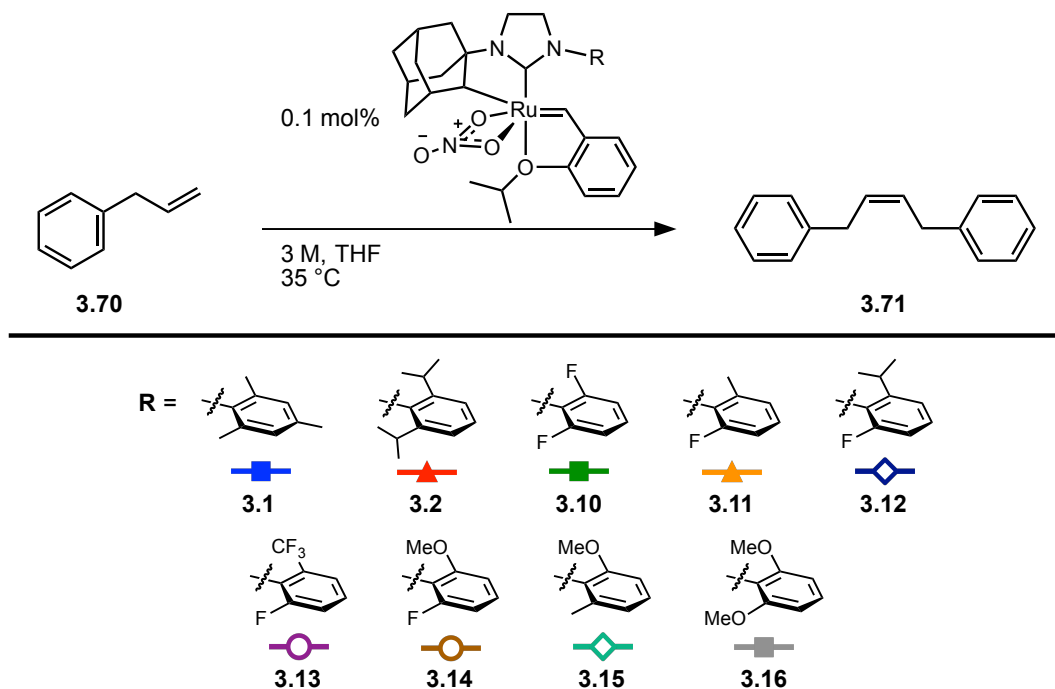
While the limited stability of the catalysts in solution, particularly at higher temperatures, has limited our ability to study the behavior of these catalysts, significant insight into the dynamic behavior of catalyst **3.10** has been elucidated. In addition, we have probed a through-space C–H \cdots F–C interaction that displays characteristics of an

intramolecular hydrogen-bond, which has not been observed previously for a transition metal carbene, to the best of our knowledge. Further studies on the nature of this interaction and the dynamic behavior of catalysts **3.10–3.16** are currently being pursued *via* both computational and NMR spectroscopy approaches.

Reactivity

Homodimerization of Allylbenzene

We then set out to probe the reactivity of the new series of catalysts, **3.10–3.16**, and compare them to the previous catalysts **3.1** and **3.2**. The homodimerization of allylbenzene (**3.70**) to form (*Z*)-1,4-diphenylbut-2-ene (**3.71**) has proved a useful benchmark reaction for probing *Z*-selective metathesis catalysts (**Scheme 3.11**).^{1,12,15,21} **3.70** is a relatively unhindered olefin, which readily undergoes homodimerization and the reaction allows for easy monitoring by either GC or NMR spectroscopy. A significant decomposition route in the case of the cyclometallated catalysts involves decomposition of the catalyst to a Ru hydride species, which are known to effect olefin migration. **3.70** is particularly susceptible to olefin migration isomerization, as this results in the formation of β -methylstyrene (**3.72**), which is stabilized by conjugation.⁴³ As such, it can also serve as a useful measurement of the stability of the catalysts with respect to hydride formation.



Scheme 3.11. Homodimerization of allylbenzene at 0.1 mol% catalyst loading.

Given the high activity observed with **3.1** and **3.2**, a low catalyst loading of 0.1 mol% was used in the homodimerization of allylbenzene in order to maximize observation of differences between the catalysts. The reactions were conducted at 3 M in THF and monitored by $^1\text{H-NMR}$ spectroscopy. **Figure 3.15A** is a plot of conversion vs. time for the nine catalysts. Initial observations include that **3.1** has a higher conversion than **3.2** at 15 minutes, which is consistent with its higher activity in CM of allylic-substituted olefins (**Chapter 2**), although by 1 h. the two catalysts have reached high conversion. Both catalysts are more active than the catalysts **3.10–3.16**, which demonstrate lower conversions than either **3.1** or **3.2** at early timepoints. Over the course of 7 h., all of the catalysts apart from **3.14** reach a conversion of >95%, demonstrating good homodimerization activity. In addition, excellent selectivity for homodimerization

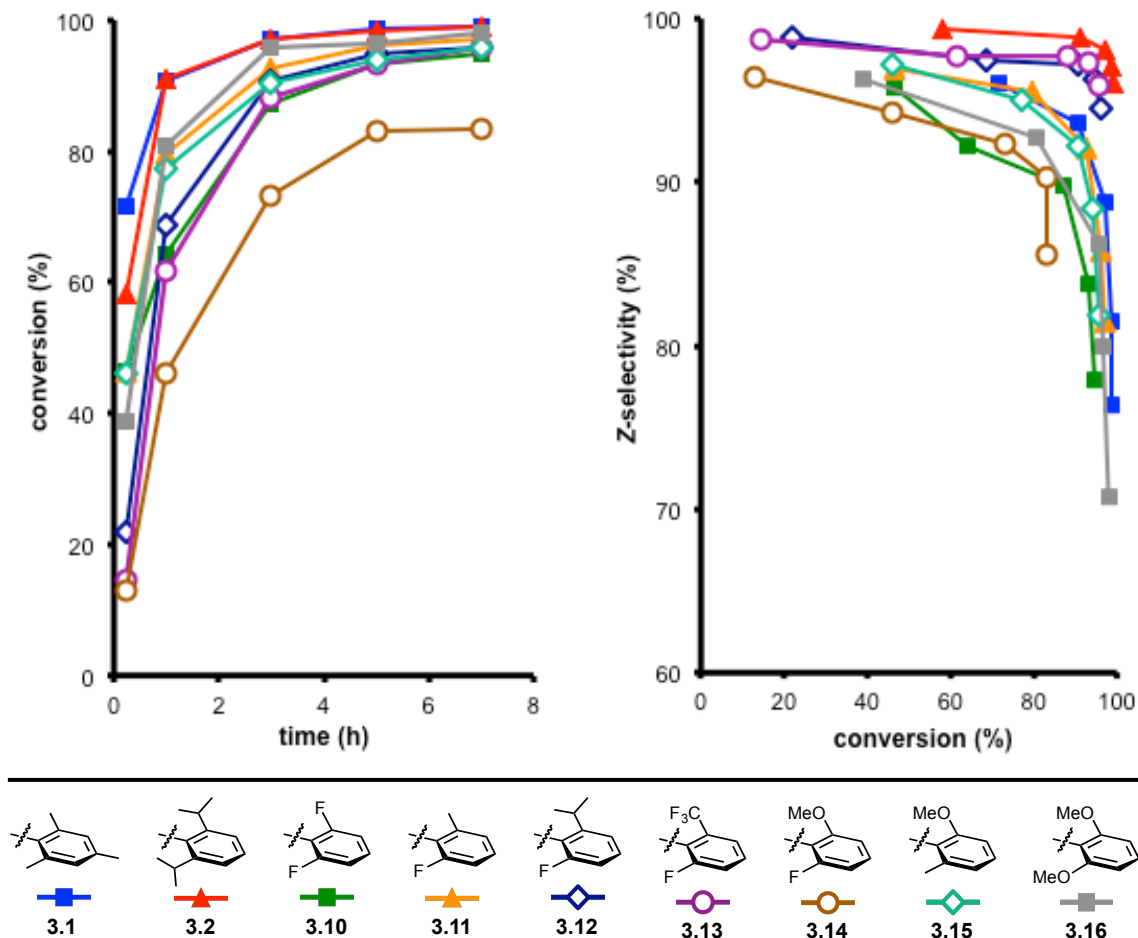


Figure 3.15. A) Plot of conversion vs. time and B) Z-selectivity vs. conversion in the homodimerization of allylbenzene, under conditions outlined in **Scheme 3.11**.

over olefin migration was observed (>30:1 at 7 h.), suggesting little decomposition to Ru hydride species.

Replacement of an ortho-alkyl substituent with either a fluoro or methoxy group of **3.1** and **3.2** results in a catalyst that displays lower reactivity (**Figure 3.16**). In addition, **3.10**, which has two ortho-F substituents, is less active than **3.11**, which has one ortho-F substituent. This is suggestive that altering the electronic nature of the N-aryl group is having an effect on the reactivity of the catalyst. The C–F⋯H–C interaction may

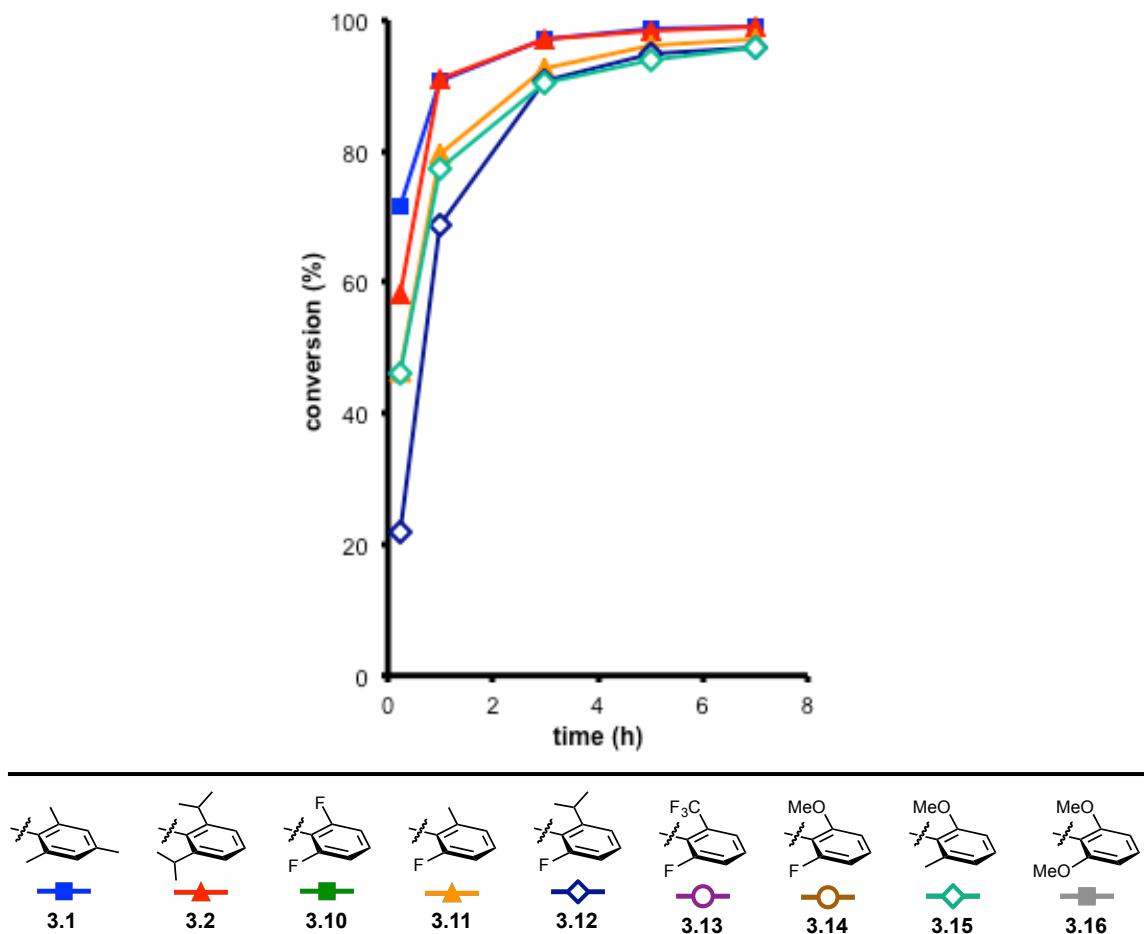


Figure 3.16. Plot of conversion vs. time in the homodimerization of allylbenzene, illustrating the influence of ortho-fluoro and ortho-methoxy substituents.

also play a role in the reactivity of the catalysts, as this may stabilize the pre-catalyst, adding an additional barrier to be overcome in order to undergo reaction. In complexes that have relatively similar electronic characteristics, the one with the smaller ortho substituent displays higher activity (for example, reactivity of **3.1** > **3.2** and **3.11** > **3.12**).

Figure 3.15B is a plot of the *Z*-selectivity of the allylbenzene homodimer vs. conversion for the nine catalysts. In all cases, the *Z*-selectivity of the homodimer is eroded at high conversion, as has previously been observed for other *Z*-selective

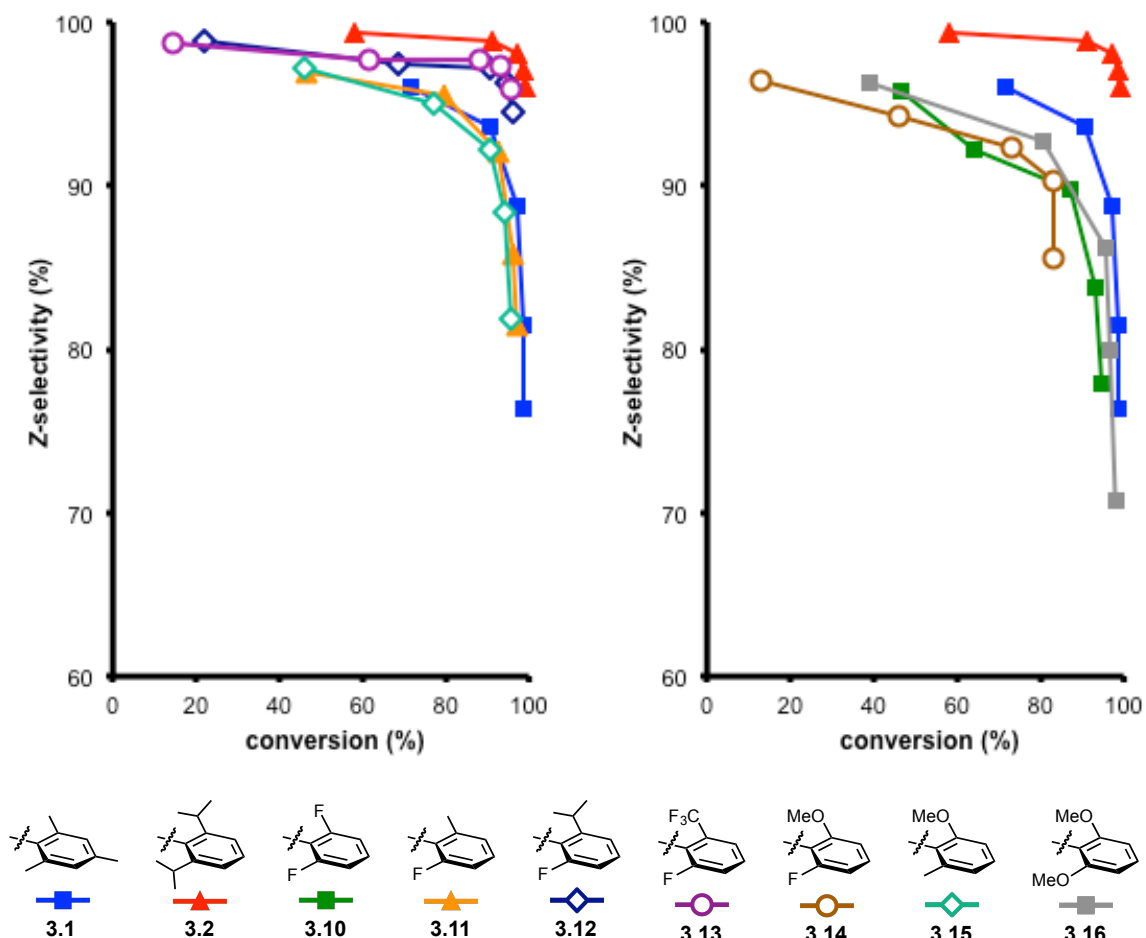


Figure 3.17. Plots of Z-selectivity vs. conversion for homodimerization of allylbenzene, illustrating **A)** Catalysts whose larger N-aryl o-substituent is similar behave similarly. **B)** Catalysts with ortho-F or ortho-OMe substituents are less Z-selective.

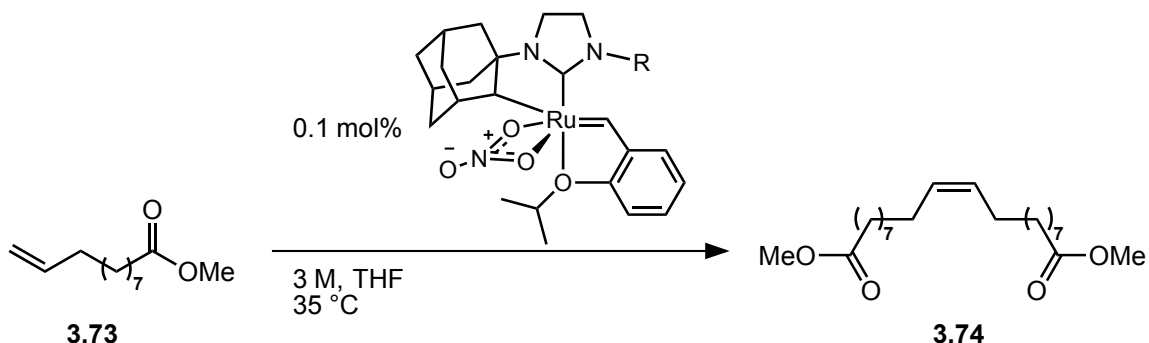
metathesis catalysts.^{1,44,45} A closer look at select series of catalysts highlights some key observations about the nature of the N-aryl group and the observed Z-selectivity with respect to conversion.

Of the catalysts studied, **3.2** displays the highest initial Z-selectivity and the smallest decrease in Z-selectivity with increasing reaction time (**Figure 3.17A**). **3.12** and **3.13** outperform the commercially available catalyst, **3.1**, demonstrating higher Z-selectivity at comparable conversion. They display low degradation of Z-content at high

conversion, comparable to **3.2** and distinct from the more significant degradation observed with other catalysts. At 7h., both catalysts achieve 96% conversion with a Z-selectivity of 94% and 96%, respectively. Although catalysts **3.11** and **3.15** display lower activity than **3.1**, the three catalysts display very similar profiles in the plot of conversion vs. Z-selectivity. The common feature of these three catalysts is that they possess one ortho-Me substituent on the N-aryl group, while the other ortho substituent varies, being F (**3.11**), OMe (**3.15**) or Me (**3.1**). **Figure 3.17B** demonstrates that catalysts **3.10**, **3.14** and **3.16**, which contain only ortho-F and/or ortho-OMe groups display lower Z-selectivity than the other catalysts in this reaction.

These trends are consistent with the larger of the two ortho substituents of the N-aryl group playing a dominant role in determining the Z-selectivity vs. conversion profile across the series of catalysts, with the smaller ortho-substituent playing a lesser role in affecting catalyst behavior. The effective size of the ortho-substituent in these systems follows the trend $\text{CF}_3 \sim \text{}^i\text{Pr} > \text{Me} > \text{OMe} \sim \text{F}$, which shows some semblance to the order predicted by various steric parameters (including A-values, Charton and Taft): $\text{CF}_3 > \text{}^i\text{Pr} > \text{Me} > \text{OMe} > \text{F}$.⁴⁶⁻⁴⁸ The sterically congested nature of the cyclometallated catalyst system is likely to impose unique steric constraints that influence the effective size of the substituents and so a direct correlation with any of these parameters is not expected or observed. The generality of the observed trends was then examined in the homodimerization of methyl-10-undecenoate and 4-penten-1-ol.

Homodimerizations of Methyl-10-undecenoate and 4-Penten-1-ol



Scheme 3.12. Homodimerization of methyl-10-undecenoate at 0.1 mol% catalyst loading.

The catalysts were then examined in the homodimerization of methyl-10-undecenoate (**3.73**) (**Scheme 3.12**). Methyl-10-undecenoate has been demonstrated to be a less reactive substrate in CM reactions and so can be used to further discriminate between the catalysts. Here, there was a greater difference between catalysts with regard to conversion vs. time was observed, although the same trends as observed in the case of allylbenzene homodimerization were generally conserved (**Figure 3.18**). Again, the most active catalysts are **3.1** and **3.2**, which both reach 95% conversion by 3 h. and the least active catalyst is **3.14**, which has only reached 68% conversion by 9 h. The other catalysts all perform between these two extremes, reaching 85-95% conversion by 9 h. While initial levels of *Z*-selectivity reflect the order observed in the case of allylbenzene homodimerization, increased *Z*-degradation is observed **3.10–3.16** compared to **3.1** and **3.2**. In particular, catalysts **3.12** and **3.13**, which showed a low decrease in the *Z*-selectivity of **3.71** at high conversion, showed a much more significant decrease in the case of **3.74**. The catalysts that showed the lowest decrease in *Z*-selectivity were **3.11** and **3.12**.

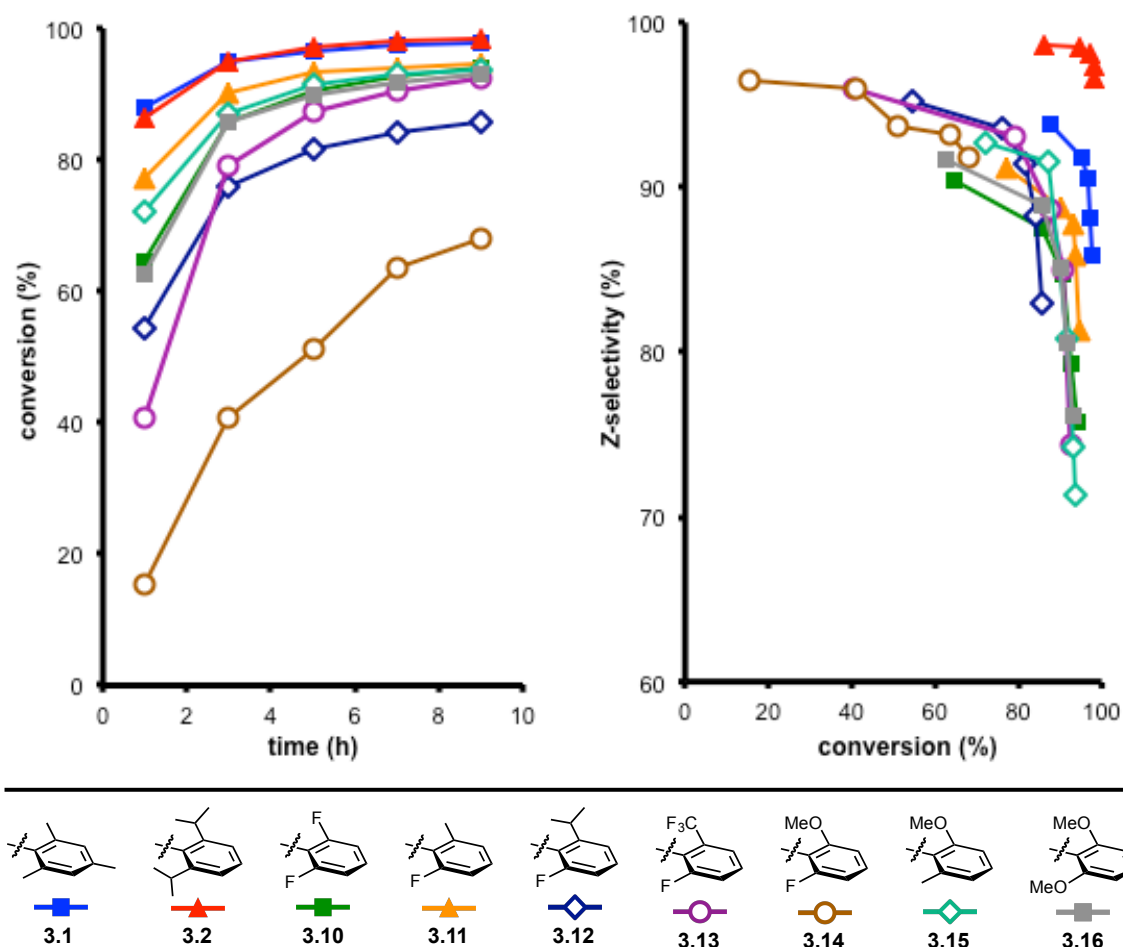
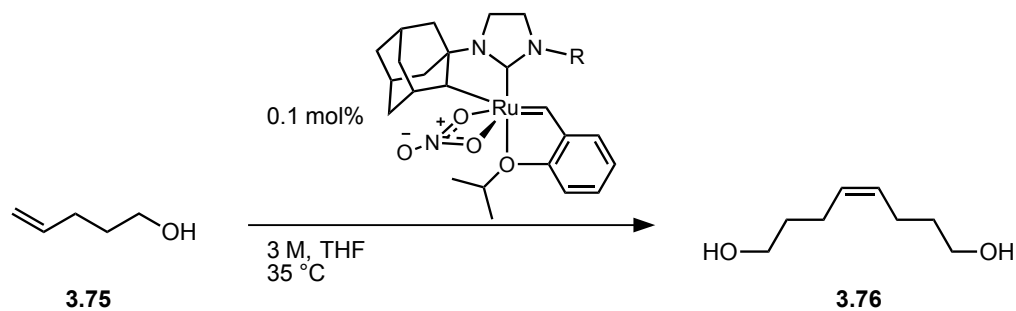


Figure 3.18. A) Plot of conversion vs. time and B) Z-selectivity vs. conversion in the homodimerization of methyl-10-undecenoate, under conditions outlined in **Scheme 3.12**.

4-penten-1-ol (**3.75**) is another substrate that has proved challenging in Z-selective CM reactions, as it is typically less reactive than other substrates and also tends to show enhanced degradation of Z-content in comparison to other substrates (**Scheme 3.13**).^{1,21} In homodimerization of **3.75**, the order of activity of the catalysts was significantly changed from that for homodimerization of **3.70** or **3.73** (**Figure 3.19**). While **3.1** and **3.2** displayed the highest conversion at 1 h., they were closely followed by methoxy-substituted catalysts **3.15** and **3.16**, which displayed significantly higher



Scheme 3.13. Homodimerization of 4-penten-1-ol at 0.1 mol% catalyst loading.

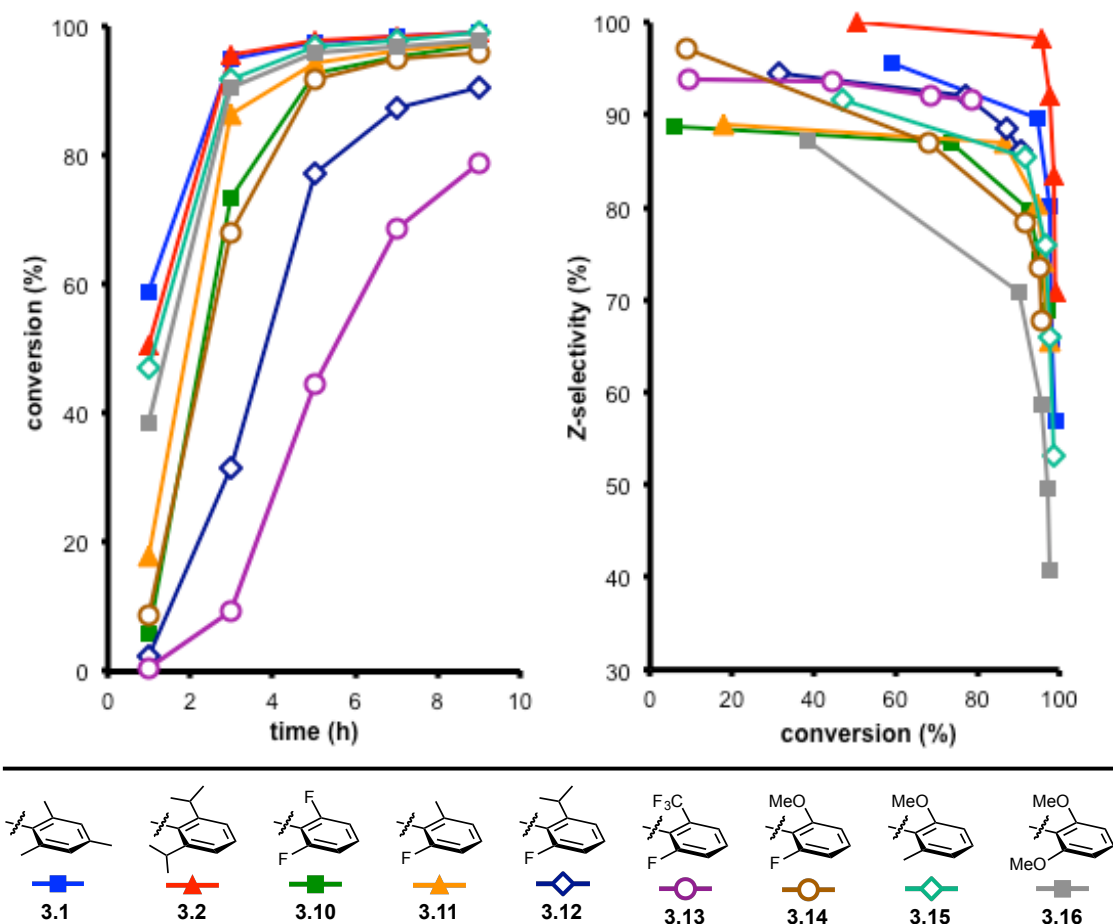


Figure 3.19. A) Plot of conversion vs. time and B) Z-selectivity vs. conversion in the homodimerization of 4-penten-1-ol, under conditions outlined in **Scheme 3.13**.

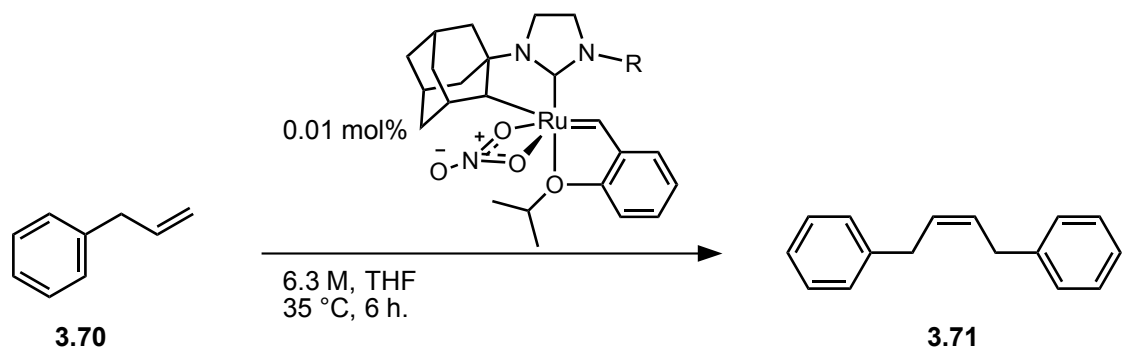
conversions than the remaining catalysts. In addition, catalyst **3.14**, which displayed the lowest rate of conversion to **3.70** and **3.73** (and did not reach full conversion in the same

timeframe as the other catalysts), displayed significantly enhanced activity in 4-penten-1-ol homodimerization. The enhanced reactivity of catalysts **3.14–3.16**, which have an N-aryl group bearing an ortho-methoxy substituent, may be a consequence of a secondary interaction with the alcohol functionality in the substrate. Catalysts **3.12** and **3.13** displayed the lowest activity for this substrate.

Significantly higher Z-degradation is observed in the case of 4-penten-1-ol than in the case of the other two substrates examined. This is particularly noted in the case of catalyst **3.16**, where the Z-selectivity drops below 50% at ~7 h. In addition, catalyst **3.2**, which displays a very limited decrease in Z-selectivity at high conversions in the other homodimerization reactions, here demonstrates rapid erosion of Z-content at high conversion. The vastly different behavior for Z-degradation in homodimerization of **3.76** compared to other substrates suggests that there may be another mechanism contributing to the Z-degradation in the homodimerization of 4-penten-1-ol.

T.O.N. Experiments

In order to further probe the activity and stability of these catalysts and to investigate their overall stability, we decided to investigate the homodimerization of



Scheme 3.14. Homodimerization of allylbenzene at 0.01 mol% catalyst loading.

allylbenzene at 0.01 mol% catalyst loading (**Scheme 3.14**). Consistent with previous results, catalysts **3.1** and **3.2** demonstrated the highest activity with T.O.N. of 8800 and 8700, respectively (**Figure 3.20**). The next most active catalysts were the catalysts without an ortho-F, **3.15** and **3.16**, which both gave a T.O.N. of 7200, followed closely by **3.11** with a T.O.N. of 6800. Notably, all of the catalysts demonstrated a T.O.N. of >5,000 under these conditions, indicating that they are all relatively active for this substrate. The Z-selectivity largely reflects the same trends observed at higher catalyst loading. Again there is a loose correlation between increasing bulk of the N-aryl ortho substituents and decreasing activity, although there also appears to be an electronic component, which may be an indirect electronic effect or, in the case of the fluoro-aryl

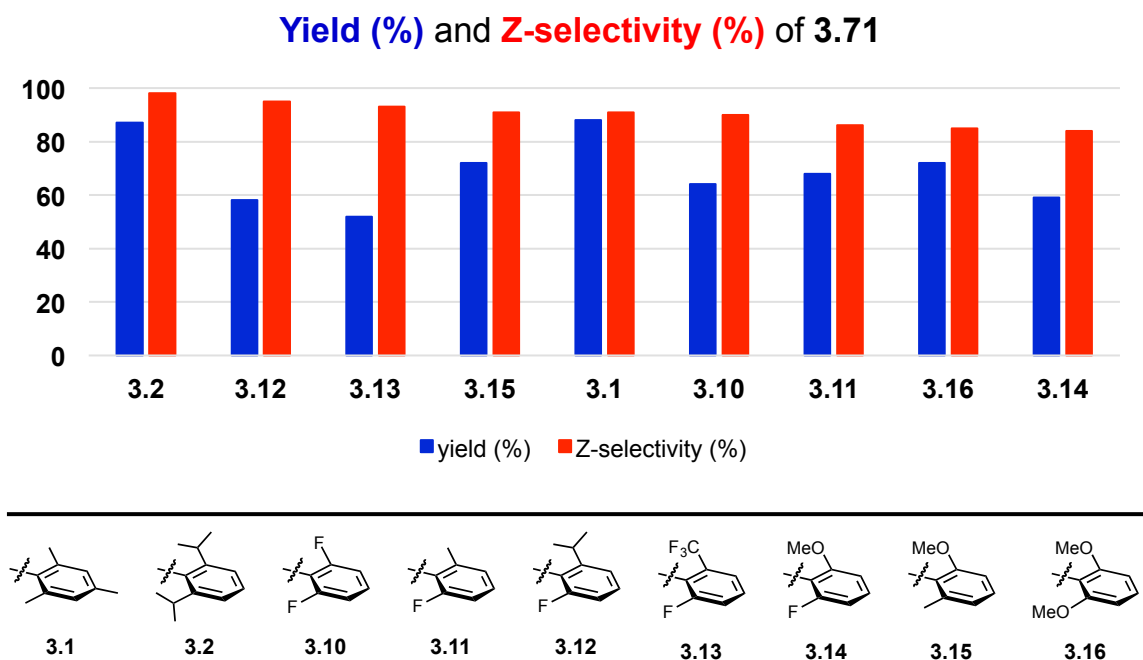
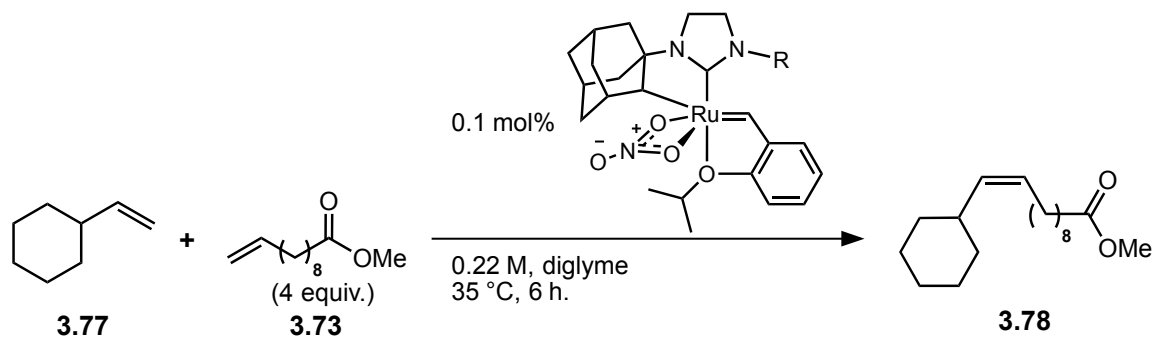


Figure 3.20. Yield and Z-selectivity of homodimer **3.71** at 6 h. in the homodimerization of allylbenzene (ordered by decreasing Z-selectivity) according to **Scheme 3.14**. Yield and Z-selectivity determined by GC, using tridecane as an internal standard.

groups, a direct result of the C–F⋯H–C interaction between the N-aryl group and the benzylidene.

CM of Allylic-substituted Olefins

Given the larger difference observed between catalyst **3.1** and **3.2** in reactions of allylic-substituted olefins, we wanted to examine the new catalysts **3.10–3.16** in one of these reactions. While CM of vinyl dioxolane or other vinyl acetals could be carried out in good yield and high Z-selectivity using catalyst **3.2** (Chapter 2), vinyl cyclohexane **3.77** proved a much more challenging substrate (Scheme 3.15). Under optimized conditions, cross product **3.78** could be formed in 50% yield and with 74% Z-selectivity using catalyst **3.1**, whereas catalyst **3.2** furnished a significantly lower yield of product (16%), albeit with a higher Z-selectivity of 93% (Figure 3.21). The series of catalysts, **3.10–3.16**, were screened under the same conditions and several interesting observations about the reactivity were noted. The activity observed across the series of catalysts can be correlated with two major features. Firstly, the size of the larger ortho substituent seems to have a significant impact on the overall activity, with catalysts **3.2**, **3.12**, and **3.13** all



Scheme 3.15. CM of vinyl cyclohexane and methyl-10-undecenoate

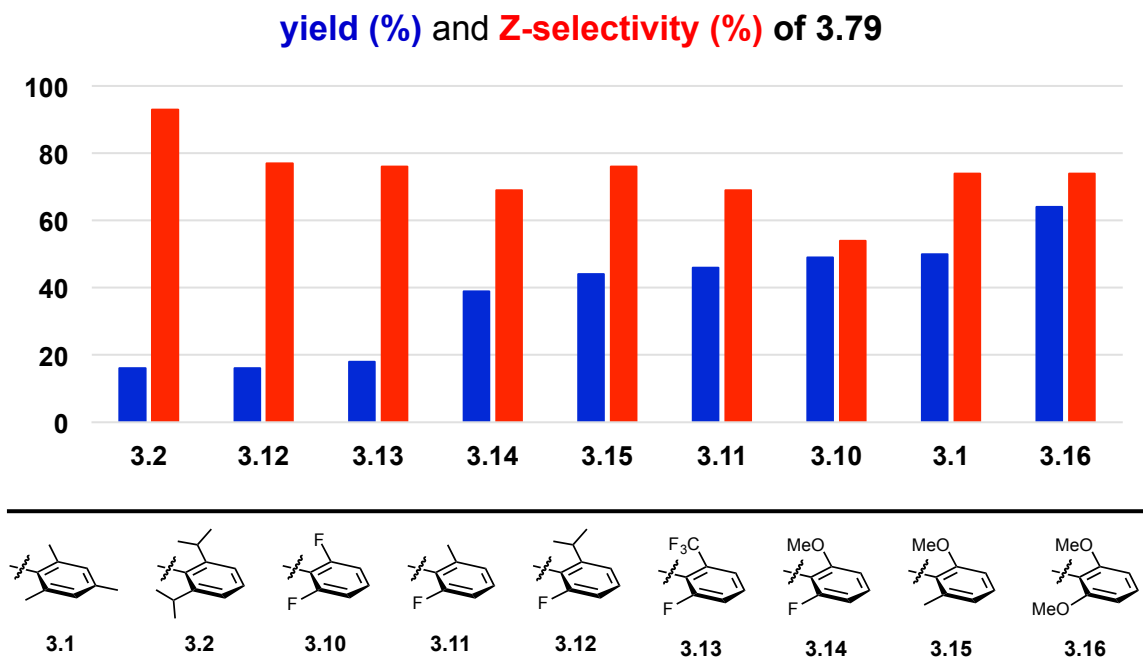


Figure 3.21. Yield and Z-selectivity of cross product **3.79** at 6 h. (ordered by increasing yield). Reaction conducted according to **Scheme 3.15**. Yield and Z-selectivity determined by GC, using tridecane as an internal standard.

giving low yields ranging from 16–18%. This seems to be balanced somewhat by an electronic effect of the ortho substituents, which was observed in the case of the homodimerization reactions discussed previously, in which o-F substituents led to reduced reactivity. **3.14**, which was the least reactive catalyst in homodimerizations of allylbenzene and methyl-10-undecenoate, gives a significantly higher yield of 39%. While the relative order of reactivity in homodimerization reactions was **3.1** > **3.11** > **3.10**, the three catalysts all generate a similar yield of cross product **3.78** (50%, 46%, and 49%, respectively). Unexpectedly, catalyst **3.16** gives the highest yield of **3.78** (64%) in this reaction, surpassing the previous best result with **3.1** (50%) and the product is formed with similar Z-selectivity (74%).

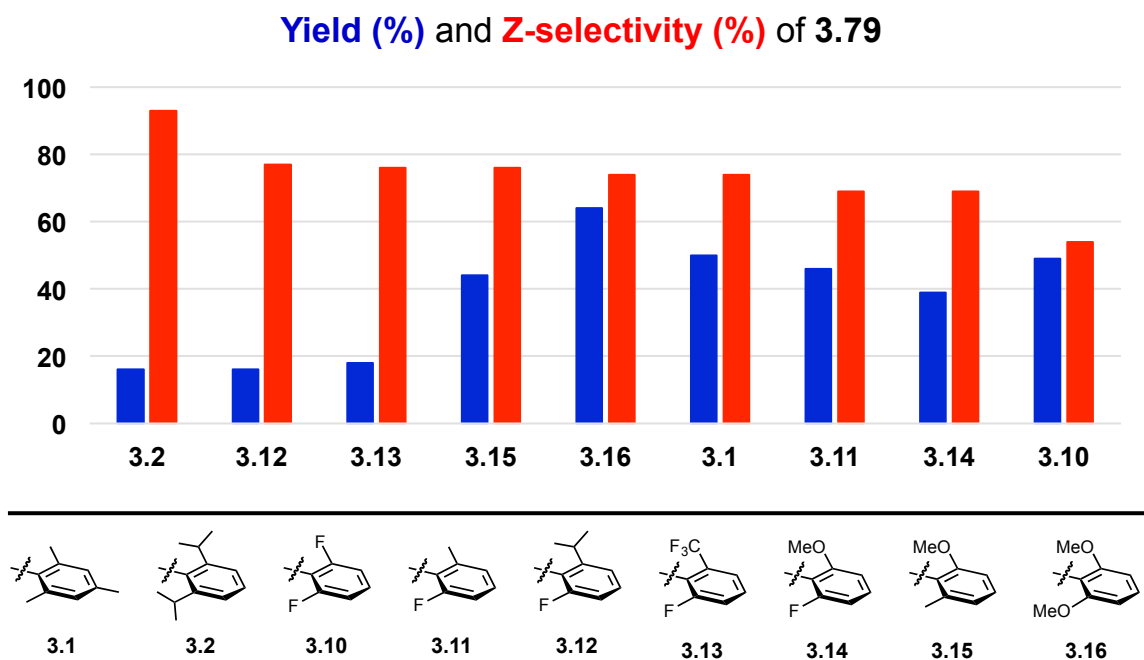


Figure 3.22. Yield and Z-selectivity of cross product **3.79** at 6 h. (ordered by descending Z-selectivity). Reaction conducted according to **Scheme 3.15**. Yield and Z-selectivity determined by GC, using tridecane as an internal standard.

While the larger of the two ortho substituents seems to play a dominant role in the reactivity of the complexes, both of the ortho substituents seem to be significant in governing the Z-selectivity of the catalysts (**Figure 3.22**). Catalyst **3.2** is the only catalyst that exceeds 90% Z-selectivity. Conversely, catalyst **3.10**, which bears the least bulky N-aryl group, displays the lowest Z-selectivity with only a marginal preference for the Z-isomer (54%). All of the other catalysts fall in a relatively narrow range of 69 to 77% Z-selectivity despite significant variance in the size of their substituents. While catalysts **3.12** and **3.13** demonstrated significantly higher Z-selectivity than catalyst **3.1** in homodimerization reactions, they were only marginally more Z-selective in the formation of **3.78** (76–77% vs. 74%) (**Figure 3.23**). Catalyst **3.16** displayed identical Z-selectivity to **3.1** in this CM reaction, which contrasted with its homodimerization reactivity, where

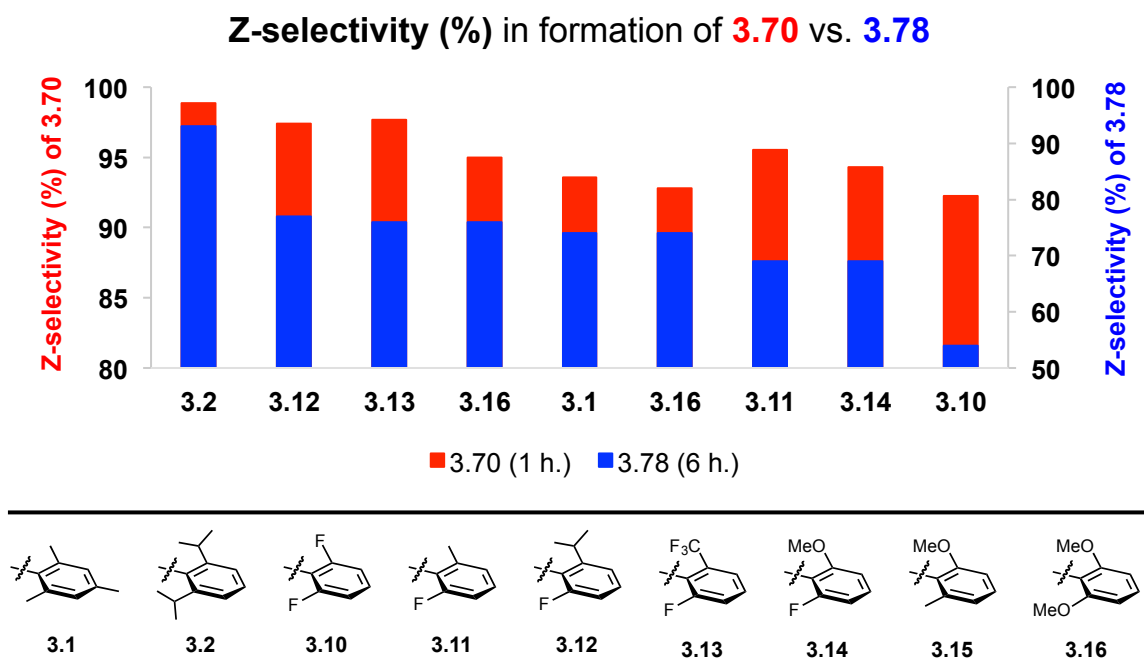


Figure 3.23. Comparison of Z-selectivity observed in formation of **3.70** (Scheme 3.11) at 1h. compared to Z-selectivity observed in formation of **3.78** (Scheme 3.15) at 6 h. (ordered by descending Z-selectivity for the latter reaction). Z-selectivity determined by GC, using tridecane as an internal standard.

it displayed lower Z-selectivity than **3.1**. The improved performance of **3.16** in these systems may be a result of the steric flexibility of the methoxy group, which may allow improved reactivity while still maintaining Z-selectivity comparable to **3.1**.

Conclusion

A series of seven new cyclometallated Ru-based metathesis catalysts that differ in the identity of the N-aryl group have been prepared. In these catalysts, the unique constraints imposed by the cyclometallated NHC ligand have introduced a number of interesting features with respect to their solution-phase behavior. The dynamic behavior of the catalysts arising from rotation about the N–C(aryl) bond is studied by NMR

spectroscopy. In a number of the catalysts bearing an NHC with an unsymmetrical N-aryl group, this results in the presence of two distinct conformational isomers, which differ in the orientation of the N-aryl group with respect to the benzyldiene. In addition, an unusual intramolecular C–H···F–C interaction between the benzyldiene hydrogen and the ortho-fluorine of the N-aryl group is observed in a number of the catalysts and studied by NMR spectroscopy.

The reactivity of these seven catalysts was compared to previous catalysts **3.1** and **3.2** in a number of CM applications, which has allowed us to determine which features of the N-aryl group are key for determining the activity and selectivity of the cyclometallated catalysts. In CM of unhindered terminal olefins, the size of the larger of the two ortho substituents of the N-aryl group plays a dominant role in determining the Z-selectivity, with the second ortho substituent having a less significant effect. The activity of the catalysts seems to be largely dominated by electronic effects, with increased size of the ortho substituents playing a lesser role in attenuating activity. Distinct patterns are observed in CM of an allylic-substituted olefin. Here, the Z-selectivity is found to more closely correlate with the size of the smaller ortho-substituent of the N-aryl group. In contrast, the activity of the catalyst is most closely correlated with the size of the larger of the two ortho substituents, with less bulky N-aryl groups leading to significantly higher yields. Newly prepared catalyst **3.16** generated the highest yield of cross product in CM of vinyl cyclohexane, outperforming both **3.1** and **3.2**, and may find further applications in Z-selective CM of hindered substrates.

The differences in the influence of the N-aryl group on the activity and selectivity of the catalyst between these two classes of olefins are significant. For those catalysts

bearing unsymmetrical N-aryl groups, the results suggest the possibility that the two conformational isomers of the catalyst, differing by rotation about the N–C(aryl) bond, may have different reactivity profiles. The conformer that is more active in the metathesis of unhindered olefins may not be the same conformer that is more active in the metathesis of allylic-substituted olefins. These results suggest that a static picture of catalyst structure may not be sufficient to understand these catalysts and further studies on the dynamic behavior of Ru metathesis catalysts may lead a better understanding of their reactivity. The substrate scope for CM with the cyclometallated Z-selective metathesis catalysts, as explored in this thesis, is currently more limited than for previous generations of metathesis catalysts. The rigid steric constraints necessary to impose high Z-selectivity in these catalysts result in an increased sensitivity to variations in substrate structure, which could potentially be exploited for chemoselective metathesis applications. An improved understanding of the interplay between substrate and catalyst structure in controlling activity and selectivity may result in further improved catalysts for challenging Z-selective metathesis applications.

Experimental Section

Materials and Methods

Unless otherwise stated, solvents and reagents were of reagent quality, obtained from commercial sources and used without further purification. Reactions involving organometallic catalysts were carried out in a nitrogen-filled glovebox or under Ar using standard Schlenk techniques, unless otherwise described. Diglyme was sparged with Ar, stored over 4 Å molecular sieves and filtered over basic alumina prior to use. MeOH used in the preparation of metathesis catalysts was dried over 3 Å molecular sieves, distilled from CaH₂ and degassed by sparging with Ar prior to use. Other solvents involved in the reaction or preparation of organometallic species were purified by passage through solvent purification columns and degassed prior to use.¹ C₆D₆ was purified by passage through a solvent purification column and degassed prior to use. Liquid substrates for cross metathesis were degassed by sparging with Ar and filtered through a short plug of basic alumina prior to use. DCM and CDCl₃ used for the analysis of CM reactions were filtered through a plug of basic alumina prior to use. Flash chromatography was carried out with silica gel 60 (230-400 mesh).

Gas chromatography data was obtained using an Agilent 6850 FID gas chromatograph equipped with a HP-5 (5%-phenyl)-methylpolysiloxane capillary column (Agilent). High-resolution mass spectroscopy was completed at the California Institute of Technology Mass Spectrometry Facility. NMR spectra were recorded on a Varian Inova 400 (400 MHz for ¹H, 128 MHz for ¹¹B, 101 MHz for ¹³C), automated Varian Inova 500 (500 MHz for ¹H, 126 MHz for ¹³C), Varian Inova 600 (500 MHz for ¹H, 151 MHz for ¹³C) or Bruker Avance III 400 (400 MHz for ¹H, 101 MHz for ¹³C). ¹H and ¹³C chemical

shifts are expressed in ppm downfield from tetramethylsilane using the residual protiated solvent (for ^1H) or the solvent (for ^{13}C) as an internal standard (CDCl_3 ^1H : 7.26 ppm and ^{13}C : 77.2 ppm; $\text{DMSO-}d^6$ ^1H : 2.50 ppm and ^{13}C : 39.5 ppm; CD_3OD ^1H : 3.31 ppm and ^{13}C : 49.0 ppm). ^{19}F chemical shifts are expressed in ppm downfield from CFCl_3 using the deuterium signal of the solvent as an internal standard.

Screening-scale Reactions

Typical procedure: CM of vinylcyclohexane and methyl 10-undecenoate

In a nitrogen-filled glovebox, vinylcyclohexane (73 mL, 0.53 mmol, 6 equiv.) and methyl 10-undecenoate (20 mL, 0.09 mmol, 1 equiv.) were combined in a 4 mL vial, to which tridecane (10 mL) was added as an internal standard. A solution of the appropriate catalyst (4.4 mmol, 5 mol%) in diglyme (300 mL) was added and the reaction was stirred open to the atmosphere at 35 °C.

Samples for GC analysis were obtained by taking a 5 mL reaction aliquot and diluting to 1 mL with a 10% v/v solution of ethyl vinyl ether in DCM. Samples were shaken vigorously and allowed to stand for 10 minutes before GC analysis.

GC response factors were obtained for all starting materials and products using tridecane as an internal standard. Data was analysed as previously described.⁵

Instrument conditions: inlet temperature: 250 °C, detector temperature 300 °C, H_2 flow: 30 mL/min, air flow: 400 mL/min, makeup flow: 30 mL/min.

GC method: 80 °C for 2 minutes, followed by a temperature increase of 30 °C/min to 250 °C and held at that temperature for 3 minutes, then a temperature increase

of 5 °C/min to 270 °C, and finally a temperature increase of 30 °C/min to 300 °C and held at that temperature for 3 minutes. Total run time: 18.7 minutes.

Compound	Response Factor	Retention Time (min)
tridecane	-	5.86
vinylcyclohexane	1.71	2.27
methyl-10-undecenoate	1.24	6.44
methyl (Z)-11-cyclohexylundec-10-enoate	0.79	9.21
methyl (E)-11-cyclohexylundec-10-enoate	0.79	9.36
dimethyl (Z)-icos-10-enedioate	0.71	13.90
dimethyl (E)-icos-10-enedioate	0.71	13.97

Typical procedure: homodimerization of allylbenzene at 0.01 mol% catalyst loading

In a nitrogen-filled glovebox, allylbenzene (200 mL, 1.51 mmol, 1 equiv.) and tridecane (20 mL) were combined in a 4 mL vial, to which a solution of the appropriate catalyst (0.15 mmol, 0.01 mol%) in THF (20 mL) was added. The reaction was stirred open to the atmosphere at 35 °C.

Samples for GC analysis were obtained by taking a 5 mL reaction aliquot and diluting to 1 mL with a 10% v/v solution of ethyl vinyl ether in DCM. Samples were shaken vigorously and allowed to stand for 10 minutes before GC analysis. All reactions were carried out in duplicate.

GC response factors were obtained for all starting materials and products using tridecane as an internal standard. Data was analysed as previously described.⁵

Instrument conditions: inlet temperature: 250 °C, detector temperature 300 °C, H₂ flow: 30 mL/min, air flow: 400 mL/min, makeup flow: 30 mL/min.

GC method: 80 °C for 1.5 minutes, followed by a temperature increase of 40 °C/min to 230 °C and held at that temperature for 2 minutes, then a temperature increase of 40 °C/min to 300 °C and held at that temperature for 2.5 minutes. Total run time: 11.5 minutes.

Compound	Response Factor	Retention Time (min)
tridecane	-	4.57
allylbenzene	1.52	2.96
(<i>E</i>)-1,4-diphenylbut-2-ene	0.76	6.22
(<i>Z</i>)-1,4-diphenylbut-2-ene	0.76	6.31

Typical procedures: homodimerization reactions

In a nitrogen-filled glovebox, allylbenzene (150 mL, 1.1 mmol, 1 equiv.) and THF (130 mL) were combined in a 4 mL vial, to which a solution of the appropriate catalyst (1.1 mmol, 0.1 mol%) in THF (100 mL) was added. The reaction was stirred open to the atmosphere at 35 °C.

In a nitrogen-filled glovebox, methyl-10-undecenoate (130 mL, 0.57 mmol, 1 equiv.) and THF (10 mL) were combined in a 4 mL vial, to which a solution of the appropriate catalyst (0.57 mmol, 0.1 mol%) in THF (50 mL) was added. The reaction was stirred open to the atmosphere at 35 °C.

In a nitrogen-filled glovebox, 4-penten-1-ol (117 mL, 1.1 mmol, 1 equiv.) and THF (160 mL) were combined in a 4 mL vial, to which a solution of the appropriate catalyst (1.1 mmol, 0.1 mol%) in THF (100 mL) was added. The reaction was stirred open to the atmosphere at 35 °C.

Samples for $^1\text{H-NMR}$ analysis were obtained by taking a 5 mL reaction aliquot and diluting to 0.65 mL with a 5% v/v solution of ethyl vinyl ether in CDCl_3 . $^1\text{H-NMR}$ spectra were analysed as previously described to determine conversion and *Z*-selectivity.

General Procedures – Catalyst Synthesis

General Procedure 0:

Adapted from a previously reported procedure. To a solution of the carboxylic acid (19.2 mmol, 1 equiv.) in benzene (60 mL, 0.3 M) was added Et_3N (20.2 mmol, 1.05 equiv.) and DPPA (20.2 mmol, 1.05 equiv.). The reaction mixture was then heated to reflux for 12 h. and subsequently cooled to r.t. The solution was poured into a mixture of NaOH (2M, 40 mL/1 g of RCOOH) and THF (40 mL/1 g of RCOOH) with stirring. The organic layer was separated and the aqueous layer extracted with EtOAc (3 x 50 mL). The combined organic layer was washed with brine, dried over Na_2SO_4 and concentrated *in vacuo*. The resultant residue was redissolved in EtOAc , filtered, concentrated *in vacuo*, and purified by flash chromatography on silica gel.

General Procedure 1:

Anhydrous K_2CO_3 (32.8 mmol, 2 equiv.) was added to a solution of the aniline (16.4 mmol, 1 equiv.) in MeCN (200 mL, 0.07 M). Bromoacetyl chloride (16.4 mmol, 1 equiv.) was then added dropwise and the reaction mixture allowed to stir at 20 °C for 3 h. The mixture was filtered, concentrated under reduced pressure, and the resultant residue purified by recrystallization or flash chromatography on silica gel.

General Procedure 2a:

Anhydrous K_2CO_3 (19.7 mmol, 2 equiv.) was added to a solution of the amido bromide (9.8 mmol, 1 equiv.) in MeCN (200 mL, 0.05 M). 1-adamantylamine (14.8 mmol, 2.5 equiv.) was added to the reaction mixture, which was then heated at reflux for 12 h. The mixture was then filtered, concentrated, and the resultant residue was purified by flash chromatography on silica gel.

General Procedure 2b:

Anhydrous K_2CO_3 (19.7 mmol, 2 equiv.) was added to a solution of the amido bromide (9.8 mmol, 1 equiv.) in MeCN (200 mL, 0.05 M). 1-adamantylamine (14.8 mmol, 2 equiv.) was added to the reaction mixture, which was then heated at reflux for 8 h. The mixture was then filtered, concentrated, and the resultant residue was purified by flash chromatography on silica gel.

General Procedure 3a:

THF (100 mL, 0.2 M) was added to a flame-dried, two-neck flask under an atmosphere of argon and cooled to 0 °C. $LiAlH_4$ (51.5 mmol, 3 equiv.) was added portionwise with stirring. The amido amine (17.2 mmol, 1 equiv.) was dissolved in THF (20 mL) and added to the reaction mixture dropwise. The reaction was then warmed to reflux for 36 h. before cooling to room temperature. H_2O (2 mL), 15 w/w% NaOH (2 mL) and H_2O (6 mL) were added slowly sequentially to the reaction mixture. THF was removed *in vacuo* and the residue partitioned between EtOAc (125 mL) and H_2O (50 mL). The aqueous layer was extracted with EtOAc (2 x 50 mL) and the combined organic

layers were washed with H₂O (100 mL), dried over Na₂SO₄, filtered, and concentrated *in vacuo*.

General Procedure 3b:

Amido amine (2.9 mmol, 1 equiv.) was added to a flame-dried, heavy-walled Schlenk flask under an atmosphere of argon. BH₃.THF in THF (1.0 M, 8.7 mmol, 3 equiv.) was then added slowly. When gas evolution had ceased, the Schlenk flask was sealed and heated to reflux for 8 h. The reaction mixture was then cooled to r.t. and MeOH (20 mL) was added slowly and then removed *in vacuo*. A further portion of MeOH (40 mL) was added and then removed *in vacuo*. The resulting residue was then dissolved in MeOH (40 mL) and HCl in Et₂O (2.0 M, 14.5 mmol, 5 equiv.) was added and stirred at 20 °C for 30 min. The reaction mixture was then concentrated *in vacuo* and the resultant solid triturated with Et₂O (40 mL), filtered, washed with Et₂O (3 x 20 mL), and dried *in vacuo*.

General Procedure 4a:

To a solution of diamine (2.0 mmol, 1 equiv.) in Et₂O (10 mL) was added HCl in Et₂O (2.0 M, 4.0 mmol, 2 equiv.) and the reaction mixture was stirred at 20 °C for 30 min. The resultant precipitate was filtered, washed with Et₂O (2 x 20 mL), and dried *in vacuo*. To the resultant solid was added HC(OEt)₃ (30 mmol, 15 equiv.) and MeCN (v/v with HC(OEt)₃). The reaction mixture was heated to reflux for 12 h. and subsequently cooled to r.t. MeCN was removed *in vacuo* and the resulting residue triturated with Et₂O

(20 mL). The Et₂O was decanted and the resulting solid triturated with two further portions of Et₂O (2 x 20 mL). The product was dried *in vacuo* at 35 °C.

General Procedure 4b:

To the diamine dihydrochloride salt (1.3 mmol, 1 equiv.) was added HC(OEt)₃ (19.5 mmol, 15 equiv.) and MeCN (v/v with HC(OEt)₃). The reaction mixture was heated to reflux for 12 h. and subsequently cooled to r.t. MeCN was removed *in vacuo* and the resulting residue triturated with Et₂O (20 mL). The Et₂O was decanted and the resulting solid triturated with two further portions of Et₂O (2 x 20 mL). The product was dried *in vacuo* at 35 °C.

General Procedure 5a:

In a nitrogen-filled glovebox, the NHC salt (1.15 mmol, 1.0 equiv.) and KHMDS (1.11 mmol, 0.96 equiv.) were weighed into a vial, to which benzene (6 mL, 0.2 M) was added. The suspension was stirred at 20 °C for 15 mins, at which stage PCy₃-Hov (0.82 mmol, 0.71 equiv.) was added and the reaction stirred at 35 °C for 3 h. The solution was then removed from the glovebox and pentane (6 mL, v/v with benzene) was added. The green precipitate was filtered and washed with pentane and then 1:1 pentane:Et₂O until the washings were clear. The residue was purified by silica gel plug using DCM as eluant and the product concentrated *in vacuo*.

General Procedure 5b:

The NHC salt (0.66 mmol, 1.0 equiv.) and KHMDS (0.63 mmol, 0.96 equiv.) were weighed into a vial, to which benzene (4 mL, 0.2 M) was added. The suspension

was stirred at 20 °C for 15 mins, at which stage PCy₃-Hov (0.55 mmol, 0.83 equiv.) was added and the reaction stirred at 35 °C for 3 h. The solution was then removed from the glovebox and pentane (4 mL, v/v with benzene) was added. The green precipitate was filtered and washed with 1:1 pentane:Et₂O until the washings were colourless. The residue was purified by silica gel plug using DCM as eluant.

General Procedure 6

In a nitrogen-filled glovebox, to the Ru-complex (0.24 mmol, 1.0 equiv.) and NaOPiv (2.4 mmol, 10 equiv.) was added 2:1 MeOH:THF (7.3 mL, 0.03 M). The reaction mixture was stirred at 35 °C until the solution became purple in colour and no further colour change was noted after 30 min. The solution was concentrated *in vacuo* and the resulting solids triturated with 2:1 pentane:Et₂O (10 mL), filtered, and washed with 2:1 pentane:Et₂O until the washings were colourless. DCM was then added to elute the product, which was obtained after concentration *in vacuo*. To the resulting solid (0.20 mmol) was added NH₄NO₃ (5.9 mmol, 30 equiv.) and 2:1 THF:MeOH (4.0 mL, 0.05 M). The reaction mixture was stirred at 20 °C for 2 h. and then concentrated *in vacuo*. The resultant solids were triturated with 1:1 pentane:Et₂O (5 mL), filtered, and washed with 1:1 pentane:Et₂O (2 x 5 mL). The product was obtained by elution of the solid with DCM and concentration of the resultant solution *in vacuo*.

Experimental Data

3.18

2-fluoro-6-methoxybenzoic acid (2.00 g, 11.8 mmol), TEA (1.72 mL, 1.25 g, 12.3 mmol), and DPPA (2.66 mL, 3.40 g, 12.3 mmol) were reacted according to **general procedure 0**. After purification by silica gel chromatography (gradient elution, hexanes to 80:20 hexanes:EtOAc), product **S0.2** was obtained as an off-white solid (81% yield, 1.34 g). Analytical data matched that previously reported.

3.19

2,6-dimethoxybenzoic acid (3.50 g, 19.2 mmol), TEA (2.81 mL, 2.04 g, 20.2 mmol), and DPPA (4.34 mL, 5.55 g, 20.2 mmol) were reacted according to general procedure 0. After purification by silica gel chromatography (85:15 hexanes:EtOAc), product S0.7 was obtained as a pale yellow solid (70% yield, 2.06 g). Analytical data matched that previously reported.

3.20

Adapted from a previously reported procedure. 2-fluoro-6-bromoaniline (3.00 g, 15.8 mmol), Pd(OAc)₂ (0.071 g, 0.32 mmol), CPhos (0.276 g, 0.63 mmol), and THF (15.8 mL) were added to a flame-dried, three-neck flask under an atmosphere of argon. The reaction was cooled to 0 °C and ⁱPrZnBr in THF (0.5 M, 47.3 mL, 23.7 mmol) was added via cannula. The reaction mixture was then heated to 50 °C and allowed to stir for 3 h. After cooling the mixture to r.t., the reaction was quenched by addition of 1M HCl (20 mL) and extracted with EtOAc (3 x 80 mL). The combined organic layers were washed with brine, dried over MgSO₄, and concentrated *in vacuo*. The crude product was

obtained as a pale yellow oil (93% yield, 2.05 g), which was consistent with previously reported data and used without further purification in the next step.

3.21

2,6-difluoroaniline (6.00 g, 46.5 mmol), K_2CO_3 (12.8 g, 92.9 mmol), and bromoacetyl chloride (3.87 mL, 7.31 g, 46.5 mmol) were reacted according to **general procedure 1**. After purification by silica gel chromatography (70:30 hexanes:EtOAc), product **3.21** was obtained as a white solid (82% yield, 9.37 g as an 89:11 mixture of the Br:Cl products).

1H NMR (500 MHz, $CDCl_3$) δ 7.82 (br s, 1H), 7.30 – 7.20 (m, 1H), 7.02 – 6.92 (m, 2H), 4.06 (s, 2H) ppm.

^{19}F NMR (282 MHz, $CDCl_3$) δ -117.63 – -117.74 (m) ppm.

^{13}C NMR (126 MHz, $CDCl_3$) δ 164.3, 157.9 (dd, $J = 251.9, 4.5$ Hz), 128.5 (t, $J = 9.6$ Hz), 113.2 (t, $J = 16.5$ Hz), 112.0 (dd, $J = 19.3, 4.2$ Hz), 28.6 ppm.

HRMS (FAB) calcd. for $C_8H_7BrF_2NO$ $[M+H]^+$ 249.9679; found 249.9680.

3.22

2-fluoro-6-methylaniline (3.25 g, 26.0 mmol), K_2CO_3 (7.18 g, 51.9 mmol), and bromoacetyl chloride (2.16 mL, 4.09 g, 26.0 mmol) were reacted according to **general procedure 1**. After purification by silica gel chromatography (75:25 hexanes:EtOAc), product **3.22** was obtained as a white solid (92% yield, 5.77 g as a 92:8 mixture of Br:Cl products).

^1H NMR (400 MHz, CDCl_3) δ 7.75 (br s, 1H), 7.24 – 7.14 (m, 1H), 7.03 (d, $J = 7.6$ Hz, 1H), 6.98 (t, $J = 8.9$ Hz, 1H), 4.07 (s, 2H), 2.27 (s, 3H) ppm.

^{13}C NMR (101 MHz, CDCl_3) δ 7.75 (s, 1H), 7.24 – 7.14 (m, 1H), 7.03 (d, $J = 7.6$ Hz, 1H), 6.98 (t, $J = 8.9$ Hz, 4H), 4.07 (s, 2H), 2.27 (s, 3H) ppm.

HRMS (FAB) calcd. for $\text{C}_9\text{H}_{10}\text{BrFNO}$ $[\text{M}+\text{H}]^+$ 245.9930; found 245.9918.

3.23

2-fluoro-6-isopropylaniline (1.20 g, 7.83 mmol), K_2CO_3 (2.17 g, 15.7 mmol), and bromoacetyl chloride (0.65 mL, 1.23 g, 7.83 mmol) were reacted according to **general procedure 1**. After purification by silica gel chromatography (gradient elution, hexanes to 60:40 hexanes:EtOAc), product **3.23** was obtained as a white solid (62% yield, 1.31 g as a 95:5 mixture of Br:Cl products).

^1H NMR (400 MHz, CDCl_3) δ 7.70 (br s, 1H), 7.32 – 7.25 (m, 1H), 7.12 (d, $J = 7.9$ Hz, 1H), 6.98 (t, $J = 8.8$ Hz, 1H), 4.08 (s, 2H), 3.06 (hept, $J = 6.9$ Hz, 1H), 1.23 (d, $J = 6.9$ Hz, 6H) ppm.

^{13}C NMR (101 MHz, CDCl_3) δ 164.25, 157.89 (d, $J = 251.9$ Hz), 128.52 (t, $J = 9.6$ Hz), 113.20 (t, $J = 16.5$ Hz), 111.99 (dd, $J = 19.3, 4.2$ Hz), 28.63 ppm.

HRMS (FAB) calcd. for $\text{C}_{11}\text{H}_{14}\text{BrFNO}$ $[\text{M}+\text{H}]^+$ 274.0243; found 274.0235.

3.24

2-fluoro-6-trifluoromethylaniline (2.00 g, 11.2 mmol), K_2CO_3 (3.09 g, 22.3 mmol), and bromoacetyl chloride (0.93 mL, 1.76 g, 11.2 mmol) were reacted according to **general**

procedure 1. After purification by silica gel chromatography (75:25 hexanes:EtOAc), product **3.24** was obtained as a white solid (97% yield, 3.21 g as a 92:8 mixture of Br:Cl products).

^1H NMR (400 MHz, CDCl_3) δ 7.96 (br s, 1H), 7.49 (d, $J = 7.7$ Hz, 1H), 7.47 – 7.32 (m, 2H), 4.06 (s, 2H) ppm.

^{13}C NMR (101 MHz, CDCl_3) δ 164.25, 157.89 (d, $J = 251.9$ Hz), 128.52 (t, $J = 9.6$ Hz), 113.20 (t, $J = 16.5$ Hz), 111.99 (dd, $J = 19.3, 4.2$ Hz), 28.63 ppm.

HRMS (FAB) calcd. for $\text{C}_9\text{H}_7\text{BrF}_4\text{NO}$ $[\text{M}+\text{H}]^+$ 299.9647; found 299.9643.

3.25

2-fluoro-6-methoxyaniline (1.29 g, 9.14 mmol), K_2CO_3 (2.53 g, 18.3 mmol), and bromoacetyl chloride (0.76 mL, 1.44 g, 9.14 mmol) were reacted according to **general procedure 1**. After recrystallization from EtOAc / hexanes, product **3.25** was obtained as an off-white solid (74% yield, 1.76 g) as a 96:4 mixture of Br:Cl products.

^1H NMR (400 MHz, CDCl_3) δ 7.72 (br s, 1H), 7.21 (td, $J = 8.4, 6.4$ Hz, 1H), 6.82 – 6.74 (m, 1H), 6.72 (d, $J = 8.4$ Hz, 1H), 4.06 (s, 2H), 3.86 (s, 3H) ppm.

^{13}C NMR (101 MHz, CDCl_3) δ 164.25, 157.89 (d, $J = 251.9$ Hz), 128.52 (t, $J = 9.6$ Hz), 113.20 (t, $J = 16.5$ Hz), 111.99 (dd, $J = 19.3, 4.2$ Hz), 28.63 ppm.

HRMS (FAB) calcd. for $\text{C}_9\text{H}_{10}\text{BrFNO}_2^+$ $[\text{M}+\text{H}]^+$ 261.9879; found 261.9879.

3.26

2-methoxy-6-methylaniline (2.25 g, 16.4 mmol), K_2CO_3 (4.54 g, 32.8 mmol), and bromoacetyl chloride (1.37 mL, 2.58 g, 16.4 mmol) were reacted according to **general procedure 1**. After purification by silica gel chromatography (60:40 hexanes:EtOAc), product **3.26** was obtained as an off-white solid (80% yield, 3.34 g as an 89:11 mixture of Br:Cl products).

1H NMR (400 MHz, $CDCl_3$) δ 7.78 (br s, 1H), 7.17 (t, $J = 8.1$ Hz, 1H), 6.85 (d, $J = 7.7$ Hz, 1H), 6.76 (d, $J = 8.3$ Hz, 1H), 4.06 (s, 2H), 3.82 (s, 3H), 2.24 (s, 3H) ppm.

^{13}C NMR (101 MHz, $CDCl_3$) δ 164.2, 154.1, 136.8, 128.0, 123.4, 122.9, 108.6, 55.9, 29.4, 18.4 ppm.

HRMS (FAB) calcd. for $C_{10}H_{13}BrNO_2^+$ $[M+H]^+$ 258.0130; found 258.0132.

3.27

2,6-dimethoxyaniline (3.00 g, 19.6 mmol), K_2CO_3 (5.41 g, 39.2 mmol), and bromoacetyl chloride (1.63 mL, 3.08 g, 19.6 mmol) were reacted according to **general procedure 1**. After trituration of the solid with Et_2O and pentane, product **3.27** was obtained as a white solid (85% yield, 4.50 g as an 88:12 mixture of Br:Cl products).

1H NMR (400 MHz, $CDCl_3$) δ 7.56 (br s, 1H), 7.22 (t, $J = 8.4$ Hz, 1H), 6.60 (d, $J = 8.4$ Hz, 2H), 4.04 (br s, 2H), 3.84 (s, 6H) ppm.

^{13}C NMR (101 MHz, $CDCl_3$) δ 163.9, 155.5, 128.5, 113.4, 104.4, 56.2, 29.5 ppm.

HRMS (FAB) calcd. for $C_{10}H_{13}BrNO_3$ $[M+H]^+$ 274.0079; found 274.0073.

3.28

3.21 (1.50 g, 6.18 mmol), K_2CO_3 (1.66 g, 12.0 mmol), and 1-adamantylamine (2.26 g, 15.0 mmol) were reacted according to **general procedure 2a**. After purification by silica gel chromatography (96:4 DCM:MeOH), product **3.28** was obtained as a white solid (95% yield, 1.98 g).

1H NMR (500 MHz, $CDCl_3$) δ 9.22 (br s, 1H), 7.21 – 7.13 (m, 1H), 6.99 – 6.91 (m, 2H), 3.44 (s, 2H), 2.09 (s, 3H), 1.73 – 1.47 (m, 13H) ppm.

^{13}C NMR (126 MHz, $CDCl_3$) δ 172.0, 157.9 (dd, $J = 250.6, 5.1$ Hz), 127.2 (t, $J = 9.7$ Hz), 114.2 (t, $J = 16.5$ Hz), 111.8 (dd, $J = 19.1, 4.7$ Hz), 51.4, 44.4, 42.8, 36.6, 29.6 ppm.

HRMS (FAB) calcd. for $C_{18}H_{23}F_2N_2O$ $[M+H]^+$ 321.1779; found 321.1764.

3.29

3.22 (4.50 g, 18.5 mmol), K_2CO_3 (5.05 g, 36.6 mmol), and 1-adamantylamine (6.91 g, 45.7 mmol) were reacted according to **general procedure 2a**. After purification by silica gel chromatography (96:4 DCM:MeOH), product **3.29** was obtained as a white solid (92% yield, 5.42 g).

1H NMR (400 MHz, $CDCl_3$) δ 9.17 (br s, 1H), 7.16 – 7.07 (m, 1H), 7.01 (d, $J = 7.6$ Hz, 1H), 6.95 (t, $J = 9.0$ Hz, 1H), 3.43 (s, 2H), 2.26 (s, 3H), 2.10 (s, 3H), 1.75 – 1.52 (m, 13H) ppm.

^{13}C NMR (101 MHz, $CDCl_3$) δ 7.75 (s, 1H), 7.24 – 7.14 (m, 1H), 7.03 (d, $J = 7.6$ Hz, 1H), 6.98 (t, $J = 8.9$ Hz, 4H), 4.07 (s, 2H), 2.27 (s, 3H) ppm.

HRMS (FAB) calcd. for $C_{19}H_{26}FN_2O$ $[M+H]^+$ 317.2029; found 317.2017.

3.30

3.23 (1.16 g, 4.26 mmol), K_2CO_3 (1.17 g, 8.46 mmol), and 1-adamantylamine (1.28 g, 8.46 mmol) were reacted according to **general procedure 2b**. After purification by silica gel chromatography (96:4 DCM:MeOH), product **3.30** was obtained as a white solid (94% yield, 1.39 g).

1H NMR (400 MHz, $CDCl_3$) δ 9.11 (br s, 1H), 7.25 – 7.17 (m, 1H), 7.09 (d, $J = 7.9$ Hz, 1H), 6.96 (t, $J = 8.9$ Hz, 1H), 3.44 (s, 2H), 3.06 (hept, $J = 6.9$ Hz, 1H), 2.10 (s, 3H), 1.78 – 1.53 (m, 13H), 1.22 (d, $J = 6.9$ Hz, 6H) ppm.

^{13}C NMR (101 MHz, $CDCl_3$) δ 164.25, 157.89 (d, $J = 251.9$ Hz), 128.52 (t, $J = 9.6$ Hz), 113.20 (t, $J = 16.5$ Hz), 111.99 (dd, $J = 19.3, 4.2$ Hz), 28.63 ppm.

HRMS (FAB) calcd. for $C_{21}H_{30}FN_2O$ $[M+H]^+$ 345.2342; found 345.2354.

3.31

3.24 (1.50 g, 5.05 mmol), K_2CO_3 (1.38 g, 10.0 mmol), and 1-adamantylamine (1.89 g, 12.5 mmol) were reacted according to **general procedure 2a**. After purification by silica gel chromatography (98:2 DCM:MeOH, then 96:4 DCM:MeOH), product **3.31** was obtained as a white solid (96% yield, 1.79 g).

1H NMR (400 MHz, $CDCl_3$) δ 9.49 (br s, 1H), 7.49 – 7.43 (m, 1H), 7.39 – 7.31 (m, 2H), 3.43 (s, 2H), 2.10 (s, 3H), 1.72 – 1.58 (m, 12H) 1.55 (br s, 1H) ppm.

^{13}C NMR (101 MHz, $CDCl_3$) δ 164.25, 157.89 (d, $J = 251.9$ Hz), 128.52 (t, $J = 9.6$ Hz), 113.20 (t, $J = 16.5$ Hz), 111.99 (dd, $J = 19.3, 4.2$ Hz), 28.63 ppm.

HRMS (FAB) calcd. for $C_{19}H_{23}F_4N_2O$ $[M+H]^+$ 371.1747; found 371.1738.

3.32

3.25 (1.76 g, 6.76 mmol), K_2CO_3 (1.86 g, 13.4 mmol), and 1-adamantylamine (2.03 g, 13.4 mmol) were reacted according to **general procedure 2b**. After purification by silica gel chromatography (97:3 DCM:MeOH), product **3.32** was obtained as an off-white solid (91% yield, 2.05 g).

1H NMR (400 MHz, $CDCl_3$) δ 9.07 (br s, 1H), 7.19 – 7.09 (m, 1H), 6.77 (t, $J = 8.9$ Hz, 1H), 6.70 (d, $J = 8.3$ Hz, 1H), 3.84 (s, 3H), 3.43 (s, 2H), 2.09 (s, 3H), 1.85 – 1.36 (m, 12H) ppm.

^{13}C NMR (101 MHz, $CDCl_3$) δ 164.25, 157.89 (d, $J = 251.9$ Hz), 128.52 (t, $J = 9.6$ Hz), 113.20 (t, $J = 16.5$ Hz), 111.99 (dd, $J = 19.3, 4.2$ Hz), 28.63 ppm.

HRMS (FAB) calcd. for $C_{19}H_{26}FN_2O_2$ $[M+H]^+$ 333.1978; found 333.1962.

3.33

3.26 (2.00 g, 7.90 mmol), K_2CO_3 (2.14 g, 15.5 mmol), and 1-adamantylamine (2.34 g, 15.5 mmol) were reacted according to **general procedure 2b**. After purification by silica gel chromatography (95:5 DCM:MeOH), product **3.33** was obtained as a white solid (95% yield, 2.48 g).

1H NMR (400 MHz, $CDCl_3$) δ 9.11 (br s, 1H), 7.11 (t, $J = 8.0$ Hz, 1H), 6.84 (d, $J = 7.6$ Hz, 1H), 6.74 (d, $J = 8.2$ Hz, 1H), 3.79 (s, 3H), 3.41 (s, 2H), 2.24 (s, 3H), 2.09 (s, 3H), 1.77 – 1.56 (m, 12H), 1.48 (br s, 1H) ppm.

^{13}C NMR (101 MHz, CDCl_3) δ 171.9, 154.0, 136.5, 127.0, 124.5, 122.8, 108.4, 55.7, 51.2, 44.5, 42.8, 36.7, 29.6, 18.8 ppm.

HRMS (FAB) calcd. for $\text{C}_{20}\text{H}_{29}\text{N}_2\text{O}_2$ $[\text{M}+\text{H}]^+$ 329.2229; found 329.2213.

3.34

3.27 (2.40 g, 8.93 mmol), K_2CO_3 (2.42 g, 17.5 mmol), and 1-adamantylamine (2.65 g, 17.5 mmol) were reacted according to **general procedure 2b**. After purification by silica gel chromatography (94:6 DCM:MeOH), product **3.34** was obtained as a white solid (97% yield, 3.00 g).

^1H NMR (400 MHz, CDCl_3) δ 8.82 (br s, 1H), 7.16 (t, $J = 8.4$ Hz, 1H), 6.59 (d, $J = 8.4$ Hz, 2H), 3.82 (s, 6H), 3.41 (s, 2H), 2.09 (s, 3H), 1.80 – 1.48 (m, 13H) ppm.

^{13}C NMR (101 MHz, CDCl_3) δ 172.1, 155.7, 127.5, 114.6, 104.6, 56.2, 51.2, 44.7, 42.8, 36.8, 29.7 ppm.

HRMS (FAB) calcd. for $\text{C}_{20}\text{H}_{29}\text{N}_2\text{O}_3$ $[\text{M}+\text{H}]^+$ 345.2180; found 345.2178.

3.35

3.28 (1.25 g, 3.90 mmol) and LiAlH_4 (0.444 g, 11.7 mmol) were reacted according to **general procedure 3a**. The product **3.35** was obtained as a pale-yellow solid (98% yield, 1.19 g), which was used without further purification.

^1H NMR (400 MHz, CDCl_3) δ 6.85 – 6.73 (m, 2H), 6.67 – 6.57 (m, 1H), 4.22 (s, 1H), 3.40 – 3.29 (m, 2H), 2.79 (t, $J = 5.8$ Hz, 2H), 2.06 (s, 3H), 1.71 – 1.54 (m, 12H), 1.10 (br s, 1H) ppm.

^{13}C NMR (101 MHz, CDCl_3) δ 153.7 (dd, $J = 241.0, 7.8$ Hz), 126.4 (t, $J = 13.9$ Hz), 117.4 (t, $J = 9.5$ Hz), 111.8 – 111.3 (m), 50.4, 47.4 (t, $J = 3.8$ Hz), 43.1, 40.4, 36.9, 29.7 ppm.

HRMS (FAB) calcd. for $\text{C}_{18}\text{H}_{25}\text{F}_2\text{N}_2$ $[\text{M}+\text{H}]^+$ 307.1986; found 307.1974.

3.36

3.29 (5.00 g, 15.8 mmol) and LiAlH_4 (1.79 g, 47.4 mmol) were reacted according to **general procedure 3a**. The product **3.36** was obtained as a pale-yellow solid (93% yield, 4.43 g), which was used without further purification.

^1H NMR (400 MHz, CDCl_3) δ 6.91 – 6.80 (m, 2H), 6.67 (td, $J = 7.9, 5.2$ Hz, 1H), 4.04 (s, 1H), 3.33 – 3.21 (m, 2H), 2.79 (t, $J = 5.8$ Hz, 2H), 2.26 (s, 3H), 2.06 (s, 3H), 1.72 – 1.53 (m, 12H) 0.92 (br s, 1H) ppm.

^{13}C NMR (101 MHz, CDCl_3) δ 7.75 (s, 1H), 7.24 – 7.14 (m, 1H), 7.03 (d, $J = 7.6$ Hz, 1H), 6.98 (t, $J = 8.9$ Hz, 4H), 4.07 (s, 2H), 2.27 (s, 3H) ppm.

HRMS (FAB) calcd. for $\text{C}_{19}\text{H}_{28}\text{FN}_2$ $[\text{M}+\text{H}]^+$ 303.2236; found 303.2229.

3.40

3.30 (1.00 g, 2.90 mmol) and $\text{BH}_3\cdot\text{THF}$ (1 M, 8.7 mL, 8.7 mmol) were reacted according to **general procedure 3b**. Product **3.40** was obtained as a white solid (91% yield, 1.06 g).

^1H NMR (400 MHz, CD_3OD) δ 7.13 (d, $J = 7.4$ Hz, 1H), 7.05 (td, $J = 7.9, 5.5$ Hz, 1H), 6.98 (ddd, $J = 11.7, 8.1, 1.6$ Hz, 1H), 3.49 (t, $J = 6.4$ Hz, 2H), 3.30 – 3.15 (m, 3H), 2.23 (s, 3H), 1.98 (s, 3H), 1.98 (s, 3H), 1.87 – 1.69 (m, 6H), 1.27 (d, $J = 6.8$ Hz, 6H) ppm.

^{13}C NMR (101 MHz, CD_3OD) δ 164.25, 157.89 (d, $J = 251.9$ Hz), 128.52 (t, $J = 9.6$ Hz), 113.20 (t, $J = 16.5$ Hz), 111.99 (dd, $J = 19.3, 4.2$ Hz), 28.63 ppm.

HRMS (FAB) calcd. for $\text{C}_{21}\text{H}_{32}\text{FN}_2$ $[\text{M-H}]^+$ 331.2550; found 331.2534.

3.41

3.31 (2.50 g, 6.75 mmol) and $\text{BH}_3\cdot\text{THF}$ (1 M, 20.3 mL, 20.3 mmol) were reacted according to **general procedure 3b**. Product **3.41** was obtained as a white solid (84% yield, 2.44 g).

^1H NMR (400 MHz, CD_3OD) δ 7.40 – 7.28 (m, 2H), 6.97 (td, $J = 8.2, 5.1$ Hz, 1H), 3.60 (td, $J = 6.6, 1.6$ Hz, 2H), 3.23 (t, $J = 6.6$ Hz, 2H), 2.22 (s, 3H), 1.97 (s, 3H), 1.97 (s, 3H), 1.77 (app q, $J = 12.5$ Hz, 6H) ppm.

^{13}C NMR (101 MHz, CD_3OD) δ 164.25, 157.89 (d, $J = 251.9$ Hz), 128.52 (t, $J = 9.6$ Hz), 113.20 (t, $J = 16.5$ Hz), 111.99 (dd, $J = 19.3, 4.2$ Hz), 28.63 ppm.

HRMS (FAB) calcd. for $\text{C}_{19}\text{H}_{25}\text{F}_4\text{N}_2$ $[\text{M-H}]^+$ 357.1954; found 357.1954.

3.42

3.32 (1.55 g, 4.66 mmol) and $\text{BH}_3\cdot\text{THF}$ (1 M, 18.7 mL, 18.7 mmol) were reacted according to **general procedure 3b**. Product **3.42** was obtained as a white solid (89% yield, 1.63 g).

^1H NMR (400 MHz, CD_3OD) δ 7.33 (td, $J = 8.5, 6.7$ Hz, 1H), 7.03 (d, $J = 8.5$ Hz, 1H), 6.98 – 6.89 (m, 1H), 4.01 (s, 3H), 3.71 (t, $J = 6.6$ Hz, 2H), 3.35 (t, $J = 6.6$ Hz, 2H), 2.23 (s, 3H), 1.99 (s, 3H), 1.99 (s, 3H), 1.77 (app q, $J = 12.8$ Hz, 6H) ppm.

^{13}C NMR (101 MHz, CD_3OD) δ 164.25, 157.89 (d, $J = 251.9$ Hz), 128.52 (t, $J = 9.6$ Hz), 113.20 (t, $J = 16.5$ Hz), 111.99 (dd, $J = 19.3, 4.2$ Hz), 28.63 ppm.

HRMS (FAB) calcd. for $\text{C}_{19}\text{H}_{28}\text{FN}_2\text{O}$ $[\text{M}-\text{H}]^+$ 319.2186; found 319.2173.

3.43

3.33 (1.50 g, 4.57 mmol) and $\text{BH}_3\cdot\text{THF}$ (18.3 mL, 18.3 mmol) were reacted according to **general procedure 3b**. Product **3.43** was obtained as a white solid (85% yield, 1.51 g).

^1H NMR (400 MHz, CD_3OD) δ 7.41 (t, $J = 8.1$ Hz, 1H), 7.11 (d, $J = 8.3$ Hz, 1H), 6.99 (d, $J = 7.8$ Hz, 1H), 4.01 (s, 3H), 3.76 (t, $J = 6.6$ Hz, 2H), 3.54 (t, $J = 6.6$ Hz, 2H), 2.57 (s, 3H), 2.23 (s, 3H), 2.05 (s, 3H), 2.04 (s, 3H), 1.78 (app q, $J = 12.6$ Hz, 6H) ppm.

^{13}C NMR (101 MHz, CD_3OD) δ 153.8, 134.3, 132.2, 125.2, 123.5, 111.5, 59.7, 57.2, 47.9, 39.4, 36.9, 36.5, 30.6, 17.8 ppm.

HRMS (FAB) calcd. for $\text{C}_{20}\text{H}_{31}\text{N}_2\text{O}$ $[\text{M}-\text{H}]^+$ 315.2436; found 315.2440.

3.44

3.34 (2.00 g, 5.80 mmol) and $\text{BH}_3\cdot\text{THF}$ (17.4 mL, 17.4 mmol) were reacted for 3 h. according to **general procedure 3b**. After work-up the product was recrystallized from MeOH / EtOAc to give **3.44** as a white crystalline solid (60% yield, 1.41 g).

^1H NMR (400 MHz, CD_3OD) δ 7.49 (t, $J = 8.5$ Hz, 1H), 6.90 (d, $J = 8.5$ Hz, 2H), 4.01 (s, 6H), 3.70 (t, $J = 7.0$ Hz, 2H), 3.37 (t, $J = 7.0$ Hz, 2H), 2.23 (s, 3H), 1.99 (s, 3H), 1.99 (s, 3H), 1.78 (app q, $J = 12.5$ Hz, 6H) ppm.

^{13}C NMR (101 MHz, CD_3OD) δ 154.7, 132.9, 112.8, 106.3, 59.6, 57.4, 47.2, 39.4, 36.6, 36.4, 30.6 ppm.

HRMS (FAB) calcd. for $\text{C}_{20}\text{H}_{31}\text{N}_2\text{O}_2$ $[\text{M}-\text{H}]^+$ 331.2375; found 331.2386.

3.45

3.35 (1.50 g, 4.90 mmol), HCl in Et_2O (2 M, 4.90 mL, 9.79 mmol) and $\text{HC}(\text{OEt})_3$ (12.0 mL, 73.4 mmol) were reacted according to **general procedure 4a**. The product **3.45** was obtained as a pale-yellow solid (59% yield, 1.02 g).

^1H NMR (400 MHz, CDCl_3) δ 10.02 (s, 1H), 7.35 (tt, $J = 8.4, 6.2$ Hz, 1H), 7.05 (t, $J = 8.4$ Hz, 2H), 4.50 – 4.26 (m, 4H), 2.27 (s, 3H), 2.13 (s, 3H), 2.13 (s, 3H), 1.73 (s, 6H) ppm.

^{13}C NMR (101 MHz, CDCl_3) δ 157.6, 157.3 (dd, $J = 253.4, 3.6$ Hz), 130.4 (t, $J = 9.9$ Hz), 114.0 (t, $J = 15.0$ Hz), 113.0 – 112.6 (m), 59.1, 50.8 (t, $J = 2.7$ Hz), 45.3, 41.0, 35.5, 29.2 ppm.

HRMS (FAB) calcd. for $\text{C}_{19}\text{H}_{23}\text{F}_2\text{N}_2$ M^+ 317.1829; found 317.1835.

3.46

3.36 (0.500 g, 1.65 mmol), HCl in Et_2O (2 M, 1.65 mL, 3.31 mmol) and $\text{HC}(\text{OEt})_3$ (4.12 mL, 24.8 mmol) were reacted according to **general procedure 4a**. The product **3.46** was obtained as an off-white solid (63% yield, 361 mg).

^1H NMR (400 MHz, CDCl_3) δ 9.31 (s, 1H), 7.24 – 7.16 (m, 1H), 7.00 (d, $J = 7.8$ Hz, 1H), 6.93 (t, $J = 9.1$ Hz, 1H), 4.37 – 4.19 (m, 4H), 2.42 (s, 3H), 2.17 (s, 3H), 2.05 (s, 6H), 1.65 (s, 6H) ppm.

^{13}C NMR (101 MHz, CDCl_3) δ 7.75 (s, 1H), 7.24 – 7.14 (m, 1H), 7.03 (d, $J = 7.6$ Hz, 1H), 6.98 (t, $J = 8.9$ Hz, 4H), 4.07 (s, 2H), 2.27 (s, 3H) ppm.

HRMS (FAB) calcd. for $\text{C}_{20}\text{H}_{26}\text{FN}_2$ M^+ 313.2080; found 313.2084.

3.47

3.40 (0.283 g, 0.70 mmol), and $\text{HC}(\text{OEt})_3$ (1.80 mL, 10.8 mmol) were reacted according to **general procedure 4b**. Product **3.47** was obtained as an off-white solid (74% yield, 196 mg).

^1H NMR (400 MHz, CDCl_3) δ 9.24 (s, 1H), 7.42 – 7.32 (m, 1H), 7.18 (d, $J = 7.8$ Hz, 1H), 7.00 (t, $J = 8.8$ Hz, 1H), 4.42 (s, 2H), 4.30 (s, 2H), 3.25 (s, 1H), 2.24 (s, 3H), 2.12 (s, 6H), 1.72 (s, 6H), 1.29 (s, 6H) ppm.

^{13}C NMR (101 MHz, CDCl_3) δ 164.25, 157.89 (d, $J = 251.9$ Hz), 128.52 (t, $J = 9.6$ Hz), 113.20 (t, $J = 16.5$ Hz), 111.99 (dd, $J = 19.3, 4.2$ Hz), 28.63 ppm.

HRMS (FAB) calcd. for $\text{C}_{22}\text{H}_{30}\text{FN}_2$ M^+ 341.2393; found 341.2401.

3.48

3.41 (0.600 g, 1.40 mmol) and $\text{HC}(\text{OEt})_3$ (3.50 mL, 21.0 mmol) were reacted in MeCN (10.5 mL) according to **general procedure 4b**, except that 3 equiv. of MeCN (v/v with $\text{HC}(\text{OEt})_3$) were used. Product **3.48** was obtained as a white solid (62% yield, 350 mg).

^1H NMR (400 MHz, CDCl_3) δ 10.00 (s, 1H), 7.65 – 7.56 (m, 1H), 7.53 (d, $J = 7.7$ Hz, 1H), 7.46 (t, $J = 8.3$ Hz, 1H), 4.30 (s, 4H), 2.21 (s, 3H), 2.06 (s, 6H), 1.68 (s, 6H) ppm.

^{13}C NMR (101 MHz, CDCl_3) δ 164.25, 157.89 (d, $J = 251.9$ Hz), 128.52 (t, $J = 9.6$ Hz), 113.20 (t, $J = 16.5$ Hz), 111.99 (dd, $J = 19.3, 4.2$ Hz), 28.63 ppm.

HRMS (FAB) calcd. for $C_{20}H_{23}F_4N_2 M^+$ 367.1797; found 367.1781.

3.49

3.42 (1.00 g, 2.56 mmol) and $HC(OEt)_3$ (6.50 mL, 39.1 mmol) were reacted according to **general procedure 4b**, except that 3 equiv. of MeCN (v/v with $HC(OEt)_3$) were used.

Product **3.49** was obtained as a white solid (72% yield, 676 mg).

1H NMR (400 MHz, $CDCl_3$) δ 9.19 (s, 1H), 7.21 (td, $J = 8.5, 6.6$ Hz, 1H), 6.74 – 6.63 (m, 2H), 4.29 (s, 4H), 3.83 (s, 3H), 2.15 (s, 3H), 2.00 (s, 3H), 1.99 (s, 3H), 1.63 (s, 6H) ppm.

^{13}C NMR (101 MHz, $CDCl_3$) δ 164.25, 157.89 (d, $J = 251.9$ Hz), 128.52 (t, $J = 9.6$ Hz), 113.20 (t, $J = 16.5$ Hz), 111.99 (dd, $J = 19.3, 4.2$ Hz), 28.63 ppm.

HRMS (FAB) calcd. for $C_{20}H_{26}FN_2O M^+$ 329.2029; found 329.2021.

3.50

3.43 (0.600 g, 1.55 mmol) and $HC(OEt)_3$ (3.86 mL, 23.2 mmol) were reacted according to general procedure 4. The product **3.50** was obtained as an off-white solid (76% yield, 424 mg).

1H NMR (400 MHz, $CDCl_3$) δ 8.79 (s, 1H), 7.20 (t, $J = 8.0$ Hz, 1H), 6.80 (d, $J = 7.6$ Hz, 1H), 6.75 (d, $J = 8.3$ Hz, 1H), 4.38 – 4.28 (m, 2H), 4.26 – 4.15 (m, 2H), 3.81 (s, 3H), 2.38 (s, 3H), 2.20 (s, 3H), 2.06 (s, 3H), 2.06 (s, 3H), 1.68 (s, 6H) ppm.

^{13}C NMR (101 MHz, $CDCl_3$) δ 157.4, 154.9, 137.4, 130.5, 123.6, 123.3, 109.3, 58.0, 56.2, 50.7, 45.4, 41.1, 35.5, 29.2, 18.2 ppm.

HRMS (FAB) calcd. for $C_{21}H_{29}N_2O$ M^+ 325.2280; found 325.2276.

3.51

3.44 (0.350 g, 1.06 mmol) and $HC(OEt)_3$ (2.64 mL, 15.8 mmol) were reacted according to general procedure 4. After trituration of the solid with Et_2O , it was dissolved in a mixture of acetone (4 mL) and H_2O (2 mL) and $NaBF_4$ (0.186 g, 1.69 mmol) was added. The solution was stirred at room temperature for 1 h, at which stage the acetone was removed *in vacuo*. The product was partitioned between DCM (15 mL) and H_2O (5 mL). The aqueous layer was extracted a further portion of DCM (15 mL) and the combined organic layers were dried over Na_2SO_4 , filtered, concentrated, and dried *in vacuo* at 35 °C overnight. Product **3.51** was obtained as a white solid (59% yield, 269 mg).

1H NMR (400 MHz, $CDCl_3$) δ 7.90 (s, 1H), 7.30 (t, $J = 8.5$ Hz, 1H), 6.62 (d, $J = 8.5$ Hz, 2H), 4.40 – 4.18 (m, 4H), 3.89 (s, 6H), 2.26 (s, 3H), 2.01 (s, 3H), 2.00 (s, 3H), 1.80 – 1.67 (m, 6H) ppm.

^{13}C NMR (101 MHz, $CDCl_3$) δ 155.7, 155.3, 130.8, 113.3, 104.7, 57.9, 56.6, 50.4, 44.9, 41.1, 35.6, 29.3 ppm.

HRMS (FAB) calcd. for $C_{21}H_{29}N_2O_2$ M^+ 341.2229; found 341.2231.

3.53

3.45 (0.420 g, 1.20 mmol), KHMDS (0.232 g, 1.16 mmol) and **3.52** (0.517 g, 0.860 mmol) were reacted according to **general procedure 5**. Product **3.53** was obtained as a green solid (72% yield, 394 mg).

^1H NMR (400 MHz, CDCl_3) δ 17.25 (s, 1H), 7.57 (ddd, $J = 8.9, 7.2, 1.8$ Hz, 1H), 7.48 (tt, $J = 8.6, 6.0$ Hz, 1H), 7.14 – 7.04 (m, 2H), 6.95 (t, $J = 7.9$ Hz, 1H), 6.95 (d, $J = 7.4$ Hz, 1H), 6.89 (t, $J = 7.4$ Hz, 1H), 5.11 (hept, $J = 6.2$ Hz, 1H), 4.15 – 3.92 (m, 4H), 2.93 (s, 6H), 2.41 (s, 3H), 1.93 (d, $J = 11.9$ Hz, 3H), 1.83 (d, $J = 12.3$ Hz, 3H), 1.65 (d, $J = 6.2$ Hz, 6H) ppm.

^{13}C NMR (101 MHz, CDCl_3) δ 307.2, 211.8, 160.9 (dd, $J = 255.4, 3.8$ Hz), 153.0, 145.4, 130.9, 129.6 (t, $J = 9.8$ Hz), 123.5, 122.6 (t, $J = 15.9$ Hz), 122.5, 113.4, 112.8 – 112.4 (m), 74.5, 57.9, 52.4, 45.0, 41.9, 36.0, 29.9, 22.3 ppm.

HRMS (FAB) calcd. for $\text{C}_{29}\text{H}_{34}\text{Cl}_2\text{F}_2\text{N}_2\text{ORu}$ M^+ 636.1060; found 636.1083.

3.54

3.45 (0.400 g, 1.15 mmol), KHMDS (0.221 g, 1.11 mmol), and **3.52** (0.492 g, 0.819 mmol) were reacted according to **general procedure 5**. Product **3.54** was obtained as a green solid (80% yield, 414 mg).

^1H NMR (400 MHz, CDCl_3) δ 309.64, 209.53, 160.61 (d, $J = 252.8$ Hz), 152.62, 145.84, 141.39, 131.58 (d, $J = 12.7$ Hz), 130.99, 129.69 (d, $J = 8.4$ Hz), 126.44 (d, $J = 3.4$ Hz), 123.95, 122.72, 114.88 (d, $J = 20.1$ Hz), 113.47, 74.43, 57.62, 51.93, 44.95, 42.19, 36.20, 30.05, 22.52 (d, $J = 5.1$ Hz), 18.19 (d, $J = 2.6$ Hz) ppm.

^{13}C NMR (101 MHz, CDCl_3) δ 309.6, 209.5, 160.6 (d, $J = 252.8$ Hz), 152.6, 145.8, 141.4, 131.6 (d, $J = 12.7$ Hz), 131.0, 129.7 (d, $J = 8.4$ Hz), 126.4 (d, $J = 3.4$ Hz), 124.0, 122.7, 114.9 (d, $J = 20.1$ Hz), 113.5, 74.4, 57.6, 51.9, 45.0, 42.2, 36.2, 30.0, 22.5 (d, $J = 5.1$ Hz), 18.2 (d, $J = 2.6$ Hz) ppm.

HRMS (FAB) calcd. for $C_{30}H_{37}Cl_2FN_2ORu [(M+H_2)^{2+}]$ 634.1468; found 634.1455.

3.55

3.46 (146 mg, 0.387 mmol), KHMDS (73.4 mg, 0.368 mmol), and **3.52** (175 mg, 0.290 mmol) were reacted according to **general procedure 5**. Product **3.55** was obtained as a green solid (61% yield, 116 mg).

1H NMR (400 MHz, $CDCl_3$) δ 16.88 (s, 1H), 7.61 – 7.51 (m, 2H), 7.36 (d, $J = 7.9$ Hz, 1H), 7.13 – 7.05 (m, 1H), 6.94 (d, $J = 8.4$ Hz, 1H), 6.90 – 6.83 (m, 2H), 5.08 (hept, $J = 6.2$ Hz, 1H), 4.15 – 3.79 (m, 4H), 3.34 (hept, $J = 6.8$ Hz, 1H), 3.05 – 2.85 (m, 6H), 2.41 (s, 3H), 1.93 (d, $J = 11.9$ Hz, 3H), 1.83 (d, $J = 12.2$ Hz, 3H), 1.67 (d, $J = 6.2$ Hz, 3H), 1.61 (d, $J = 6.1$ Hz, 3H), 1.21 (d, $J = 6.9$ Hz, 3H), 1.00 (d, $J = 6.7$ Hz, 3H) ppm.

^{13}C NMR (101 MHz, $CDCl_3$) δ 308.5, 210.2, 160.0 (d, $J = 252.9$ Hz), 152.7, 151.4, 145.5, 130.8, 130.6 (d, $J = 12.5$ Hz), 130.1 (d, $J = 8.4$ Hz), 123.7, 122.6, 122.3 (d, $J = 3.5$ Hz), 114.6 (d, $J = 20.3$ Hz), 113.4, 74.4, 57.6, 53.6 – 53.0 (m), 44.9, 42.2, 36.2, 30.0, 27.6 (d, $J = 1.7$ Hz), 25.1, 23.4, 22.6 (d, $J = 28.7$ Hz) ppm.

HRMS (FAB) calcd. for $C_{32}H_{41}Cl_2FN_2ORu M^+$ 660.1624; found 660.1602.

3.56

3.47 (315 mg, 0.782 mmol), KHMDS (148 mg, 0.743 mmol), and **3.52** (352 mg, 0.586 mmol) were reacted according to **general procedure 5**. Product **3.56** was obtained as a green solid (77% yield, 309 mg).

^1H NMR (400 MHz, CDCl_3) δ 16.87 (s, 1H), 7.78 (d, $J = 8.0$ Hz, 1H), 7.68 (td, $J = 8.0$, 5.0 Hz, 1H), 7.56 (ddd, $J = 8.5$, 7.1, 1.9 Hz, 1H), 7.47 – 7.40 (m, 1H), 6.95 (d, $J = 8.5$ Hz, 1H), 6.91 – 6.79 (m, 2H), 5.10 (hept, $J = 6.1$ Hz, 1H), 4.15 – 3.71 (m, 4H), 3.09 – 2.83 (m, 6H), 2.41 (s, 3H), 1.94 (d, $J = 11.9$ Hz, 3H), 1.83 (d, $J = 12.4$ Hz, 3H), 1.68 (d, $J = 6.1$ Hz, 3H), 1.62 (d, $J = 6.1$ Hz, 3H) ppm.

^{13}C NMR (101 MHz, CDCl_3) δ 305.5, 213.5, 161.2 (d, $J = 257.3$ Hz), 153.1, 145.5, 132.5 (q, $J = 31.1$ Hz), 131.9 (d, $J = 14.9$ Hz), 131.1, 130.3 (d, $J = 8.3$ Hz), 128.4, 123.7, 122.9 (qd, $J = 274.6$, 3.3 Hz), 122.8 (p, $J = 4.9$ Hz), 122.6, 121.8 (d, $J = 20.5$ Hz), 113.6, 74.6, 58.2, 53.7, 45.4, 42.1, 36.1, 30.0, 22.5 (d, $J = 13.1$ Hz) ppm.

HRMS (FAB) calcd. for $\text{C}_{30}\text{H}_{34}\text{Cl}_2\text{F}_4\text{N}_2\text{ORu M}^+$ 686.1028; found 686.1006.

3.57

3.48 (240 mg, 0.66 mmol), KHMDS (126 mg, 0.63 mmol), and **3.52** (329 mg, 0.55 mmol) were reacted according to **general procedure 5**. Product **3.57** was obtained as a green solid (77% yield, 309 mg).

^1H NMR (400 MHz, CDCl_3) δ 17.35 (s, 1H), 7.56 (ddd, $J = 8.8$, 7.3, 1.7 Hz, 1H), 7.45 (td, $J = 8.5$, 6.3 Hz, 1H), 7.00 – 6.91 (m, 2H), 6.91 – 6.79 (m, 3H), 5.08 (hept, $J = 6.1$ Hz, 1H), 4.08 – 3.81 (m, 4H), 3.75 (s, 3H), 2.95 (s, 6H), 2.40 (s, 3H), 1.93 (d, $J = 11.9$ Hz, 3H), 1.82 (d, $J = 12.3$ Hz, 3H), 1.64 (dd, $J = 6.1$, 3.3 Hz, 6H) ppm.

^{13}C NMR (101 MHz, CDCl_3) δ 308.6 (d, $J = 41.3$ Hz), 210.7, 161.0 (d, $J = 251.7$ Hz), 159.1 (d, $J = 3.9$ Hz), 152.8, 145.6 (d, $J = 2.1$ Hz), 130.7, 129.6 (d, $J = 10.0$ Hz), 123.5,

122.6, 122.4, 113.4, 109.0 (d, $J = 20.5$ Hz), 107.9 (d, $J = 3.1$ Hz), 74.3, 57.6, 56.8, 51.8, 44.9, 42.1, 36.2, 30.0, 22.5 (d, $J = 3.3$ Hz) ppm.

HRMS (FAB) calcd. for $C_{30}H_{37}Cl_2FN_2O_2Ru$ M^+ 648.1260; found 648.1277.

3.58

3.49 (250 mg, 0.693 mmol), KHMDS (132 mg, 0.664 mmol), and **3.52** (347 mg, 0.577 mmol) were reacted according to general procedure **5**. Product **3.58** was obtained as a green solid (69% yield, 259 mg).

1H NMR (400 MHz, $CDCl_3$) δ 17.01 (s, 1H), 7.55 (ddd, $J = 8.9, 7.2, 1.8$ Hz, 1H), 7.44 (t, $J = 8.0$ Hz, 1H), 7.00 (d, $J = 7.6$ Hz, 1H), 6.96 – 6.84 (m, 4H), 5.07 (hept, $J = 6.2$ Hz, 1H), 4.11 – 3.91 (m, 3H), 3.85 – 3.71 (m, 1H), 3.66 (s, 3H), 2.96 (s, 6H), 2.41 (s, 3H), 2.32 (s, 3H), 1.94 (d, $J = 11.9$ Hz, 3H), 1.83 (d, $J = 12.3$ Hz, 3H), 1.63 (d, $J = 6.2$ Hz, 3H), 1.62 (d, $J = 6.2$ Hz, 3H) ppm.

^{13}C NMR (101 MHz, $CDCl_3$) δ 310.9 (d, $J = 18.3$ Hz), 208.9, 157.8, 152.4, 145.8, 140.0, 132.5, 130.6, 129.2, 123.7, 122.7, 122.6, 113.3, 110.2, 74.2, 57.2, 56.4, 51.1, 44.8, 42.2, 36.3, 30.1, 22.6 (d, $J = 5.8$ Hz), 18.3 ppm.

HRMS (FAB) calcd. for $C_{31}H_{40}Cl_2N_2O_2Ru$ M^+ 644.1511; found 644.1513.

3.59

3.51 (150 mg, 0.35 mmol), LiHMDS (56 mg, 0.33 mmol), and **3.52** (168 mg, 0.28 mmol) were reacted according to general procedure **5**. Product **3.59** was obtained as a green solid (64% yield, 117 mg).

^1H NMR (600 MHz, CDCl_3) δ 17.47 (s, 1H), 7.55 (ddd, $J = 8.6, 7.4, 1.7$ Hz, 1H), 7.44 (t, $J = 8.4$ Hz, 1H), 6.99 (dd, $J = 7.5, 1.6$ Hz, 1H), 6.93 (d, $J = 8.4$ Hz, 1H), 6.88 (t, $J = 7.4$ Hz, 1H), 6.69 (d, $J = 8.4$ Hz, 2H), 5.06 (hept, $J = 6.1$ Hz, 1H), 4.06 – 3.95 (m, 2H), 3.92 – 3.84 (m, 2H), 3.70 (s, 6H), 2.96 (s, 6H), 2.40 (s, 3H), 1.94 (d, $J = 11.9$ Hz, 3H), 1.82 (d, $J = 12.3$ Hz, 3H), 1.63 (d, $J = 6.2$ Hz, 6H) ppm.

^{13}C NMR (101 MHz, CDCl_3) δ 309.8 (d, $J = 43.5$ Hz), 209.6, 158.7, 152.6, 145.6, 130.4, 129.4, 123.4, 122.9, 122.6, 113.4, 104.9, 74.1, 57.3, 56.6, 51.4, 44.8, 42.2, 36.3, 30.1, 22.6 ppm.

HRMS (FAB) calcd. for $\text{C}_{31}\text{H}_{40}\text{Cl}_2\text{N}_2\text{O}_3\text{Ru}$ M^+ 660.1460; found 660.1477.

3.10

3.53 (200 mg, 0.31 mmol) and NaOPiv (389 mg, 3.1 mmol) were reacted according to **general procedure 6** to give **3.60** as a purple solid (177 mg). A portion of this material (150 mg) and NH_4NO_3 (540 mg, 6.8 mmol) were then reacted to give product **3.10** as a purple solid (66% yield, 110 mg).

^1H NMR (400 MHz, C_6D_6) δ 15.40 – 15.36 (m, 1H), 7.41 (dd, $J = 7.6, 1.4$ Hz, 1H), 7.13 (dd, $J = 8.6, 1.2$ Hz, 1H), 6.82 – 6.73 (m, 2H), 6.58 (tt, $J = 8.6, 6.5$ Hz, 1H), 6.47 (d, $J = 8.3$ Hz, 1H), 6.42 (t, $J = 8.9$ Hz, 1H), 4.58 (hept, $J = 5.9$ Hz, 1H), 4.09 (s, 1H), 3.59 (q, $J = 10.6$ Hz, 1H), 3.33 – 3.25 (m, 1H), 3.17 – 3.00 (m, 2H), 2.23 (s, 1H), 2.06 (s, 1H), 1.96 (d, $J = 11.7$ Hz, 1H), 1.84 (s, 2H), 1.73 (d, $J = 12.3$ Hz, 1H), 1.60 (s, 1H), 1.45 (d, $J = 6.4$ Hz, 3H), 1.52 – 1.34 (m, 3H), 1.10 – 1.02 (m, 2H), 0.97 (d, $J = 6.2$ Hz, 3H), 0.54 (d, $J = 12.7$ Hz, 1H) ppm.

^{19}F NMR (376 MHz, C_6D_6) δ -118.1 (dt, $J = 9.1, 4.5$ Hz), -119.5 – -119.6 (m).

HRMS (FAB) calcd. for $\text{C}_{29}\text{H}_{32}\text{F}_2\text{N}_3\text{O}_4\text{Ru}$ [(M+H)- H_2] $^+$ 626.1405; found 626.1419.

3.11

3.54 (150 mg, 0.24 mmol), NaOPiv (294 mg, 2.4 mmol), and NH_4NO_3 (471 mg, 5.9 mmol) were reacted according to **general procedure 6** to give product **3.11** as a purple solid (76% yield, 93 mg).

^1H NMR (600 MHz, C_6D_6) δ 15.56 – 15.54 (m, 1H), 15.05 (s, 1H), 7.45 (dd, $J = 7.5, 1.7$ Hz, 1H), 7.34 (dd, $J = 7.5, 1.7$ Hz, 1H), 7.18 (dddd, $J = 17.4, 8.4, 7.5, 1.7$ Hz, 5H), 7.01 (t, $J = 9.0$ Hz, 1H), 6.89 (d, $J = 7.7$ Hz, 1H), 6.89 – 6.82 (m, 1H), 6.85 – 6.74 (m, 4H), 6.65 (ddd, $J = 8.6, 6.0, 2.8$ Hz, 3H), 6.51 (dd, $J = 8.3, 1.0$ Hz, 1H), 6.48 (dd, $J = 8.2, 1.0$ Hz, 1H), 4.59 (dhept, $J = 12.6, 6.3$ Hz, 2H), 4.18 (s, 1H), 4.09 (s, 1H), 3.62 (ddd, $J = 11.7, 10.7, 9.4$ Hz, 1H), 3.44 (dt, $J = 10.9, 9.5$ Hz, 1H), 3.35 (ddd, $J = 11.2, 9.5, 6.1$ Hz, 1H), 3.29 – 3.08 (m, 7H), 2.33 (s, 2H), 2.31 (s, 3H), 2.25 (dp, $J = 12.3, 3.3$ Hz, 2H), 2.09 (dp, $J = 6.5, 3.2$ Hz, 2H), 1.99 (dt, $J = 12.1, 2.7$ Hz, 2H), 1.93 (tdd, $J = 14.6, 3.1, 1.8$ Hz, 2H), 1.90 – 1.87 (m, 1H), 1.87 – 1.82 (m, 1H), 1.80 – 1.73 (m, 2H), 1.65 (s, 3H), 1.51 (dddt, $J = 12.0, 10.7, 3.7, 1.7$ Hz, 2H), 1.46 (d, $J = 6.4$ Hz, 5H), 1.49 – 1.41 (m, 1H), 1.46 (d, $J = 6.3$ Hz, 5H), 1.16 – 1.07 (m, 4H), 1.04 (dq, $J = 11.2, 2.7$ Hz, 1H), 1.00 (d, $J = 6.2$ Hz, 3H), 0.96 (d, $J = 6.2$ Hz, 4H), 0.57 (tt, $J = 13.1, 2.6$ Hz, 2H) ppm.

^{13}C NMR (101 MHz, C_6D_6) δ 267.8 – 267.4 (m), 265.2 – 264.5 (m), 216.2, 215.4, 161.0 (d, $J = 249.0$ Hz), 159.8 (d, $J = 245.3$ Hz), 154.4, 154.32, 143.2, 143.1, 140.7, 138.2, 128.8 (d, $J = 8.9$ Hz), 128.8 (d, $J = 8.9$ Hz), 126.6, 126.5, 126.2 (d, $J = 3.2$ Hz), 125.6 (d, $J = 3.2$ Hz), 123.1 (d, $J = 4.2$ Hz), 122.9 (d, $J = 6.4$ Hz), 114.1 (d, $J = 20.4$ Hz), 113.3 (d,

$J = 21.1$ Hz), 112.6, 112.4, 74.1, 73.8, 66.4, 66.4, 63.1, 63.0, 53.0, 51.4 (d, $J = 2.5$ Hz), 51.0, 42.4, 42.2, 41.8, 41.8, 39.9, 39.8, 37.5, 37.5, 37.4, 37.3, 33.0, 32.9, 30.5, 30.5, 29.4, 29.4, 21.0, 20.9, 19.9, 17.4 (d, $J = 2.6$ Hz), 16.5 (d, $J = 2.6$ Hz) ppm.

HRMS (FAB) calcd. for $C_{30}H_{36}FN_3O_4Ru$ M^+ 650.1805; found 623.1719.

3.12

3.55 (150 mg, 0.23 mmol) and NaOPiv (280 mg, 2.3 mmol) were reacted according to **general procedure 6** to give **3.62** as a purple solid (123 mg). A portion of this material (46 mg) and NH_4NO_3 (160 mg, 2.0 mmol) were then reacted to give product **3.12** as a purple solid (54% yield, 30 mg).

1H NMR (400 MHz, CD_2Cl_2) δ 14.85 (s, 1H), 7.53 – 7.43 (m, 1H), 7.39 (dd, $J = 7.4, 1.3$ Hz, 1H), 7.22 (td, $J = 8.0, 5.8$ Hz, 1H), 7.06 (d, $J = 7.9$ Hz, 1H), 7.02 – 6.93 (m, 2H), 6.88 (ddd, $J = 9.6, 8.2, 1.1$ Hz, 1H), 5.13 (hept, $J = 6.2$ Hz, 1H), 4.06 – 3.93 (m, 1H), 3.93 – 3.68 (m, 5H), 2.27 – 2.14 (m, 2H), 2.08 – 2.01 (m, 2H), 1.93 (d, $J = 12.0$ Hz, 1H), 1.77 – 1.63 (m, 2H), 1.60 (s, 1H), 1.55 (s, 2H), 1.50 (d, $J = 6.4$ Hz, 3H), 1.26 (d, $J = 6.9$ Hz, 3H), 1.19 (d, $J = 6.2$ Hz, 3H), 1.17 (d, $J = 7.0$ Hz, 3H), 1.06 – 0.88 (m, 2H), 0.23 (d, $J = 12.0$ Hz, 1H) ppm.

^{19}F NMR (376 MHz, C_6D_6) δ -120.30 (dd, $J = 9.7, 5.8$ Hz) ppm.

^{13}C NMR (101 MHz, CD_2Cl_2) δ 265.9 (d, $J = 20.1$ Hz), 216.4, 160.7 (d, $J = 248.0$ Hz), 154.7, 150.1, 142.9, 129.4 (d, $J = 8.9$ Hz), 127.2, 126.9 (d, $J = 12.9$ Hz), 123.4, 123.3, 121.8 (d, $J = 3.3$ Hz), 113.4 (d, $J = 20.6$ Hz), 112.9, 74.5, 67.7, 63.8, 53.2 (d, $J = 2.3$ Hz), 42.9, 42.6, 40.2, 37.9, 37.8, 37.6, 33.2, 30.9, 29.7, 27.9 (d, $J = 2.3$ Hz), 25.7, 23.2, 21.4, 20.6 ppm.

HRMS (FAB) calcd. for $C_{32}H_{39}FN_3O_4Ru [(M+H)-H_2]^+$ 650.1969; found 650.1978.

3.13

3.56 (200 mg, 0.29 mmol) and NaOPiv (360 mg, 2.9 mmol) were reacted according to **general procedure 6** to give **3.63** as a purple solid (154 mg). A portion of this material (80 mg) and NH_4NO_3 (270 mg, 3.3 mmol) were then reacted to give product **3.13** as a purple solid (48% yield, 49 mg).

1H NMR (400 MHz, C_6D_6) δ 15.38 (d, $J = 3.9$ Hz, 1H), 15.15 (s, 1H), 7.49 (dd, $J = 7.4$, 1.4 Hz, 1H), 7.37 (dd, $J = 7.4$, 1.3 Hz, 1H), 7.26 – 7.21 (m, 1H), 7.16 – 7.07 (m, 3H), 6.96 (d, $J = 8.0$ Hz, 1H), 6.81 (t, $J = 7.4$ Hz, 1H), 6.75 (t, $J = 7.4$ Hz, 1H), 6.69 – 6.55 (m, 3H), 6.50 – 6.40 (m, 2H), 4.58 (hept, $J = 6.3$ Hz, 2H), 4.15 (s, 1H), 4.05 (s, 1H), 3.82 – 3.72 (m, 1H), 3.53 – 3.31 (m, 3H), 3.27 – 3.00 (m, 4H), 2.21 (s, 2H), 2.05 (s, 2H), 1.98 – 1.66 (m, 8H), 1.65 – 1.55 (m, 2H), 1.52 – 1.33 (m, 12H), 1.16 – 1.01 (m, 6H), 0.98 (d, $J = 6.2$ Hz, 3H), 0.94 (d, $J = 6.2$ Hz, 3H), 0.60 – 0.47 (m, 2H) ppm.

^{19}F NMR (376 MHz, C_6D_6) δ -58.6 (s), -59.6 (s), -117.7 (dd, $J = 9.2$, 5.2 Hz), -117.9 – -118.0 (m) ppm.

^{13}C NMR (101 MHz, C_6D_6) δ 268.7, 267.9, 218.5 (d, $J = 1.4$ Hz), 215.5, 161.9 (d, $J = 251.8$ Hz), 160.7 (d, $J = 247.7$ Hz), 154.8, 154.7, 143.5, 143.1, 131.2 (q, $J = 30.6$ Hz), 130.6 (q, $J = 29.8$ Hz), 130.0 (d, $J = 8.8$ Hz), 129.8 (d, $J = 8.9$ Hz), 128.8 – 128.5 (m), 127.2, 127.0, 125.4 (app. d, $J = 3.7$ Hz), 125.3, 123.7, 123.5, 123.4, 123.4, 123.3 – 123.1 (m), 122.8 – 122.4 (m), 120.9 (d, $J = 20.9$ Hz), 120.2 (d, $J = 21.3$ Hz), 112.9, 112.8, 74.6, 74.4, 66.1, 66.0, 63.8, 63.7, 53.0, 52.8, 42.5, 42.5, 42.4, 40.1, 38.2, 37.8, 37.8, 37.7, 37.6, 33.2, 30.8, 30.8, 29.8, 29.7, 21.2, 21.1, 20.4 ppm.

HRMS (FAB) calcd. for $C_{30}H_{34}F_4N_3O_4Ru$ (M+H)⁺ 678.1529; found 678.1552.

3.14

3.57 (79 mg, 0.12 mmol), NaOPiv (150 mg, 1.2 mmol), and NH_4NO_3 (255 mg, 3.2 mmol) were reacted according to **general procedure 6** to give product **3.14** as a purple solid (62% yield, 48 mg).

¹H NMR (600 MHz, C_6D_6) δ 15.51 (s, 1H), 15.38 (s, 1H), 7.49 – 7.39 (m, 2H), 7.21 (s, 1H), 7.16 – 7.11 (m, 2H), 6.88 (s, 1H), 6.84 – 6.75 (m, 3H), 6.51 (s, 1H), 6.49 – 6.43 (m, 2H), 6.41 (d, $J = 8.5$ Hz, 1H), 6.08 (s, 1H), 4.58 (hept, $J = 6.0$ Hz, 2H), 4.17 (s, 1H), 4.12 (s, 1H), 3.93 (q, $J = 10.6$ Hz, 1H), 3.72 – 3.62 (m, 1H), 3.58 (s, 3H), 3.51 (s, 1H), 3.40 (td, $J = 9.9, 4.1$ Hz, 1H), 3.33 – 3.08 (m, 5H), 2.30 – 2.21 (m, 2H), 2.07 (s, 1H), 2.03 (s, 1H), 2.00 – 1.93 (m, 2H), 1.89 – 1.81 (m, 3H), 1.81 – 1.71 (m, 3H), 1.65 (s, 1H), 1.62 (s, 1H), 1.51 – 1.38 (m, 13H), 1.15 – 1.04 (m, 3H), 0.99 – 0.91 (m, 6H), 0.63 – 0.53 (m, 2H) ppm.

¹⁹F NMR (376 MHz, C_6D_6) δ -119.82– -119.92 (m), -121.43 – -121.52 (m) ppm.

¹³C NMR (101 MHz, CD_2Cl_2) δ 267.5 – 266.8 (m), 216.4, 215.9, 161.8 (d, $J = 247.4$ Hz), 160.5 (d, $J = 246.1$ Hz), 159.3, 158.2, 154.6, 143.1, 129.2 (d, $J = 10.4$ Hz), 127.1, 123.4, 123.1, 118.6 (d, $J = 15.0$ Hz), 112.7, 108.3 (d, $J = 23.3$ Hz), 108.0 (d, $J = 21.3$ Hz), 107.0, 74.2, 67.7, 63.8, 56.3, 51.9, 51.5, 42.9, 42.8, 40.2, 37.8, 37.7, 37.6, 33.3, 30.9, 29.7, 21.5, 20.6 ppm.

HRMS (FAB) calcd. for $C_{30}H_{35}FN_3O_3Ru$ [(M+H)-H₂]⁺ 638.1605; found 638.1601.

3.15

3.58 (150 mg, 0.23 mmol), NaOPiv (290 mg, 2.3 mmol), and NH_4NO_3 (260 mg, 3.3 mmol) were reacted according to **general procedure 6** to give product **3.15** as a purple solid (53% yield, 79 mg).

^1H NMR (400 MHz, C_6D_6) δ 15.53 (s, 1H), 15.17 (s, 2H), 7.48 – 7.42 (m, 1H), 7.36 (dd, $J = 7.4, 1.7$ Hz, 2H), 7.26 – 7.17 (m, 3H), 7.05 (t, $J = 8.0$ Hz, 2H), 6.98 (t, $J = 7.9$ Hz, 1H), 6.93 – 6.86 (m, 2H), 6.82 (t, $J = 7.4$ Hz, 2H), 6.70 – 6.62 (m, 4H), 6.55 – 6.44 (m, 3H), 6.29 (dd, $J = 8.1, 1.4$ Hz, 1H), 4.56 (pd, $J = 6.3, 2.1$ Hz, 3H), 4.19 (s, 2H), 4.16 (s, 1H), 3.98 – 3.84 (m, 2H), 3.68 (s, 6H), 3.60 – 3.41 (m, 3H), 3.39 (s, 3H), 3.35 – 3.06 (m, 8H), 2.45 (s, 6H), 2.38 (s, 3H), 2.29 (d, $J = 2.7$ Hz, 1H), 2.23 (q, $J = 2.8$ Hz, 2H), 2.15 – 1.84 (m, 11H), 1.82 – 1.70 (m, 5H), 1.71 – 1.59 (m, 3H), 1.58 – 1.36 (m, 18H), 1.24 – 1.02 (m, 8H), 0.98 – 0.90 (m, 9H), 0.60 (ddt, $J = 20.4, 12.2, 2.6$ Hz, 3H) ppm.

^{13}C NMR (101 MHz, CD_2Cl_2) δ 267.6 – 267.3 (m), 265.4 – 264.8 (m), 215.9, 214.1, 157.9, 156.8, 154.6, 154.5, 143.2, 143.1, 140.2, 137.9, 129.0, 128.9, 128.5, 128.5, 127.1, 126.9, 123.5, 123.4, 123.3, 123.1, 122.5, 122.0, 112.8, 112.7, 108.7, 108.7, 74.3, 74.1, 68.1, 67.6, 67.6, 63.4, 63.4, 55.6, 55.5, 51.6, 51.3, 43.0, 42.6, 42.6, 40.3, 40.2, 37.8, 37.8, 37.7, 37.7, 37.6, 33.3, 33.2, 31.0, 30.9, 29.8, 29.8, 26.0, 21.5, 21.4, 20.6, 18.2, 16.7 ppm.

HRMS (FAB) calcd. for $\text{C}_{31}\text{H}_{38}\text{N}_3\text{O}_5\text{Ru}$ [(M+H)- H_2] $^+$ 634.1855; found 634.1883.

3.16

3.59 (75 mg, 0.11 mmol) and NaOPiv (140 mg, 1.1 mmol) were reacted according to **general procedure 6** to give **3.66** as a purple solid (53 mg). A portion of this material

(32 mg) and NH_4NO_3 (75 mg, 0.94 mmol) were then reacted to give product **3.16** as a purple solid (54% yield, 24 mg).

^1H NMR (600 MHz, C_6D_6) δ 15.53 (s, 1H), 7.46 (d, $J = 7.4$ Hz, 1H), 7.25 – 7.19 (m, 1H), 7.01 (t, $J = 8.4$ Hz, 1H), 6.89 (t, $J = 7.4$ Hz, 1H), 6.52 (d, $J = 8.4$ Hz, 1H), 6.47 (d, $J = 8.4$ Hz, 1H), 6.14 (d, $J = 8.4$ Hz, 1H), 4.58 (hept, $J = 6.3$ Hz, 1H), 4.19 (s, 1H), 3.99 (q, $J = 10.9$ Hz, 1H), 3.67 (s, 3H), 3.64 – 3.56 (m, 1H), 3.42 (s, 3H), 3.31 (q, $J = 10.9$ Hz, 1H), 3.26 – 3.20 (m, 1H), 2.28 (s, 1H), 2.03 (s, 1H), 2.00 (d, $J = 12.1$ Hz, 1H), 1.86 (d, $J = 10.9$ Hz, 1H), 1.77 (t, $J = 11.5$ Hz, 2H), 1.66 (s, 1H), 1.50 (t, $J = 10.5$ Hz, 2H), 1.46 (d, $J = 6.3$ Hz, 3H), 1.41 (d, $J = 12.4$ Hz, 1H), 1.17 (d, $J = 11.2$ Hz, 1H), 1.12 (d, $J = 12.0$ Hz, 1H), 0.94 (d, $J = 6.2$ Hz, 3H), 0.61 (d, $J = 12.1$ Hz, 1H) ppm.

^{13}C NMR (101 MHz, C_6D_6) δ 266.4 (d, $J = 7.9$ Hz), 216.0, 159.2, 157.5, 154.8, 143.7, 129.1, 126.4, 123.2, 122.8, 118.7, 113.0, 104.5, 104.0, 74.0, 66.9, 63.2, 55.7, 55.1, 51.1, 42.6, 42.1, 40.4, 37.9, 37.9, 37.8, 33.6, 30.9, 30.0, 21.5, 20.4 ppm.

HRMS (FAB) calcd. for $\text{C}_{31}\text{H}_{38}\text{N}_3\text{O}_6\text{Ru}$ [(M+H)- H_2] $^+$ 650.1805; found 650.1816.

References

- (1) Keitz, B. K.; Endo, K.; Patel, P. R.; Herbert, M. B.; Grubbs, R. H. *J. Am. Chem. Soc.* **2012**, *134* (1), 693–699.
- (2) Keitz, B. K.; Fedorov, A.; Grubbs, R. H. *J. Am. Chem. Soc.* **2012**, *134* (4), 2040–2043.
- (3) Miyazaki, H.; Herbert, M. B.; Liu, P.; Dong, X.; Xu, X.; Keitz, B. K.; Ung, T.; Mkrtumyan, G.; Houk, K. N.; Grubbs, R. H. *J. Am. Chem. Soc.* **2013**, *135* (15), 5848–5858.
- (4) Rosebrugh, L. E.; Marx, V. M.; Keitz, B. K.; Grubbs, R. H. *J. Am. Chem. Soc.* **2013**, *135* (27), 10032–10035.
- (5) Cannon, J. S.; Grubbs, R. H. *Angew. Chem. Int. Ed.* **2013**, *52* (34), 9001–9004.

- (6) Herbert, M. B.; Marx, V. M.; Pederson, R. L.; Grubbs, R. H. *Angew. Chem. Int. Ed.* **2013**, *52* (1), 310–314.
- (7) Hartung, J.; Grubbs, R. H. *J. Am. Chem. Soc.* **2013**, *135* (28), 10183–10185.
- (8) Quigley, B. L.; Grubbs, R. H. *Chem. Sci.* **2014**, *5* (2), 501–506.
- (9) Hartung, J.; Dornan, P. K.; Grubbs, R. H. *J. Am. Chem. Soc.* **2014**, *136* (37), 13029–13037.
- (10) Herbert, M. B.; Grubbs, R. H. *Angew. Chem. Int. Ed.* **2015**, *54* (17), 5018–5024.
- (11) Rosebrugh, L. E.; Ahmed, T. S.; Marx, V. M.; Hartung, J.; Liu, P.; López, J. G.; Houk, K. N.; Grubbs, R. H. *J. Am. Chem. Soc.* **2016**, *138* (4), 1394–1405.
- (12) Rosebrugh, L. E.; Herbert, M. B.; Marx, V. M.; Keitz, B. K.; Grubbs, R. H. *J. Am. Chem. Soc.* **2013**, *135* (4), 1276–1279.
- (13) Mangold, S. L.; Grubbs, R. H. *Chem. Sci.* **2015**, *6* (8), 4561–4569.
- (14) Mangold, S. L.; O’Leary, D. J.; Grubbs, R. H. *J. Am. Chem. Soc.* **2014**, *136* (35), 12469–12478.
- (15) Pribisko, M. A.; Ahmed, T. S.; Grubbs, R. H. *Polyhedron* **2014**, *84*, 144–149.
- (16) Endo, K.; Herbert, M. B.; Grubbs, R. H. *Organometallics* **2013**, *32* (18).
- (17) Endo, K.; Grubbs, R. H. *J. Am. Chem. Soc.* **2011**, *133* (22), 8525–8527.
- (18) Herbert, M. B.; Suslick, B. A.; Liu, P.; Zou, L.; Dornan, P. K.; Houk, K. N.; Grubbs, R. H. *Organometallics* **2015**, *34* (12), 2858–2869.
- (19) Bronner, S. M.; Herbert, M. B.; Patel, P. R.; Marx, V. M.; Grubbs, R. H. *Chem. Sci.* **2014**, *5* (10), 4091–4098.
- (20) Herbert, M. B.; Lan, Y.; Keitz, B. K.; Liu, P.; Endo, K.; Day, M. W.; Houk, K. N.; Grubbs, R. H. *J. Am. Chem. Soc.* **2012**, *134* (18), 7861–7866.
- (21) Keitz, B. K.; Endo, K.; Herbert, M. B.; Grubbs, R. H. *J. Am. Chem. Soc.* **2011**, *133* (25), 9686–9688.
- (22) Paczal, A.; Bényei, A. C.; Kotschy, A. *J. Org. Chem.* **2006**, *71* (16), 5969–5979.
- (23) Thomas, R. M.; Keitz, B. K.; Champagne, T. M.; Grubbs, R. H. *J. Am. Chem. Soc.* **2011**, *133* (19), 7490–7496.
- (24) Thomas, R. M.; Fedorov, A.; Keitz, B. K.; Grubbs, R. H. *Organometallics* **2011**, *30* (24), 6713–6717.
- (25) Benhamou, L.; Chardon, E.; Lavigne, G.; Bellemin-Laponnaz, S.; César, V. *Chem. Rev.* **2011**, *111* (4), 2705–2733.
- (26) Altenburger, J. M.; Fossey, V.; Galtier, D.; Petit, F. 5,6-bisaryl-2-pyridine-carboxamide derivatives, preparation thereof and therapeutic application thereof as urotensin II receptor antagonists. US Patent US8466292 B2, Jun 18, 2013.
- (27) Song, Y. M.; Ha, Y. M.; Kim, J.-A.; Chung, K. W.; Uehara, Y.; Lee, K. J.; Chun,

- P.; Byun, Y.; Chung, H. Y.; Moon, H. R. *Bioorg. Med. Chem. Lett.* **2012**, *22* (24), 7451–7455.
- (28) Han, C.; Buchwald, S. L. *J. Am. Chem. Soc.* **2009**, *131* (22), 7532–7533.
- (29) Gilman, N. W.; Sternbach, L. H. *J. Chem. Soc. D: Chem. Comm.* **1971**, No. 9, 465a.
- (30) Vougioukalakis, G. C.; Grubbs, R. H. *Chem. Eur. J.* **2008**, *14* (25), 7545–7556.
- (31) Wenzel, A. G.; Grubbs, R. H. *J. Am. Chem. Soc.* **2006**, *128* (50), 16048–16049.
- (32) Ritter, T.; Day, M. W.; Grubbs, R. H. *J. Am. Chem. Soc.* **2006**, *128* (36), 11768–11769.
- (33) Ledoux, N.; Linden, A.; Allaert, B.; Mierde, H. V.; Verpoort, F. *Adv. Synth. Catal.* **2007**, *349* (10), 1692–1700.
- (34) Vehlow, K.; Maechling, S.; Blechert, S. *Organometallics* **2006**, *25* (1), 25–28.
- (35) Ritter, T.; Hejl, A.; Wenzel, A. G.; Funk, T. W.; Grubbs, R. H. *Organometallics* **2006**, *25* (24), 5740–5745.
- (36) Anderson, D. R.; O’Leary, D. J.; Grubbs, R. H. *Chem. Eur. J.* **2008**, *14* (25), 7536–7544.
- (37) Jeffrey, G. A. *An Introduction to Hydrogen Bonding*; Oxford University Press: New York, 1997.
- (38) Mitani, M.; Saito, J.; Ishii, S.-I.; Nakayama, Y.; Makio, H.; Matsukawa, N.; Matsui, S.; Mohri, J.-I.; Furuyama, R.; Terao, H.; Bando, H.; Tanaka, H.; Fujita, T. *Chem. Record* **2004**, *4* (3), 137–158.
- (39) Weberski, M. P., Jr.; Chen, C.; Delferro, M.; Zuccaccia, C.; Macchioni, A.; Marks, T. J. *Organometallics* **2012**, *31* (9), 3773–3789.
- (40) Kui, S. C. F.; Zhu, N.; Chan, M. C. W. *Angew. Chem. Int. Ed.* **2003**, *42* (14), 1628–1632.
- (41) Iwashita, A.; Chan, M. C. W.; Makio, H.; Fujita, T. *Catal. Sci. Technol.* **2014**, *4* (3), 599–610.
- (42) Vougioukalakis, G. C.; Grubbs, R. H. *Organometallics* **2007**, *26* (9), 2469–2472.
- (43) Hassam, M.; Taher, A.; Arnott, G. E.; Green, I. R.; van Otterlo, W. A. L. *Chem. Rev.* **2015**, *115* (11), 5462–5569.
- (44) Occhipinti, G.; Koudriavtsev, V.; Törnroos, K. W.; Jensen, V. R. *Dalton Trans* **2014**, *43* (29), 11106–11117.
- (45) Speed, A. W. H.; Mann, T. J.; O’Brien, R. V.; Schrock, R. R.; Hoveyda, A. H. *J. Am. Chem. Soc.* **2014**, *136* (46), 16136–16139.
- (46) Anslyn, E. V.; Dougherty, D. A. In *Modern Physical Organic Chemistry*; University Science Books: Sausalito, CA; p 103.

- (47) MacPhee, J. A.; Panaye, A.; Dubois, J.-E. *Tetrahedron* **1978**, *34* (24), 3553–3562.
- (48) Charton, M. In *Steric effects in drug design*; Topics in Current Chemistry; Springer Berlin Heidelberg: Berlin, Heidelberg, 1983; Vol. 114, pp 57–91.